MSc. Dissertation

A morphological study of the kidney and renal portal system of the Cape griffon vulture (*Gyps coprotheres*)

Lauren N. Havenga

A dissertation submitted in partial fulfilment of the requirement for the degree of Magister Scientiae in the Department of Anatomy and Physiology in the Faculty of Veterinary Science, University of Pretoria

November 2015

A morphological study of the kidney and renal portal system of the Cape griffon vulture (*Gyps coprotheres*)
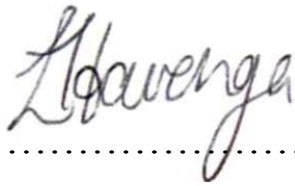
By: Dr. Lauren N. Havenga
Department of Anatomy and Physiology
Faculty of Veterinary Science
University of Pretoria
South Africa

Supervisor: Prof. Hermanus B. Groenewald
Department of Anatomy and Physiology
Faculty of Veterinary Science
University of Pretoria
South Africa

Co-supervisor: Prof. Neil Duncan
Department of Paraclinical Sciences
Faculty of Veterinary Science
University of Pretoria
South Africa

Ⅰ. **Declaration**

I, Lauren N. Havenga, declare that the dissertation, which I hereby submit for the degree of Magister Scientiae at the University of Pretoria, is my own work and has not previously been submitted by me for a degree at this or any other tertiary institution.

…………………………………………………

Havenga, L.N.

November 2015

II. Ethics Statement

The author, whose name appears on the title page of this dissertation, has obtained, for the research described in this work, the applicable research approval. The author declares that she has observed the ethical standards required in terms of the University of Pretoria's Code of ethics for researchers and the Policy guidelines for responsible research.

III. Acknowledgements

I would like to thank my supervisors Prof Groenewald and Prof Duncan for their hard work and dedication in making this project a success. You have challenged me and taught me to question in order to understand rather than to passively accept statements. You have truly been an inspiration to me.

To my parents. You have encouraged my love for animals since a toddler. You have given me the most amazing opportunity in life by believing in and supporting my dream to study veterinary medicine and enter a career in research. Thank you for your unwavering love and support. I have the most amazing parents I could imagine. Through the head start you have given me, I know I can make a difference.

Kerri and her eco-ambassadors at Vulpro (Percy, PJ and Cody) - through the time spent at Vulpro, working with these incredible birds, and interacting with the selfless people who dedicate their lives to rescuing and saving a species that to some seems insignificant, I had a curious fascination that has been kindled and developed into a deep passion for research and vultures. I pledge to continue doing ecological research and fighting for the survival of these birds that play such a vital role in the circle of life.

To my husband Vinny. My rock, my inspiration and my driving force. You have stood by me through every challenge, been my sounding board, picked me up when I've thought things were going awry and been my cheerleader when things fell into place. To have you in my life is to be blessed.

This project has taught me the values of discipline, consistency and passion. I thank everyone who has been involved directly or indirectly in making it something I am so incredibly proud of.

Ⅳ. **Abstract**

In the 1990's, diclofenac was responsible for the inadvertent deaths of over ten million vultures on the Asian subcontinent. While the pathology associated with their deaths was clearly evident as visceral and articular gout, the mechanism behind their death remains an enigma. In one of the supposition proposed on a potential mechanism of toxicity, it was postulated that the acute necrosis of the proximal convoluted tubules was caused by ischaemia. More specifically, toxicity was related to the avian renal vascular anatomy, whereby a renal portal blood supply exists viz. venous blood originating from the hind-quarters co-perfuses the kidney with arterial blood from the aorta. A further uniqueness of this system, is the presence of the renal portal valve in the *v. iliaca communis*, which appears to control the shunting of venous blood from the hind limbs to the vena cava, thereby bypassing the cranial renal lobe in times of stress.

In the theory put forward, it was suggested that the valve could be under prostaglandin control and that diclofenac (a potent cyclooxygenase inhibitor) would potentially induce a change in the valve functionality with the net effect being the shunting of blood away from the cranial renal lobe resulting in hypoperfusion, ischaemia and necrosis of this lobe. While the theory appears plausible, the *valva renalis portalis* has only been described in a small number of other bird species such as the chicken (*Gallus domesticus*) and ostrich (*Struthio camelus*), which actually has six *valvae renales* (de Carvalho, et al. 2007). The aim of this study was to evaluate the renal anatomy and related vasculature of the Cape griffon vulture (*Gyps coprotheres*) (CGV), which is senstive to the toxic effects of diclofenac. Special attention is also being given to comparisons with the anatomy of the domestic chicken.

This study made use of 13 CGVs. Six specimens were freshly perfused with formalin within minutes of being euthansed. In all cases, the birds were euthanised on the recommendation of the treating veterinarian due severe orthopaedic injuries. The birds were otherwise deemed to be healthy. For the histological portion of the study, evaluations were made of both stored samples in the bank at the Section of veterinary pathology of the University of Pretoria, while renal and associated vascular tissue from two of the freshly fixed birds were prepared using standard H&E techniques. The other seven were recovered dead in the field. Of these four were prepared for skeletal evaluation, and the remainder used for vascular casting.

The kidneys of the CGV were present within the *fossae renales* and were well attached to the synsacrum and the *ilium*, and was trilobular. While this was similar to the chicken, the divisions with their connective tissue capsule in the vulture was much more prominent than in the chicken. The vasculature was also almost identical to the domestic chicken, with the only differences being at the entrance of the *v. portalis renalis caudalis* and the exit of the *v. renalis caudalis* into the *v. iliaca communis* on the right. The *valva renalis portalis* was also present in same location described in the chicken with a similar appearance viz. the valve was present in the *v. iliaca communis* between the *v. renalis caudalis* and the *v. renalis cranialis* and appeared as conical shaped, with finger-like processes.

Histologically, the CGV kidney was similar to that to other avian spp, with reptilian, mammalian and intermediate nephrons being evident. The kidney also had the expected appearance with the cortex consisting of the glomeruli and the medulla being made up of medullary cones. On cross-section the renal portal valve was composed of smooth muscle finger-like projections that protruded into the lumen of the lumen of the *v. iliaca communis*. The valve was well vascularised and was associated with a nerve plexus. While the plexus could not be conclusively associated with the valve, the renal portal valve is the only intravascular smooth muscle structure that has been described to have sympathetic and parasympathetic innervation.

Based on the findings of this study, the proposed mechanism of toxicity of diclofenac is anatomically possible. The similarity of the chicken and vulture in their anatomical structure may also explain previous finding that the chicken could serve as a physiological model of the study of the pathophysiology of diclofenac's toxicity.

Ⅴ. Table of Contents

VI. List of Tables

VII. List of Figures

xi

xii

xiii

xiv

xvi

xvii

xviii

VIII. **Abbreviations**

A.	Artery
Aa.	Arteries
CGV	Cape griffon vulture
COX	Cyclooxygenase 1 or 2
DCV	distal convoluted tubule
Dex.	Dextra
H&E	Haematoxylin and Eosin
NSAID	Non-steroidal anti inflammatory drug
PCT	Proximal convoluted tubule
R.	Ramus
Rr.	Rami
Sin.	Sinestra
Sp.	Species
V.	Vein
Vulpro	Vulture Conservation Programme of South Africa
Vv.	Veins

IX. Scientific and Common Names of Species

Common Name	Scientific Name
African elephant	*Loxodonta africana*
African white-backed vulture	*Gyps africanus*
Anna's hummingbird	*Caypte anna*
Bearded vulture	*Gypaetus barbatus*
Black vulture	*Coragyps atratus*
Cape griffon vulture	*Gyps coprotheres*
Collared dove	*Streptopelia decaota*
Coot	*Fulica atra*
Desert quail	*Callipepla gambelii*
Domestic chicken	*Gallus domesicus*
Domestic goose	*Anser domesticus*
Domestic pigeon	*Columbar domestica*
Dromedary camel	*Camelus dromedaries*
Egrets	Family *Aerdidae*
Egyptian vulture	*Neophron percnopterus*
Eurasian griffon vulture	*Gyps fulvus*
Perching birds	Family *Passeriformes*
Gray partridge	*Perdix perdix*
Great kiskadee	*Pitandgus sulphuratus*
Herons	Family *Ardeidae*
Holland honeyeater	*Phylidonyris novaehollandiae*
Hooded vulture	*Necrosyrtes monachus*
Hooded vulture	*Necrosyrtes monachus*
Hornbill	Family *Bucorvus*
Ibis	Family *Tresliornidae*
Japanese quail	*Coturnix coturnix japonica*
Killdeer	*Charadrius vociferous*
Kiwi	Family *Apterygidae*
Lappet-faced vulture	*Aegypius monachus*
Little wattlebird	*Anthochaera lunulata*

Common Name	Scientific Name
Long-billed vulture	*Gyps indicus*
New-world vultures	Family *Cathartidae*
Northern pintails	*Anas acuta*
Old-world vultures	Family *Accipitridae*
Oriental white backed vulture	*Gyps bengalensis*
Ostrich	*Struthio camelus*
Owl	*Athene noctua*
Palm-nut vulture	*Gypoherax angolensis*
Raptors	Family *Raptidae*
Red-tailed hawk	*Buteo jamaicensis*
Rhesus monkey	*Macaca mulatta*
Rock dove	*Columba livia*
Rüppel's griffon vulture	*Gyps rueppellii*
Slender-billed vulture	*Gyps tenuirostris*
Spiny-cheeked honeyeater	*Acanthogenys rufogularis*
Springbok	*Antidorcas marsupialis*
Storks	Family *Ciconiidae*
Turkey	*Meleagris gallapavo*
White backed vulture	*Gyps bengalensis*
White-fronted honeyeater	*Phylodonyris albifrons*
White-headed vulture	*Trigonoceps occupitalus*
Wildebeest	*Connochaetes* spp.
Zebra	*Equus* spp.

Latin Names	*English Names*
Acetabulum	Acetabulum
Ala (pars) postacetabularis ilii	Postaetabular ilium
Ala (pars) preacetabularis ilii	Preacetabular ilium
Ala ischia	Ischium
Anastomosis cum vena mesenterica caudalis	Anastamosis of the caudal mesenteric veins
Anastomosis interiliaca	Anastamosis of the common iliac trunks to form the caudal vena cava (iliac anastamosis)
Aorta descendens	Descending/ caudal aorta
Apex pubis	Tip of the pubic bone
Areae articulares vertebrae	Atricular surface of the vertebre
Arteria adrenalis	Adrenal artery
Arteria caudalis coxae	Caudal coccix artery
Arteria femoralis	Femoral artery
Arteria iliaca externa	External iliac artery
Arteria iliaca interna	Internal iliac artery
Arteria ischiadica	Ischiadic artery
Arteria ovarica	Ovarian artery
Arteria renalis caudalis	Caudal renal artery
Arteria renalis cranialis	Cranial renal artery
Arteria renalis media	Middle renal artery
Arterioles interlobulares	Interlobuar arterioles
Arterioles intralobulares	Intralobular arterioles
Arteriola glomerularis afferens	Afferent arteriole
Arteriola glomerularis efferens	Efferent arteriole
Canalis (sulcus) iliosynsacralis	Iliosacral canal
Canalis synsacri (canalis vertebralis)	Vetrebral cnal (synsacral canal)
capsule glomerularis	Glomerular (Bowman's) capsule

Latin Names	English Names
circulus (venous) portalis renalis	Venous portal circulation
complexus juxtaglomerularis	Juxtaglomerulous complex
Corpus ilii	Body of the ilim
Corpus ischia	Body of the ischium
Corpus pubis	Body of th pubis
Corpus pygostyli	Body of the pygostyle
Corpus synsacri	Body of the synsacrum
Corpusculum renale	Renal corpuscle
Cortex renalis	Renal cortex
Costae	Ribs
Crista dorsolateralis	Dorsolateral crest
Crista dorsolateralis ilii	Dorsolateral crest of the ilium
Crista iliaca dorsalis	Dorsal iliac crest
Crista iliaca intermedia	Intermedite iliac crest
Crista iliaca lateralis	Lateral iliac crest
Crista iliaca oblique	Oblique iliac crest
Crista iliosynsacralis	Iliosynsacral crest
Crista spinosa (crista dorsalis sysacri)	Spinous crest (dorsal crest of the synsacrum)
Crista ventralis	Ventral crest
Divisio renalis caudalis	Caudal renal lobe/ division
Divisio renalis cranialis	Cranial renal lobe/ division
Divisio renalis media	Middle renal lobe/ divison
Epitheliocytus maculae densae	Macula densa cells
Extermitas caudalis synsacri	Caudal border of the synsacrum
Extremetas cranialis synsacri	Cranial border of the synsacrum
Extremitas caudalis	Caudal border
Extremitas cranialis	Cranial border
Facies ventralis	Ventral surface
Facies articularis femoralis	Surface that articulates with the femoral head
Facies articularis intercostalis	Surface that articulates with the ribs

Latin Names	English Names
Facies dorsalis	Dorsal surface
Facies dorsalis synsacri	Dorsal surface of the synsacrum
Facies lateralis	Lateral surface
Facies lateralis synsacri	Lateral surface of the synsacrum
Facies renalis ilii	Renal surfae of the ilium
Facies ventralis	Ventral surface
Facies ventralis ilii	Vental surface of the ilium
Facies visceralis synsacri	Visceral serface of the synsacrum
Fascies articularis cranialis	Cranial articular surface
Fascies lateralis	Lateral surface
Fascies medialis	Medial surface
Fenestra ischiopubica	Ischiopubic fenestrations
Fenestrae intercristales	Fenestrations between crests
Fenestrae intertransversariae	Fenestrations between transverse processes
Foramen acetabula	Acetabular foramen
Foramen obturatum	Obturator foramen
Foramina intervertebralia	Intevertebral foramina
Fossa iliaca dorsalis	Dorsal iliac depression
Fossa iliocaudalis	Caudal iliac depression
Fossa renalis	Renal depression
Glomerulus	Glomerulus
Ilium	Iliim
Incisura acetabularis	Acetabular notch
Ischium	Ischium
lobulus renalis	Renal lobule
macula densa	Macula densa
Margo cranialis	Cranial border
Margo cranialis	Caudal border
Margo lateralis	Lateral border
Margo medialis	Medial border
Medulla renis	Renal medulla

Latin Names	*English Names*
Membana basilaris	Basal membrane
Mesangiocytus intraglomerularis	Mesangial cells
Nephron	Nephron
Nephron corticale	Cortical (reptilian) nephron
nephron juxtamedullare	Juxtamedullary (mammalian) nephron
Os coxae	Bones of the pelvis
Osteum cloacale ureteris (cloaca)	cloaca
Pelvis renails	Renal pelvis
Peritubulare corticale	Peritubular cortex
Plexus renales	Renal plexus
Podocytus	Podocytes
Processus antitrochantericus	Antitrochanter
Processus costis	Costal procress
Processus terminalis ischia	Ischial process
Processus transversus	Transverse process
Proessus obturatorius	Obturator process
Pubis	Pubis
Pygostylus	Pygostyle
Rete capillare glomerulare	Capillary plexus of the glomerulus
Spina dorsolateralis ilii	Dorsolateral ilial spine
Synsacrum	Synsacrum
Systema portale renale	Renal portal system
Tubulus contortus distalis	Distal convoluted tubule
tubulus contortus proximalis	Proximal convoluted tubule
tubulus distalis	Distal tubule
tubulus proximalis	Proximal tubule
ureter pars pelvica	Pelvic part of the ureter
ureter pars renalis	Renal part of the ureter
ureter pars renalis rami ureterici secundarii	Secondary branches of the renal ureter
ureter pars renalis rami ureterici primarii	Primary branches of the renal ureter
ureter pars renalis rami ureterici tertiarii	Tertiary branches of the renal ureter
Valva renalis portalis	Renal portal valve

Latin Names	English Names
Vena cava caudalis	Caudal vena cava
Vena femoris	Femoral vein
Vena iliaca communis	Common iliac trunk
Vena iliaca externa	External iliac vein
Vena iliaca interna	Internal iliac vein
Vena ischiadica	Ischiadic vein
vena metatarsalis dorsalis	Dorsal metatarsal vein
Vena portalis renalis caudalis	Caudal renal portal vein
Vena portalis renalis cranialis	Cranial renal portal vein
Vena renalis caudalis	Caudal renal vein
Vena renalis cranialis	Cranial renal vein
Venae intervertebrales	Intervertebral veins
Venae intralobulares	Intralobular veins
Venae ovaricae	Ovarian veins
Venae renales craniale	Cranial renal veins
Vertebrae caudales	Caudal vertebrae
Vertebrae thoracicae et sacrales	Thoracic and sacral vertebrae

1: Introduction

1.1. Vultures

Vultures are large, volant birds which are classically regarded as raptors (family *Raptidae*). However, unlike eagles, hawks and similar birds of prey in the family *Accipitridae*, vultures rarely (if ever) rely on predation as their food supply is derived from carrion in the veld (Mundy et al., 1992). They are morphologically characterised by their long necks covered in downy feathers, large leathery skinned heads and clumsy claws (Mundy et al., 1992). Vultures are divided into two main groups based on their evolutionary lineage and geographical location. The Old-world vultures (*Accipitridae*), which are considered to be distant relatives of eagles, are typically found in Asia, Africa and Europe, while the New-world vultures (*Cathartidae*), which are considered distant relatives of storks (family *Ciconiidae*), are found across the Americas (Mundy et al., 1992). Both families share an almost global endangered status (Anon, 2011).

1.2. The Cape griffon vulture

Eleven vulture species can be found across the African continent, namely the Egyptian vulture (*Neophron percnopterus*), Bearded vulture (*Gypaetus barbatus*), Cape griffon vulture (*Gyps coprotheres*), Rüppell's griffon vulture (*Gyps rueppellii*), African white-backed vulture (*Gyps africanus*), White-headed vulture (*Trigonoceps occipitalis*), Lappet-faced vulture (*Torgos tracheliotus*), Eurasian griffon vulture (*Gyps fulvus*), Cinereous vulture (*Aegypius* monachus), Hooded vulture (*Necrosyrtes monachus*) and the Palm-nut vulture (*Gypohierax angolensis*). However, only seven of these species are endemic to Africa (Anderson et al, 2002). The Egyptian vulture is only found as a migratory visitor to northern Africa, the Eurasian griffon vulture is a localised visitor that is extinct within Africa and the Cinereous vulture is considered a vagrant in northern Africa (Anderson et al, 2002). Of all these vulture species, only the Cape griffon vulture (CGV) is endemic to southern Africa and has the smallest known distribution of any of the Old-World vultures (Figure 1-1), which is approximately 12% of the southernmost landmass of the African continent (Mundy et al., 1992).

1
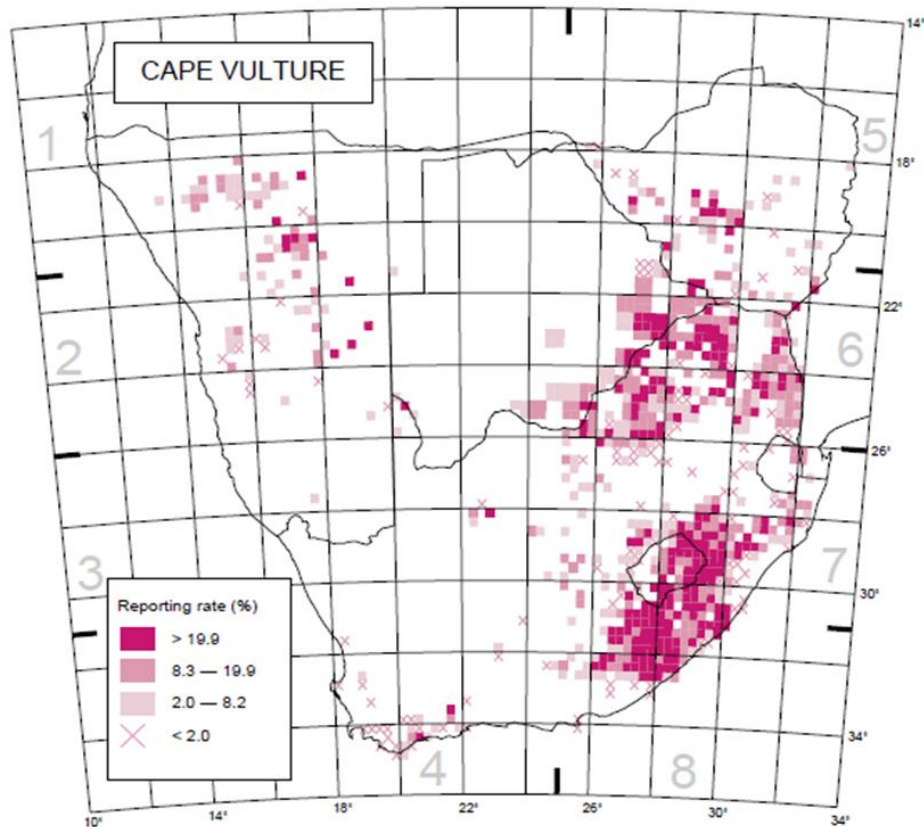
Figure 1-1: Graphic Distribution of *Gyps coprotheres* in southern Africa (excerpted from Mundy et al. 1997).

The species was first described by the early Cape settlers in 1652 with over 100 000 breeding pairs being reported, ranging from Table Mountain in Cape Town to the rest of southern Africa (Mundy et al,. 1992). Today the CGV is a red-listed endangered species, with only 2500 breeding pairs still believed to be in the country (Anon, 2011).

The CGV is the third largest of all the vulture species, with the Cinereous vulture being the largest (Mundy et al., 1992) (Figure 1-2). The average CGV has a body length of 1.10 m, a wingspan of 2.55 m, a weight of 9.35 kg and a bill length of 0.54 m (Mundy et al., 1992). More recent research has shown that these birds can reach a mass of up to 15 kg body weight (Naidoo, 2011, personal communication). Similar to other vultures, the CGV scavenges almost entirely on the soft tissues of carcasses, such as the muscle tissue and viscera (Mundy et al., 1992). These birds appear to be unable to tear the skin of a carcass unless the skin has been opened by the Lappet-faced vulture (Mundy et al., 1992) or mammalian scavengers.

2

Figure 1-2: An adult Cape griffon vulture (G. coprotheres) feeding at a vulture restaurant in South Africa. Evident in the picture is the long mainly featherless necks.

The Lappet-faced vulture is an Old-World vulture, and has a continent-wide distribution in Africa (Mundy et al., 1992). In the absence of Lappet-faced vultures or mammalian scavengers, the CGV will gain entry into a carcass by stabbing at orifices until they access the softer internal tissues (Figure 1-3). Mundy et al. (1992) noted that one major change in the behaviour of the CGV has been their feeding habits. Two hundred years ago, the birds were known to feed on the carcasses of dead migratory herbivores such as zebra (genus *equus*), springbok (genus *antidorcus*) and wildebeest (genus *connochaetes*), as well as the occasional elephant (genus *loxodonta*) or ostrich (*Struthio camelus*) carcass (Mundy et al., 1992; Mundy et al., 1997). However, with a large portion of South Africa under extensive farming practices, the CGV has become reliant on more artificial feeding systems (known colloquially as "vulture restaurants") where livestock carcasses are provided by conservationists (Gilbert et al., 2007; Deygout et al., 2009).

3

Figure 1-3: Picture showing a Cape griffon vulture trying to feed on a carcass via an orifice, since the carcass skin in still intact.

Mundy et al. (1992) studied the life and reproductive cycles of the CGV, and a brief summary follows below. The CGV displays an unusual reproductive cycle when compared to other bird species, as they only reach breeding maturity at six to seven years of age when full adult plumage and the tell-tale yellow eyes are attained. Once the birds have reached sexual maturity, they appear to pair for life. Nesting and egg lay is strictly confined to cliff ledges, with an average of one egg, with a mean incubation period of 57 days (Mundy, 1982), being produced during the breeding season (Robertson, 1986). Nesting material is collected from 10 weeks before the average laying date (Robertson, 1986). It has, however, been noted on occasions of egg infertility, for the breeding pair to produce a second egg within the same year (Robertson, 1986; Mundy, et al. 1992). Both parents care for the egg and hatchling, feeding it bill-to-bill until the chick fledges after a mean nesting period of 148-150.3 days (Robertson, 1986). In contrast, most other raptors mature at an earlier age and produce clutches of chicks (Mundy, et al. 1997). It is not known how long the adult CGV survives for in the wild.

4

1.3. The Vulture Crisis

1.3.1. *The Vulture Crisis in Asia*

Of all the vulture species globally, three have received a large degree of media exposure in the last few years, namely the Oriental white-backed vulture (*Gyps bengalensis*), the long-billed vulture (*Gyps indicus*) and the slender-billed vulture (*Gyps tenuirostris*) (Green et al., 2007; Cuthbert et al., 2011). These three vultures have declined in Eastern Asia by more than 99.9% over the past 15 years (Cuthbert et al., 2011) with the consequence they all are threatened with extinction (Green et al., 2007; Cuthbert et al., 2011). Initially, the reason for their decline was unknown with many proposed aetiologies, such as heavy metal toxicities, West Nile Viral infections and carbamate or organophosphate intoxication (Satheesan, 2000; Pain et al., 2003). However, Oakes et al. (2004) conclusively demonstrated that diclofenac, a non-steroidal anti-inflammatory drug (NSAID), was the cause of the widespread devastation of the vulture population across the Indian subcontinent. Furthermore, it was also demonstrated that the primary food source of these vultures (dead live-stock) was contaminated with varying concentrations of diclofenac (Green et al., 2007). Diclofenac was banned from importation and manufacture on the veterinary market in India in 2006 (Kumar, 2006).

The toxic effects of diclofenac were reproduced under experimental conditions in two other *Gyps* species (*G. africanus* and *G. coprotheres*) in South Africa, as well as in the domestic chicken (*Gallus domesticus*) (Swan et al., 2006; Naidoo et al., 2007), with similar clinical signs and pathological changes as seen in the vultures in eastern Asia. These clinical signs were characterised as depression and change in mentation of the birds within 24 hours post-exposure, with the birds eventually succumbing to coma and death within the next 24 hours. On necropsy, the lesions were characterised by severe visceral and articular gout with massive disruption of the normal architecture of all the major organs (Naidoo et al., 2007).

1.3.2. *Diclofenac*

Diclofenac functions in mammals through the inhibition of both the cyclooxygenase-1 (COX-1) and cyclooxygenase-2 (COX-2) enzyme systems, thereby decreasing concentrations of prostaglandins within the body (Pountos et al., 2011). Clinically this NSAID has the beneficial effects of the suppression of pain, fever and inflammation (Burke et al., 2005).

5

However, this general inhibition of the prostaglandins within the body can result in numerous side effects as these autocoids are also protective of the gastric mucosa (by reducing acid secretion and stimulating mucus production) as well as being protective of renal functioning (by modulating renal perfusion) (Pountos et al., 2011).

1.3.2.1.   Toxicity in Birds

Diclofenac is an integral part of gout management in humans through the modulation of uric acid transporters (organic anionic cassette of transporters) at the level of the nephron (Burke et al., 2005). In an unusual contrast the drug has been implicated as a cause of visceral gout in vultures (Naidoo & Swan, 2008) through an unknown mechanism. Current evidence tends to suggest that toxicity is purely secondary and results from the incidental exposure of the birds to diclofenac through the meat consumed (Oakes et al., 2004). Diclofenac was the most widely used veterinary NSAID in cattle in Eastern Asia due to a combination of effectivity and affordability as a result of governmental subsidy (Cuthbert et al., 2007; Green et al., 2007). Cattle are considered holy animals under the Hindu faith, thus precluding slaughter in cases of disease or injury. They are therefore treated in a palliative manner until death occurs (Harris et al., 1966). As a result, one in 200 carcasses contained residues of diclofenac, which was sufficient to cause the resultant devastation amongst the vulture population (Green et al., 2007). Other NSAIDS such as ketoprofen (Naidoo et al., 2010a; Naidoo et al., 2010b) and flunixin (Cuthbert et al., 2007; Zorilla, et al., 2014.) have since also been shown to be toxic in vultures.

1.3.2.2.   Pathophysiology in Vultures

Despite the vultures exposed to diclofenac displaying visceral gout and acute renal failure at death, the pathophysiology behind this phenomenon remains unknown (Oakes et al., 2004). Meteyer et al. (2005) presented histopathological evidence of acute necrosis of the proximal convoluted tubules in the kidney with absence of glomerular lesions in early mortality in conjunction with minimal inflammatory changes. It was suggested that the toxicity results from ischaemic renal necrosis through the inhibition of prostaglandin synthesis (cyclooxygenanse inhibition) with subsequent opening of the *valva renalis portalis* and shunting of venous blood away from the cranial lobe of the kidney (Meteyer et al., 2005). Despite the proposed theory being plausible, it is based on the anatomy and physiology of other avian species, i.e. no evidence is available to support the presence of the *valva renalis*

6

portalis in the CGV, even though its presence in other bird species tends to suggest that it will be present. As a first step in further evaluating the role of the circulatory system in diclofenac-induced toxicity, the gross anatomy and histology of kidneys of the CGV needs to be established.

7

2. Justification

2.1.Literature Review

The anatomy and physiology of the kidney from numerous avian species has been extensively studied (Nicholson, 1982; Nicholson & Kendall, 1983; Warui, 1989; Casotti et al., 1998; Casotti et al., 2000; Almansour, 2007; de Carvalho et al., 2007; Cazmir et al., 2008) with most focus on the domestic fowl due to its importance as a global food source (Gilbert, 1954; Akester, 1964, 1967; Akester & Mann, 1969; Siller & Hindle, 1969; Shimada & Sturkie, 1973; Warui & King, 1985; Casotti & Braun, 1995; Islam et al., 2004; Naidoo et al., 2007). As a result of the intensification of farming practices required to meet global demand, numerous diseases and disease processes have become part of the farming process (Witter, 1976). One of the most important and common conditions in chickens fed diets high in protein and calcium is gout (Peterson et al., 1971; Guo et al., 2005). Gout in chickens is characterised by hyperuricaemia and subsequent precipitation of urate tophi (crystals attached to protein) in the tissues and joints (Scott, 1978). With uric acid excretion and plasma uric acid concentration being linked to renal function, much research has focused on the structure and function of the chicken kidney. These include gross anatomical studies (Hodges, 1974; Johnson, 1979); contrast radiographic studies of the *systema portale renis* (Akester, 1964); light microscopic morphometry (Warui, 1989); stereological observations of the kidney using Alcian blue and Gomori's trichrome stains (Warui & King, 1985); transmission electron microscopy (Nicholson & Kendall, 1983; Casotti & Braun, 1995); and mathematical modelling of urine concentrating mechanisms (Layton et al., 2000).

The results from the above-mentioned studies have also been used extensively in evaluating the anatomical structure of other species such as the Desert quail (*Callipepla gambelii*) (Casotti & Braun, 1995), Anna's hummingbird (*Caypte anna*) (Casotti et al., 1998), new Holland honeyeater (*Phylidonyris novaehollandiae*), little wattlebird (*Anthochaera lunulata*), white-fronted honeyeater (*Phylidonyris albifrons*), spiny-cheeked honeyeater (*Acanthogenys rufogularis*) (Casotti & Richardson, 1993), Japanese quail (*Coturnix coturnix japonica*) (Cazimir et al., 2008) and northern pintails (*Anas acuta*) (Sherrill et al., 2001).

For the literature review which follows, the domestic chicken has been used as the reference species, as it has been studied in the most detail. Furthermore, it has been validated as a suitable model to study the mechanism of toxicity in the *Gyps spp.* (Naidoo et al., 2007).

8

2.1.1. *Osteology Associated with the Avian Kidney*

The avian kidney is described as being firmly attached to the pelvis, with the majority of the kidney lying within a depression known as the *fossa renalis*. Only the cranial portion of the kidney lies outside of the *fossa renalis* and lies wthin a shallow depression on the ventral surface of the preacetabular ilium. Not surprising, due to the close relationship of the kidney with bone, the shape and size of the kidney is in large determined by the shape of the bony cavity in which it lies. The *renal fossa* is comprised of the *synsacrum* and the *os coxae* (Baumel et al, 1993):

- The <u>*synsacrum*</u> is a rigid unit consisting of ankylosed vertebrae in mature birds. This includes one to several preacetabular thoracic vertebrae, and the lumbar verterbrae which are attached to the preacetabular ilium; the true acral vertebrae that lie directly opposite the acetabulum; and one to several proximal *vertebrae caudales* that are postacetabular (Nickel et al, 1977, Baumel et al, 1993, Lamagère, 2011). Interspecies variation exists in the number of vertebrae forming the *synsacrum*. The *synsacrum* is synostosed on each side with the *os coxae*. The latter occurs during skeletal maturation with the transverse processes of the synsacral vertebrae coalescing with the lateral borders of the *os coxae*, to produce a continuous transverse *lamina* on each side. While the fusion is prominent, it is incomplete and contains the *fenestrae intertransversariae*, which are traversed by nerves and vessels. The dorsal spinous processes of the synsacral vertebrae also ankylose to form a crest known as the *crista spinosa* (*dorsalis*) *synsacri*. The *canalis synsacri* (*vertebralis*) which runs through the centre of the *synsacrum* contains the lumbosacral intumescence of the spinal cord, an enlarged chamber. The ventral surface of the *corpus synsacri*, formed by consolidated vertebral bodies of the synsacrum, has a deep depression on each side of the midline known as the *fossa renalis* in which the kindey is partly accommodated. The *fossa renalis* is also partly formed through the fusion of the *os coxae* (mainly *ilium*) and the *synsacrum* Baumel, et al, 1993).

- The *os coxae* is formed by the fusion of the *ilium*, *ishium* and *pubis* (Nickel, et a, 1977; Baumel et al, 1993). The *corpus ilii* is the strongly developed flat bone comprising the main body of the *ilium* from which the pre- and postacetabular alae (wings) arise (Baumel et al, 1993). The *crista iliaca dorsalis* is the dorsomedial

9

border of the preacetabular *ilium*. Areas where the preacetabular *ilium* articulate with the transverse processes of the cranialmost series of synsacral vertebrae are known as *areae articulares vertebrales*. These articulations can only be seen in immature specimens where the *synsacrum* and *ilium* are disarticulated. Dorsally, the lateral free edge of the preacetabular *ilium* has a pronounced edge, the *crista iliaca lateralis*. The *os ischium* is a long bony plate (Nickel et al, 1977). Cranially it participates in the formation of the *acetabulum*, while its postacetabular dorsal border forms part of the *foramen ischiadicim*. Caudally the *ischium* fuses with the *ilium*. The *ilium* forms the ventral border of the *foramen ischiadicum* (Nickel, et al, 1977). The *os pubis* in most birds is delicate and parallel to the ventral border of the *ala ischii.* In the domestic fowl it is fused with the os *ishium* below the acetabulum (Nickel, et al, 1977) .The pelvis is formed by the consolidation of two *os coxae* and the *synsacrum*.

2.1.2. *Topography and Gross Morphology of the Avian Kidney*

The avian kidney, while historically compared to the mammalian kidney, differs greatly in its structure (Johnson, 1979):

- Similarities: Both the avian and mammalian renal systems consist of paired, retroperitoneal kidneys (King & McLelland, 1984), paired ureters and the associated blood vessels (Johnson, 1979). Internally, the avian kidney is also composed of a *cortex renalis* and *medulla renalis* (Hodges, 1974; Johnson, 1979).

- Differences: Unlike the mammalian kidney where the *cortex renalis* and *medulla renalis* are clearly defined, the avian *cortex renalis* and *medulla renalis* are randomly interspersed in cones throughout the kidney (Johnson, 1979). Additionally, the avian kidney does not possess a *pelvis renalis* (King & McLelland, 1984) and the collecting ducts join to form larger papillary ducts, which drain directly into ureteral branches at the tip of each medullary pyramid (Johnson, 1979; King & McLelland, 1984). These ureteral branches eventually coalesce along the length of the kidney to form the ureter (Johnson, 1979), which leaves the kidney as the *ureter pars pelvica* (Johnson, 1979) to join the *urodeum* (Inoue, 1953; Goodchild, 1969; Johnson, 1979). The ureter enters the cloaca at an oblique angle as a mucosal duct and forms a sac-like pocket in the mucosal wall, which functions as a pseudo-sphincter (Inoue, 1953). The most significant macroscopic difference to mammals is the presence of a renal portal

10

vasculature system in *aves* (Nickel et al., 1977; Johnson, 1979; King & McLelland, 1984; King, 1993).

The avian kidney is divided into three lobes, *divisio renalis* cranialis, *divisio renalis media* and *divisio renalis caudalis*, and is partly situated intra-pelvically in the *fossa renalis* of the synsacrum and the depressions in the *ilium* of the pelvis (Nickel et al., 1977; Johnson, 1979; King & McLelland, 1984; King, 1993); and partly extra-pelvically, with the cranial lobe abutting the lungs at the level of the thoracic vertebrae T6-T7 (Johnson, 1979; King, 1993). In the domestic fowl, the *arteria (A.) iliaca externa* and *ischiadica* form boundaries between the *divisio renalis cranialis* and *divisio renalis media*, and the *divisio renalis media* and *divisio renalis caudalis* respectively (Nickel et al., 1977; Johnson, 1979; King & McLelland, 1984; King, 1993) ("division" and "lobes" are used synonymously in literature). The *lobi renales* are joined by parenchymatous bridges (Nickel et al., 1977) with the nerves and blood vessels commonly traversing the divisions (Johnson, 1979). Not all bird species display three lobes. Two lobes have been described for the hornbill (family *Bucorvus*) (Feinstein, 1962); four lobes in long billed species such as storks (family *Ciconiidae*), herons (family *Ardeidae*), egrets (family *Aerdidae*) and ibis (family *Tresliornidae*) (Johnson, 1979; King, 1993); and five lobes in the kiwi species (family *Apterygidae*) (Kurod, 1963). However, this is often misleading, as structures crossing the kidney (for example blood vessels or ureters) may give the impression of external divisions without internal divisions being present (Johnson, 1979; King, 1993). The external surfaces of the avian *renal lobes* are covered with small round projections, which represent the *lobuli renales* reaching the cortical surface. These projections are roughly 1-2mm in diameter in the domestic fowl (King & McLelland, 1984). There are currently no reports on the topography and gross morphology of the vulture kidney.

2.1.3. *Histology of the Avian Kidney*

The mammalian kidney is comprised of a well-differentiated central *medulla renalis* (medullary area) surrounded by an outer *cortex renalis* (cortical area) (Johnson, 1979). In contrast, the avian kidney is comprised of multiple *lobuli renales* each consisting of an inner *medulla renalis* arranged in cones and an outer *cortex renalis* (Casotti et al., 2000). The kidney in the majority of avian species is approximately 70-85% *cortex renalis* and 5-15% *medulla renalis* (Warui, 1989) and the blood vessels constitute the remaining percentage. The most extreme exception to this generalization was found in the Anna's hummingbird, in

11

which 90% was *cortex renalis*, 8% vasculature and 2% *medulla renalis* (Casotti et al., 1997). It was suggested that this adaptive change may be related to the high liquid diet these birds were accustomed to, and that they therefore had less need to conserve water and consequently possessed less medullary tissue than birds living in arid environments or consuming water-poor diets (Casotti et al., 1997). In comparison to the kidneys of desert-dwelling birds, it was noted that the kidneys comprised approximately 5% more *medulla renalis* than that of non-desert dwelling birds (Warui, 1989). This finding corresponds with a well-recognised phenomenon in mammals in which the percentage of medullary tissue is directly related to the required degree of urine concentration (Johnson, 1974; Casotti et al., 1997). For example, in the Rhesus monkey (*Macaca mulatta*), which exists in a habitat in which fruit and water are readily available, the *medulla renalis* was found to constitute only 14% of the kidney (Tisher, 1971), whereas the camel (*Camelus dromedaries*) which lives in arid conditions, possesses a *medulla renalis* which constitutes 38% of the kidney (Abdalla & Abdalla, 1979; El-Gohary et al., 2011). With vultures being carnivorous, and their behaviour of finding a water source from which to drink and wash themselves after feeding is well described, it seems likely that they may display a similar cortico-medullary ratio to the majority of avian species described.

2.1.3.1. The Lobus Renalis and Lobulus Renalis

The *lobus renalis* (*diviso renalis*) is comprised of a *medulla renalis* and a *cortex renalis* (Figure 2-1) (King, 1993; Casotti et al., 2000). As mentioned above, the *lobus renalis* is not the anatomical functional unit of the avian kidney, but one based on structures crossing the ventral kidney surface. The anatomical functional unit is the *lobulus renalis*. The *lobulus renalis* is that division of the kidney, which contains all a regions' nephrons which share a common *ureter pars renalis rami ureterici secundarii* (secondary branch of the ureter) (Figure 2-1).

Anatomically the *lobuli renales* consists of a portion of the *cortex renalis* and its medullary cones. The medullary cone is best defined as a collection of a *lobuli renales* collecting ducts and loops of Henlé as they all lead to a common primary branch of the ureter (Siller & Hindle, 1969; Johnson, 1979; Casotti et al., 2000) (Figure 2-1). The medullary cone is surrounded by a connective tissue sheath (Hodges, 1974; King, 1993). The cortical region of a *lobulus renalis* surrounds a central *vena intralobularis* (Figure 2-3) (King, 1993). The

12

cortical portion of the *lobulus renalis* does not, however, have a connective tissue sheath, and adjacent cortical regions overlap and blend together (Figure 2-1) (Hodges, 1974). Due to the overlap of cortical tissue and the lack of clear connective tissue boundaries, Johnson (1979) defined the avian renal lobe as the group of medullary cones which typically drain into a *ureter pars renalis rami ureterici secundarii*, and the *cortex renalis* that is associated with these cones (Figure 2-1).

In cross-section the *lobulus renalis* consists of a *vena interlobularis* (central efferent vein), surrounded by a ring of the large *juxtamedullare glomeruli* of the mammalian *nephron juxtamedullares* lying closest to the *venae intralobulares* (Johnson, 1979). The *glomeruli* of the reptilian *nephron corticales* are the most peripheral of the *glomeruli* present in *cortex renalis* of the *lobulus renalis* (Figure 2-1). In contrast to the *nephron juxtamedullare*, the entire *nephron corticale* is contained within the *cortex renalis*. The *a. intralobularis* (afferent artery) and in combination with branches of the *v. renalis portales*, referred to as the *v. interlobularis*, gives rise to the *rete capillare peritubulare corticale*, which supplies a mixture of venous and arterial blood to tubules within the *lobulus renalis*, before draining into the *v. intralobularis* (Figure 2-2) (Siller & Hindle, 1969).

13
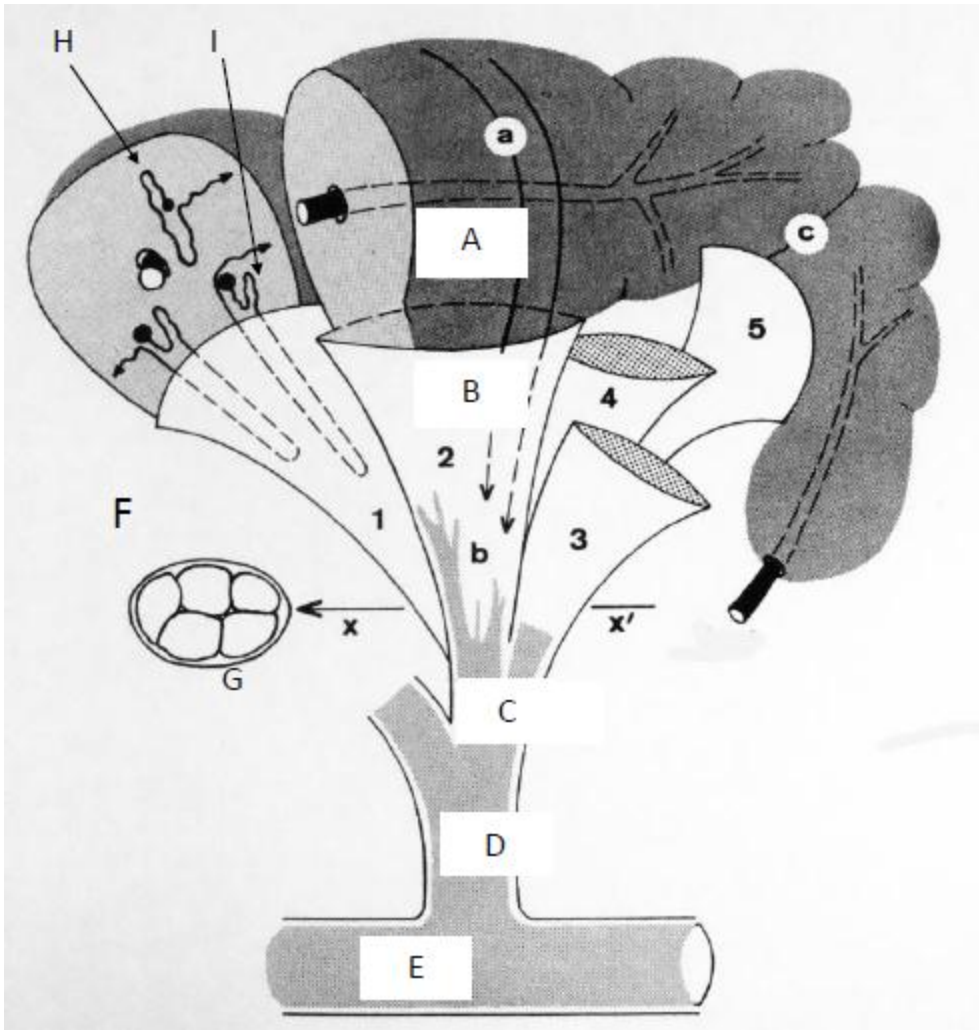
Figure 2-1: Schematic representation of lobar and lobular renal architecture (adapted from Johnson, 1979). The diagram shows a secondary ureteral branch draining a group of five *lobuli* renales (1-5), together forming one lobe. Each *lobulus renalis* is comprised of a cortical region (A) and a medullary region (B) (medullary cone). Label (c) indicates division of cortex renalis between two *lobuli renales*, secondary branch or the ureter (C); Primary branch of the ureter (D); Ureter (E); Medulla renalis (F); Cross section of the medullary cone (G); Loopless or reptilian nephron (H); Looped or mammalian nephron (I)(The loopless nephron are completely cortical, while the looped portion of the mammalian nephron extends into the medulla renalis.)

14
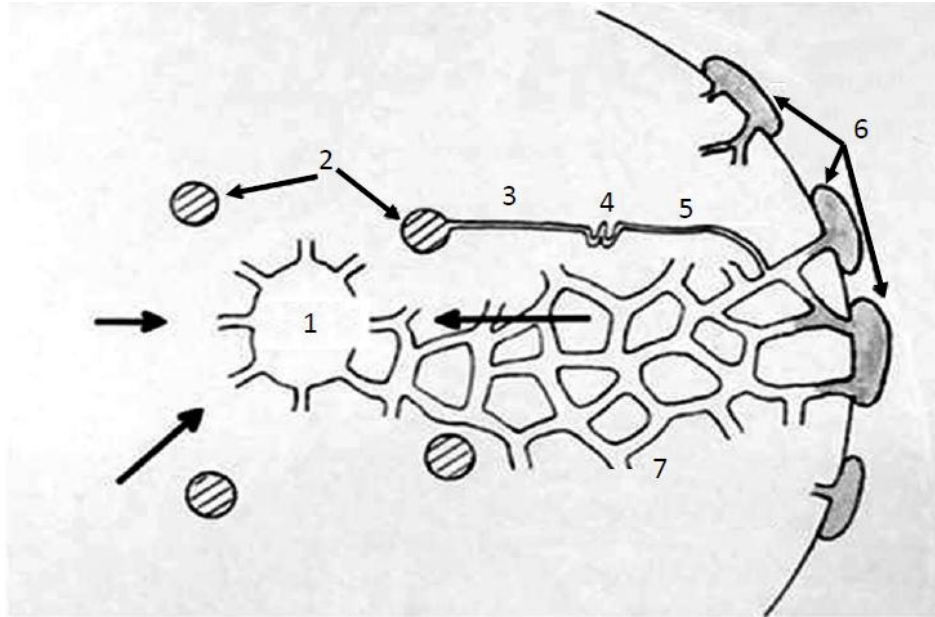
Figure 2-2: Schematic representation of the cortical blood supply (adapted from Johnson, 1979). 1: v.
intralobula*ris***; 2:** *a. intralobularis***; 3:** *a. glomerulris afferens***; 4:** *rete capillare glomeralare***; 5:** *a. glomerulris*
*afferens***; 6: Branches of the** *v***.** *portales renales* **also reffered to by some authors as the** *v. interlobularis***; 7:**
*rete capillare peritubulare corticale***). Four a.** *intralobulares* **are shown, which supply glomeruli with** *a.*
*glomerulris afferens***. Branches of the** *v***.** *portalis renales* **are perilobular. The** *rete capillare peritubulare*
corticale **surrounds and oxygenates the tubules of the nephron (not shown) and drains into the** *vena*
intralobularis **which lies centrally within the** *lobulus renalis***. Thick arrows indicate centripetal blood flow.**

2.1.3.2. *The Nephron*

The physiological functional unit of the kidney is the *nephron* (Hodges, 1974; Nabipour et
al., 2009). Histologically, the *nephron* represents the greatest point of difference between the
avian and mammalian kidney (Johnson, 1979). The avian kidney consists of both the
primitive (reptilian) *nephron* and the mammalian *nephron* with the loop of Henlé (Hodges,
1974; King, 1993; Nabipour et al., 2009). *Nephrons* are considered reptilian and loopless if
they are confined to the *cortex renalis* of the kidney and mammalian if a loop of Henlé passes
down into the *medulla renalis* (Figure 2-1) (King & McLelland, 1984). A third type, the
intermediate *nephron*, has also been described (Siller & Hindle, 1969). Part of this *nephron*
enters the *medulla renalis* for a short distance despite the loop of Henlé being absent (Siller &
Hindle, 1969). A *nephron* can consist of a single, unbranched tubule in the case of a cortical
(reptilian) nephron, or complex as in the case of a mammalian *nephron* (Johnson, 1979).

The *nephron* begins with a *corpusculum renalis* (renal corpuscle), which is the *glomerulus*
(network of capillaries) deeply embedded in the *capsule glomerularis* (Bowman's capsule),
and lies roughly midway between the *v. interlobularis* and *v. intralobularis* (King &
McLelland, 1984). The *capsule glomerularis* consists of a visceral layer of *podocytuum*
15

(podocytes), which are tightly connected to the basement membrane of the capillaries by multiple primary and secondary processes, and a parietal layer with flattened squamous epithelial cells displaying elongated nuclei (Cazmir et al., 2008). The podocytes' nuclei are oval, euchromatic and contain obvious nucleoli using standard Haematoxylin and Eosin (H&E) staining and light microscopy. The many processes give the podocytes a flattened appearance, with a single prominent area in the centre of the cell, which is occupied by the nucleus (Cazmir et al., 2008). A mass of basophilic *mesangiocytis intraglomerularis* (mesangial cells) at the centre of the corpuscle are responsible for the stability of the entire structure (Casotti et al., 2000; Cazmir et al., 2008). A complete *complexus juxtaglomerularis* (juxtaglomerular complex) is present in birds (King & McLelland, 1984). It includes the *macula densa* at the vascular pole of the renal corpuscle, which marks the origin of the *tubulus contortus distalis* (distal convoluted tubule) (Cazmir et al., 2008), and the secretory juxtaglomerular cells (modified myoepithelial cells) of the adjacent afferent arteriole (King & McLelland, 1984). The *tubulus contortus proximalis* (proximal convoluted tubule) is a continuation of the glomerular capsule and is the longest portion of the *nephron* (King and McLelland, 1984). The proximal convoluted tubule has a prominent brush-border and consists of columnar epithelial cells which appear eosinophilic under H&E staining (Casotti et al., 2000; Cazmir et al., 2008). Reptilian type proximal convoluted tubules can be divided into a thin and thick portion based on diameter of the tubule, whereas the mammalian proximal convoluted tubule can be divided into a convoluted portion and a straight portion, the transition between which occurs in the juxtamedullary *cortex renalis* (Johnson, 1979). The straight portion of the mammalian convoluted tubule tapers gradually to form a thin limb, and then very abruptly changes diameter to form a thick segment, which forms a nephronal loop of Henlé (Johnson, 1979). The thick loop returns to the *cortex renalis*, where it makes contact with its parent *glomerulus* (Johnson, 1979; Cazmir et al., 2008). The thick segment is approximately twice the width of the thin segment, both lined by cuboidal cells, with the staining intensity being more intense for the thick segments (Bacha & Bacha, 2005). The distal convoluted tubule begins at this point, and ends when it joins the collecting tubule (Johnson, 1979). The distal convoluted tubule is narrower in diameter and shorter in length (Johnson, 1979). The cells of both mammalian and reptilian distal tubules are cuboidal, stain eosinophilic with H&E, and do not have a brush border (Cazmir et al., 2008).

16

The arterial supply to the *glomerulus* enters via the *arteriola glomerularis afferens* and drains via the *arteriola glomerularis efferens* (Figure 2-3) (Casotti & Braun, 1995). The afferent arteriole has a thickened wall when compared to that of the efferent arteriole, and the oval, elongated nuclei of the juxtaglomerular cells can be seen along the wall of a short portion of the afferent arteriole (Cazmir et al., 2008).

2.1.3.3. Collecting Ducts and Ureters

The *tubulus distalis* (distal tubules) of the nephron form the *tubulus renalis colligens perilobularis* (perilobular collecting ducts) of the medullary cones, which open into the collecting tubules that run through the *lobulus renalis* and into *rami ureterici secundarii* (secondary ureteral branches), which coalesce to form *rami ureterici primarii* (primary ureteral branches) (Figure 2-1) (Johnson, 1979). A *pelvis renalis* (renal pelvis) is not present in birds. Instead, the *ureter pars renalis* arises from the coalescence of several primary ureteral branches within the cranial lobe of the kidney (Inoue, 1953; Johnson, 1979; King & McLelland, 1984). The ureter emerges from the kidney at the level of, or just caudal to, the boundary between the middle and caudal lobes of the kidney to become the *ureter pars pelvica* (Johnson, 1979).

The collecting ducts are lined by a simple cuboidal epithelium (Hodges, 1974; Johnson, 1979). As the collecting ducts emerge from the *medulla renalis*ry cones, their epithelium becomes stratified cuboidal before changing to the pseudostratified epithelium found in the ureteral branches (Johnson, 1979). As the branches coalesce to form the ureter, the walls thicken, and contain a stroma of connective tissue and circular smooth muscle that becomes thicker closer to and in the ureter (Johnson, 1979). The epithelium of the ureter is comprised of tall pseudostratified columnar cells which display multiple vacuoles containing mucopolysaccharides (Hodges, 1974). The *lamina propria* is thick and free of glands (King, 1993).

2.1.4. Blood Supply to the Avian Kidney

The avian kidney has a dual blood supply, namely an arterial and a portal system (Johnson, 1979; King & McLelland, 1984; Nabipour et al., 2009). Anatomists debated the existence of the *systema portale renis* in the avian for more than a century until it was conclusively identified in the domestic fowl (Sperber, 1949). These two systems give rise to an extensive

17

peritubular plexus (Figure 2-2) (Johnson, 1979). The plexus extends into the *cortex renalis* of the *lobuli renales* and supplies the reptilian nephrons and the cortical parts of the mammalian nephrons (Johnson, 1979; Casotti et al., 2000). Blood drains from the peritubular capillary plexus, cortical nephrons and portal system into a central efferent vein (*v. intralobularis*) situated in each medullary cone (Figure 2-2) (Johnson, 1979; King & McLelland, 1984). The v*enae intralobulares* converge to form an efferent renal radix (Casotti et al., 2000). Many radices are tributaries of the *vv. renales craniales* and *caudale*s which drain into the *vv. iliacae communii* and subsequently the *v. cava caudalis* (Casotti et al., 2000). Blood supply to a loopless nephron would thus flow from an *arterialis intralobularis*, which becomes an *arteriola glomerularis afferens* that leads to a *glomerulus*, and then into an *arteriola glomerularis efferens*, from which it will travel inwards (in a centripetal direction) along capillaries with blood from the portal system to the central vein (Figure 2-2) (Johnson, 1979).

2.1.4.1.   *Arterial Blood Supply to the Avian Kidney*

There are three pairs of renal arteries, namely the left and right *arteria (aa.) renales craniales, mediales* and *caudales* (King, 1993). All three *aa. renales* divide into primary, secondary and tertiary branches, which ramify throughout the kidney (Figure 2-3) (Siller & Hindle, 1969). In contrast to the mammalian kidney in which the arteries follow the lobar distribution of the branches of the ureter, the arteries in the avian tend to follow the distribution of the efferent veins throughout the kidney (Siller & Hindle, 1969; Johnson, 1979).

The left and right *aa. renales craniales* stem directly off the a*orta descendens* (Johnson, 1979; King, 1993); between the origin of the ventral mesenteric and femoral arteries (Siller & Hindle, 1969). The *aa. renales craniales* supply branches to the *glandulae adrenals* (*a. adrenalis*) and the *testes (a. testicularis)* in the male and a left branch to the *ovarium* (*a. ovarica*) in the female (Sperber, 1949). The *aa. renales craniales* give rise to small *divisia*r branches before dividing into three major branches which run in lateral, dorso-lateral and dorsal directions to supply the entire (Figure 2-3) (Siller & Hindle, 1969). The dorsal branch, which is hidden from view by the *vena (v.) renalis cranialis*, is very significant in that it provides the primary arterial blood supply to the ventral aspectof the *divisio renalis cranialis* before giving off braches supplying the uteri, *rami (Rr.) ureterici craniales*, and then

18

anastomosing with the ureteric branch (*Rr. ureterici medianes)* of *a. renalis mediana* (Siller & Hindle, 1969).

The *aa. renales craneles*, *mediales* and *caudales sin.* and *dext.* arise from the *aa. ischiadica sin.* and *dext.* respectively, as the *aa. ischiadiica* pass through the kidneys between the *lobales medales* and *caudales* en route to supplying the lower limb (Siller & Hindle, 1969; Johnson, 1979; King & McLelland, 1984; King, 1993). The *a. renalis mediana* curves cranially and crosses the *a. ischiadica* ventrally before dividing into two or more primary branches (Figure 2-3) (Siller & Hindle, 1969). These branches subdivide in the *divisio renalis media* (Siller & Hindle, 1969). As there is no distinct subdivision of the kidney into lobes or "divisions", the areas supplied by the *aa. renales craniales* and *caudales* tend to overlap (Siller & Hindle, 1969).

The *a. renalis caudalis* travels in a caudal direction to supply the *divisio renalis caudalis* (Figure 2-3). Ramifications of *a. renalis caudalis* penetrate the division between *divisio renalis media* and *divisio renalis caudalis* (Siller & Hindle, 1969). One of the caudo-medial branches anastomoses with the ureteric supply of the middle renal artery and forms an intricate arterial network around the ureter and its branches (Inoue, 1953; Siller & Hindle, 1969; Johnson, 1979). Siller & Hindle (1969) reported several variations to the arterial blood supply to the kidney, namely:

- the *aa. renales cranialis* may not arise directly opposite each other from the *aorta descendens*,
- an additional proximal renal artery was discovered on one side (right or left), providing arterial supply to the cranial lobe,
- the *Aa. renales medianes* and *caudales* may arise separately from the *A. ischiadica*,
- the *A. renalis caudalis* may arise from the middle sacral artery instead of the *A. ischiadica* on one side,
- an additional *A. adrenalis* may arise directly from the *aorta descendens*, instead of from the A. renalis cranialis.

Some anatomists, for example Sperber (1949), report that the *A. iliaca externa* supplies the kidney. However, it has since been shown that this vessel merely forms a division between

19

divisio renalis cranialis and *media*, and does not supply blood to the kidney (Akester, 1964; Johnson, 1979; King & McLelland, 1984; King, 1993).

As the *lobuli renales* are arranged randomly within the kidney, any branch of the *arteriae renales* may give rise to an *arterialis intralobularis* that supplies a *lobulus renalis* (Siller & Hindle, 1969; Johnson, 1979). The *arterialis intralobularis* enters at the base of the *lobulus renalis* and gives off several branches which run parallel to each other as they travel towards the apex of the *lobulus renalis* (Siller & Hindle, 1969; Johnson, 1979). These branches supply afferent arterioles to glomeruli along their course through the *lobulus renalis* (Siller & Hindle, 1969). The afferent arteriole is relatively short in the domestic fowl, and divides into glomerular capillary loops which surround a central mass of mesangial tissue (Siller & Hindle, 1969; Hodges, 1974; Casotti et al., 2000).

The glomerular capillary network is a branched network looped around the mesangium and differs according to the type of nephron it supplies (Johnson, 1979). The cortical reptilian nephrons are the smallest, and have a basic capillary arrangement consisting of an afferent arteriole which divides into two branches (Siller & Hindle, 1969). These branches form simple loops, which then re-join, forming the efferent arteriole (Siller & Hindle, 1969). The largest, juxtamedullary mammalian nephrons have a far more complicated arrangement in which the afferent arteriole divides into two branches with interconnecting bridges (Siller & Hindle, 1969). It is estimated that the glomerular capillary network in looped "mammalian"-type nephrons is approximately twice the size of that of "reptilian"-type nephrons (Casotti & Braun, 1995). The efferent glomerular arterioles arise from the coalescence of the glomerular capillary network and join the peritubular network of capillary sinuses along with blood from the *systema portale renale* (Siller & Hindle, 1969).

2.1.4.2.   The Systema portale renale

The *systema portale renale* is unique to *aves*, amphibiae, *pisceae* and *reptiliae* (Sturkie, 1986). By definition, a portal system is when an organ or organ system receives some of its blood supply through the venous system (Sturkie, 1986). In the domestic fowl, blood enters the *systema portale renale* via four routes, namely from the hind limb via the *vv. Iliacae externae* and *ishciadicae*, from the caudal pelvic region via the *vv. internae iliacae*, from the hind gut via the *vv. coccigiomesenteriae* and from the kidney itself via the *vv. renales* (Figure

20

2-3) (Akester, 1964; Hodges, 1974). The vessels merge to form two paired cranial *vv. renales portales craniales* and two paired *vv. renales portales caudales* (Akester, 1964). The *vv. renales portalis* enter the kidney and divide multiple times to become *vv. interdivisiare*s, supplying blood to the peritubular network of capillaries and finally ending as the small stellate veins of Spanner (Hodges, 1974).

The *v. renalis portalis cranialis* is considered to be a continuation of the v. *iliaca externa* and supplies the cranial lobe of the kidney (Akester, 1964). The *v. renalis portalis cranialis* is situated just caudal to the location of the *valva renalis portalis* (Figure 2-3) (Hodges, 1974). The *v. renalis portalis caudalis* proceeds caudally to supply the middle and caudal lobes of the kidney, and finally anastomoses with the contra-lateral *v. renalis portalis caudalis* caudal to the kidney (Akester, 1964). The venous branches from the hind limb, pelvis and caudal pelvic area are all tributaries of the *v. renalis portalis caudalis* (Figure 2-3) (Akester, 1964; Hodges, 1974; King, 1993). The *v. renalis* joins the *v. iliaca externa* before the *v. iliaca communis*, a common trunk formed by these two veins on either side unite along the midline to form the *v. cava caudalis* (Akester, 1964; King, 1993).

There is a great difference between venous blood sources for the two *vv. renales porales caudale*s. The *v. renalis portalis caudalis* receives blood from many areas, namely the pelvis, hind limb, pelvic viscera and abdominal viscera, whereas the *v. renalis portalis cranialis* only receives blood from the hindlimb (Akester, 1964; Johnson, 1979).
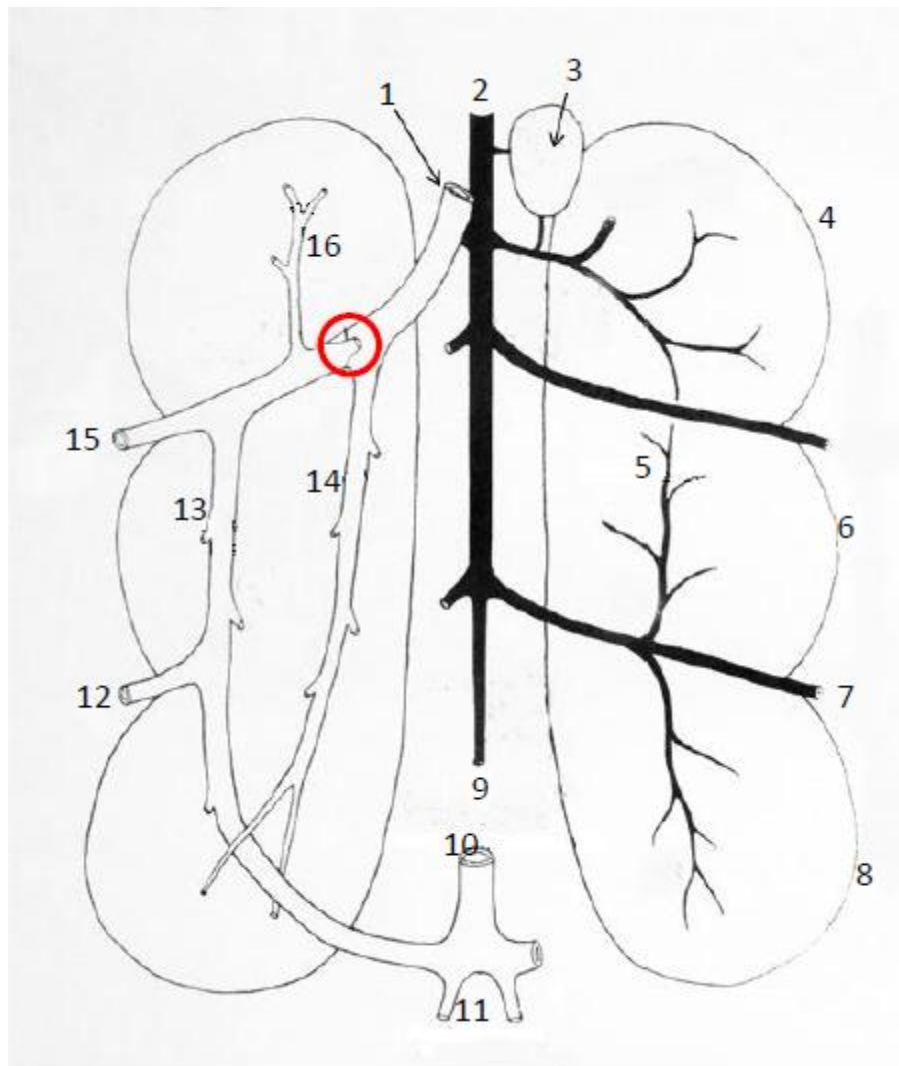
Figure 2-3: Schematic representation of the vasculature associated with the avian kidney and the location of the *valva renalis portalis* (adapted from Hodges, 1974). 1 *v. iliaca communis* formed by *v. iliaca externa* and *v. renalis caudalis*; 2: *Aorta descendens*; 3: *Glandus adrenalis*; 4: *Divisio cranialis*; 5: *a. media renalis*; 6: *Divisio renalis media*; 7: *a. schiadica*; 8: *Divisio renalis caudalis*; 9: *a. sacralis medialis*; 10: *v. coccygeomesenterica*; 11: *v. coccygii*; 12: *v. ischiadicia*; 13: *v. renalis portalis caudalis*; 14: *v. renalis caudalis*; 15: *v. iliaca externa*; 16: *v. renalis portalis cranialis*. The red circle indicates the position of the *valva renalis portalis* situated in the lumen of *v. iliaca externa*.

2.1.4.3.   The Renal Portal Valve

The *valva renalis portalis* is located in the lumen of the *v. iliaca communis* just proximal to the *v. renalis portalis cranialis*, and caudal to *v. renalis caudalis* (Figure 2-3)(Akester, 1964; Johnson 1979). In the domestic fowl, the *valva renalis portalis* is cylindrical, roughly 8mm long and consists of a single aperture valve that has a diameter of 1-2mm (Figure 2-4), and is said to be the only intravascular structure containing smooth muscle and a nerve supply (Akester, 1964). The *valva renalis portalis* consists of epithelioid cells, connective tissue and smooth muscle tracts (Gilbert, 1961). The valve is also well innervated and well vascularised

22

(Figure 2-5). In 1969, Akester notes that there is considerable innervation to the *valvus portalis renalis*. According to work published by Gilbert in 1961, there are large nerve trunks in the basal third of the valve that give off smaller nerve bundles that supply the middle third. Nerve fibres innervate the apical third of the valve. Earlier work by Spanner (1939) showed that apical third of the valve is comprised of epitheliod cells intersperced with collagen fibres and a few nerve fibres. Akester (1969) has since shown that smooth muscle cells are present throughout the entire valve and that the apical region is not entirely an epithelioid zone. Akester demonstrates that there is a fairly uniform distribution of smooth muscle throughout all parts of the valve. Unlike Gilbert 1961), Akester (1969) did not find large nerve trunks entering the base of the valve. Instead, he describes large isolated nerve trunks that do not enter the base of the valve and are not comparable by size or distribution to those described by Gilbert (1961). Peripheral ganglia innervating smooth muscle containing both adrenergic and cholinergic cell bodies which might be associated with small arteries near the valve might be a route by which the smooth muscle of the valve itself receives innervation. No large ganglia have been associated with any of the veins, although the veins have a moderate double innervation.
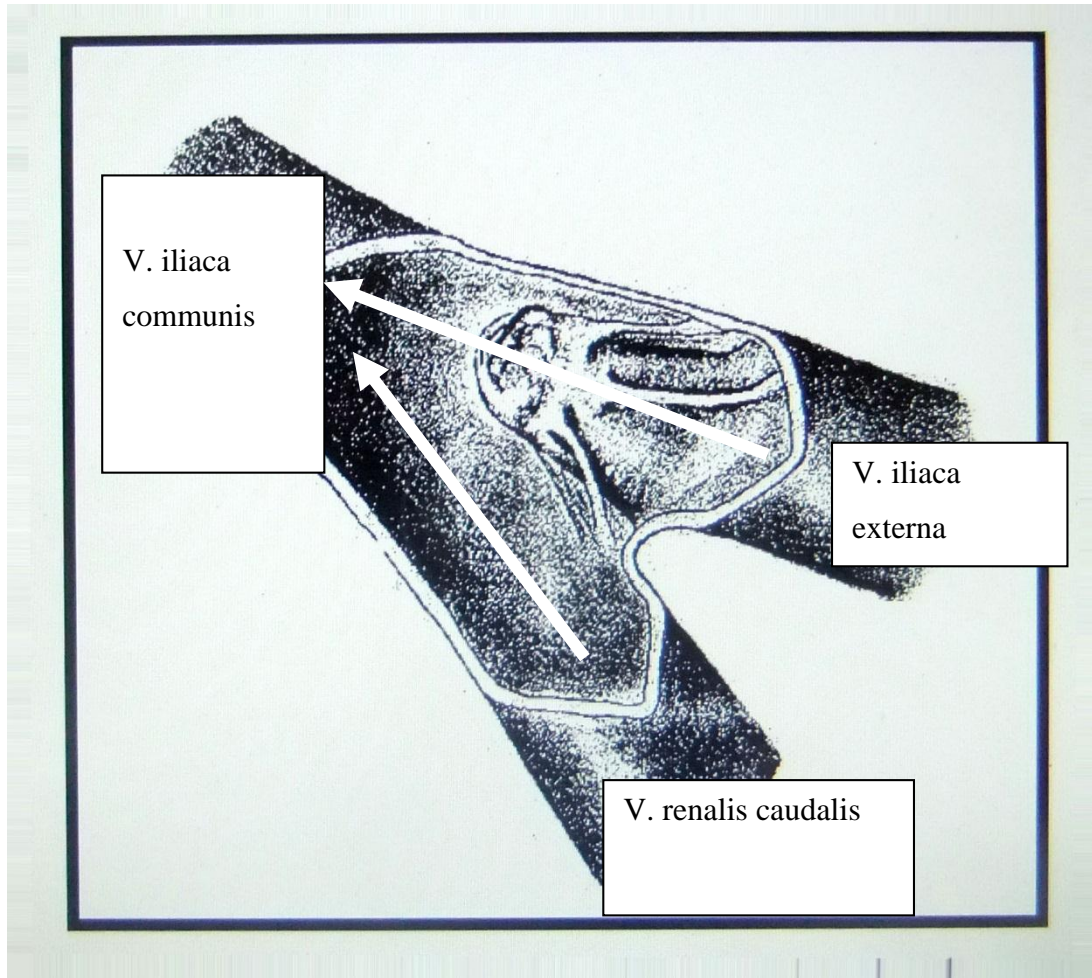
Figure 2-4: The Renal Portal Valve (adapted from Burrows et al., 1983). The *v. iliaca externa* (containing the *valva renalis portalis*) and the *v. renalis caudalis* merge to form *v. iliaca communis*. White arrows indicate the flow of blood when the *valva renalis portalis* is open.

24
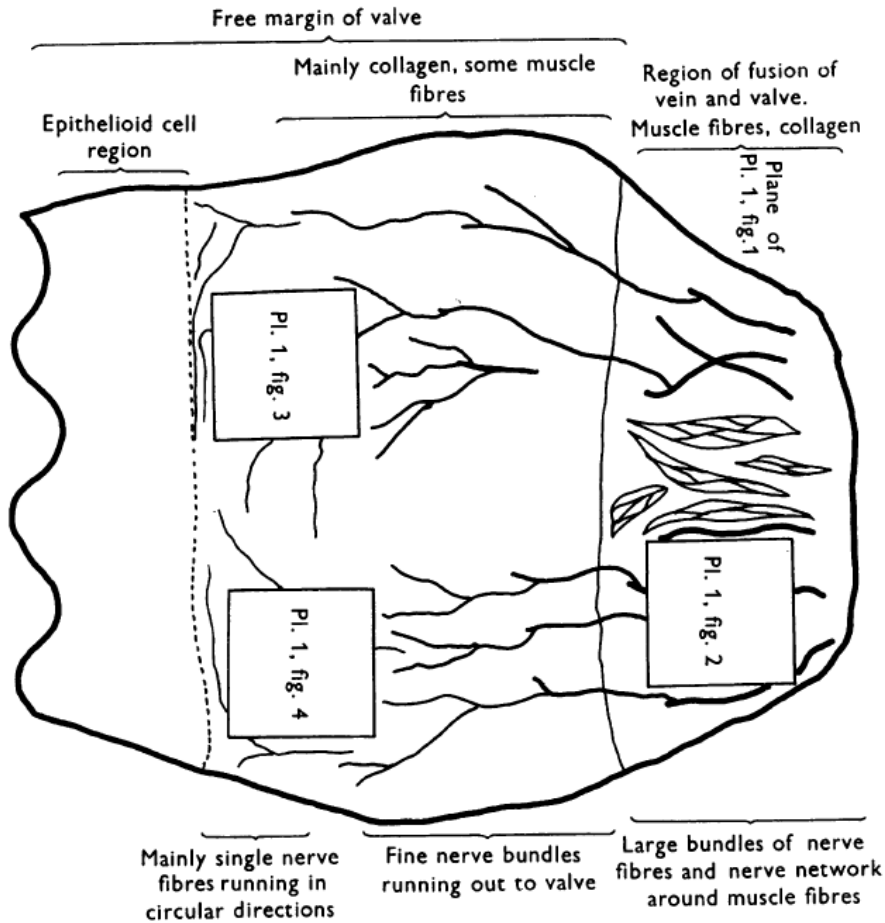
Figure 2-5: Diagram of the distribution of the nerve fibres of the renal portal valve, open along its ventral surface (Glibert, 1961)

It has been reported that when radiopaque fluid was injected into the *V. iliaca externa*, with the *valva renalis portalis* fully open, the fluid passed straight through the valve and into the caudal vena cava towards the heart, thus bypassing the *V. renalis portalis caudalis* (Figure 2-6) (Akester, 1964). With the valve closed, the radiopaque fluid entered the *V. renalis portalis cranialis*, and thus the cranial lobe of the kidney (Figure 2-7) (Akester, 1964). It was further noted that the radiopaque fluid was limited entirely to the kidney when the valve was completely closed or found in both the kidney and *vena cava caudalis* if the valve was partially open (Figure 2-8) (Akester, 1964). Through the functioning of the *valva renalis portalis*, the blood supplied by the *systema portale renalis* under normal conditions to the kidney can be diverted directly into the caudal vena cava (Akester, 1967).

25
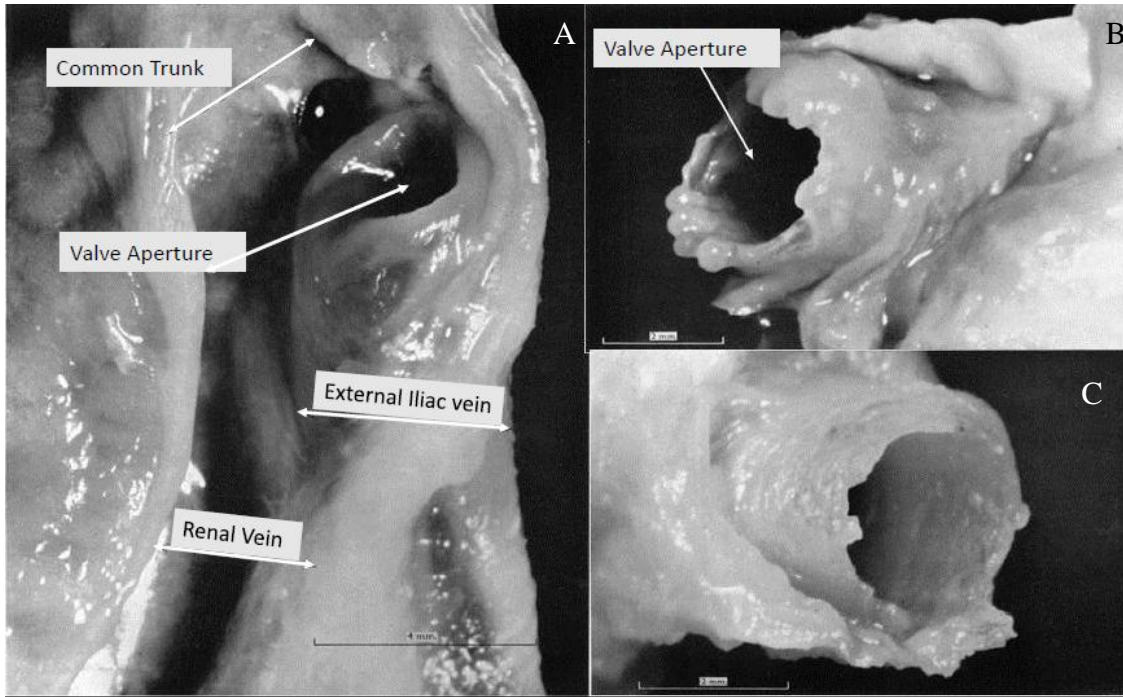
Figure 2-6: The Renal Portal Valve (valva renalis portalis) as described by Akester (1964) A. Shows the lumen of *v. renalis caudalis* that has been opened to expose the *v. renalis portalis caudalis*, which is meant to be protruding into the lumen of the *v. iliaca communis*. B. and C. show two *valvae renales portale*s with slight variation in *G.* domesticus.
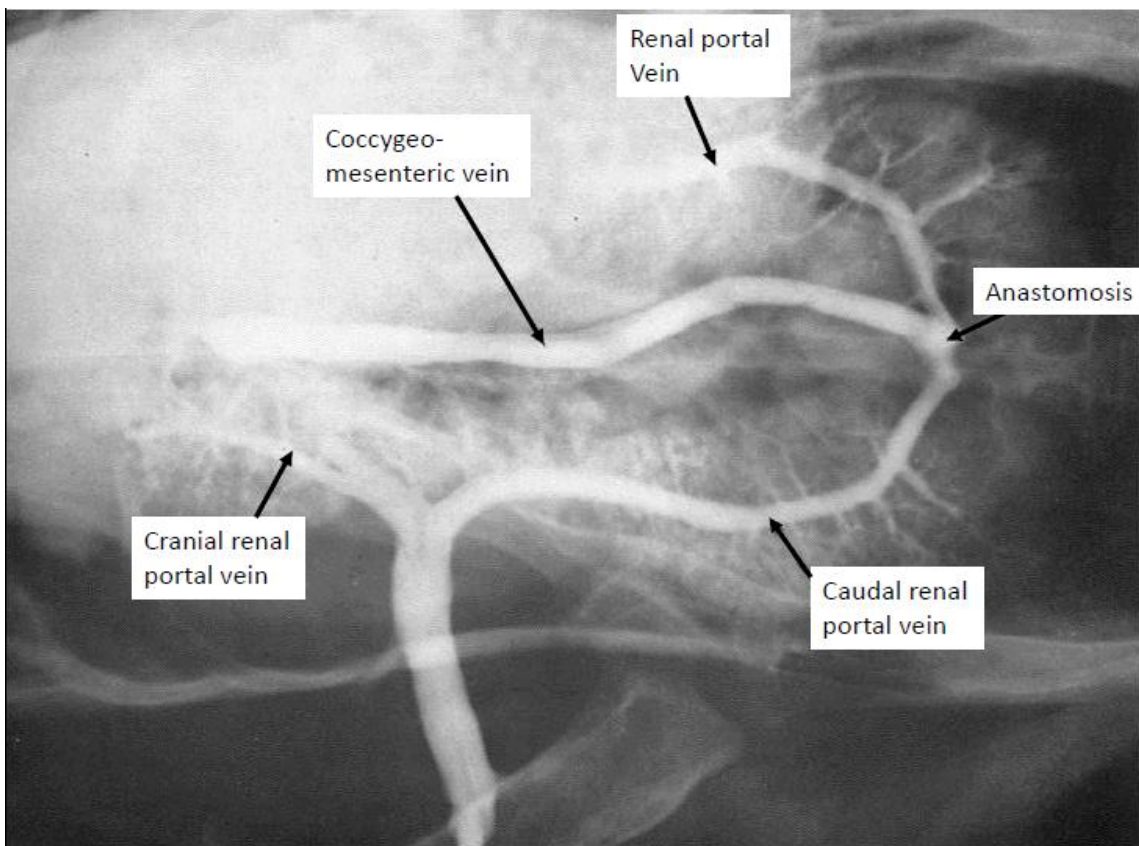
Figure 2-7: Contrast radiograph showing open *valvae renales portale*s allowing blood to move freely from the vv. *iliacae externae*, *renales porales caudales* and *renales caudales* into the *v. iliacae communii* and *vena. cava caudalis* (Akester, 1964).
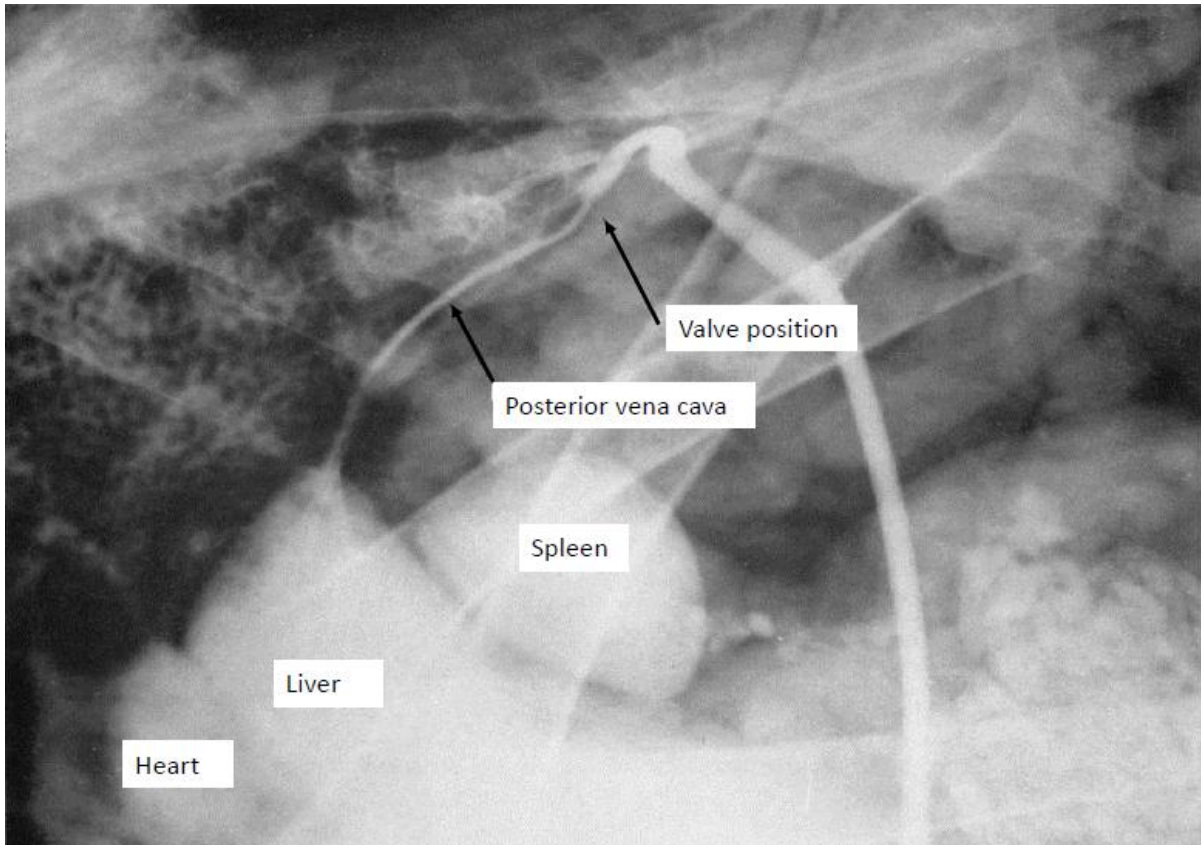
Figure 2-8: Contrast radiograph showing a closed *valva renais portalis* and reduced blood flow from the *v. iliaca externa*, *v. renalis caudalis* and *v. renalis portalis caudalis* into the *v. iliaca communis* and *vena cava caudalis* (*posterior)* (Akester, 1964)

2.1.5. *Vulture Renal Anatomy*

At present there are no studies describing the normal gross anatomy and histology of the kidney of any vulture species. The only studies pertaining to the renal system of the vulture are those which describe pathological changes following the numerous toxicological studies discussed above (Meteyer et al., 2005; Swan et al., 2006). In these studies, the vulture kidney demonstrated the standard three lobes (*cranialis*, *media* and *caudalis*) and the position in the *fossae renales* as described in the domestic fowl (Shimada & Sturkie, 1973; King & McLelland, 1984; King, 1993; Nabipour et al., 2009).

2.2. Research question

The anatomy and physiology of the *valve renalis portalis* and renal vasculature will shed light on the possible detrimental effecra of diclofenac on the Cape griffon vulture. .

2.3. Aim

The aim of this study is to evaluate the renal anatomy and related vasculature of the Cape griffon vulture which is sensitive to the toxic effects of diclofenac.

2.4. Objectives

The objectives of this study are the following:

- A comprehensive gross morphological and topographical description of the kidney of the Cape griffon vulture.
- A comprehensive histological description of the Cape griffon vulture kidney.
- A comprehensive morphological study of the renal vasculature, portal system and the *valva renalis portalis* in the Cape griffon vulture.
- A critical appraisal of the relative existing literature on the kidney and *systema portale renis* in birds.
- Correlation of the morphological characteristics in order to postulate function.
- Addition to the database of vulture biology for future comparative studies on these endangered birds and other *Raptidae*.

2.5. Benefits arising from the study

The envisaged benefits arising from this study are the following:

- Provision of a gross morphological and topographical description of the Cape griffon vulture kidney as a basis for future comparison with other vulture and raptor species,
- The establishment of a static template for future physiological and/or dynamic radiographic studies,
- The establishment of a database of normal histology to assist in the interpretation of pathological changes and/or in recognition of pathological changes,
- Postulation of functional anatomy, as it has been speculated that toxicity is believed to be closely related to the functioning of the *valva renalis portalis* and renal vasculature and
- Addition of knowledge to the database on the gross anatomy of the vulture that will later lead to more comparative studies on *Raptidae*.

28

3. Material and Methods

3.1. Experimental Animals

All animals used in this study were collected opportunistically, and represent injured birds for which euthanasia was recommended by the treating veterinarian at the Onderstepoort Veterinary Academic Hospital or dead birds found in the field. The birds in all cases originated from Vulpro, a vulture conservation organisation.

3.2. Sample Collection

Birds (n=6) were euthanized using pentobarbital at 1ml/kg of a 100mg/ml solution via a cannula placed in the *vena metatarsalis dorsalis*. Embalming fluid containing 10% formalin was introduced into the *systema portale renalis* via a catheter placed into the left ventricle (Rothwell, 1974). Birds were stored in a formalin tank at the Department of Anatomy and Physiology, University of Pretoria until evaluated. Due to the endangered status of the species, opportunistic collection was undertaken over several years. Of the six birds, two birds were used for histological evaluations as below.

Four adult carcasses found in the field following electrocution were prepared by boiling and defatting. The bones from one bird were unusable as the bird had severe osteodystrophy, and the carcass disintegrated upon processing.

Three additional carcasses that could not be preserved due to severe wound infection, fly strike and autolysis were infused with coloured latex for arterial and venous casts. For the arterial sample, arterial cannulation via the left ventricle and *aorta* (Siller & Hindle, 1969) was performed and coloured (red) latex forcefully injected. For venous casting, 18G Teflon catheters (Jelco) were inserted into each *V. iliaca externa* under a surgical dissection microscope (Zeis) (Akester, 1967) and coloured (blue) latex injected into each vein. The basic arrangement of the major blood vessels relevant to the vascularization of the kidneys was subsequently described, following the careful dissection of the tissue away from the hardened latex, also under a surgical microscope.

Four kidneys from two birds were freshly perfused using the first method mentioned above. Immediately post-perfusion, the kidneys were dissected free of the underlying structures and placed in 10% buffered formalin and used for histological examination.

29

Kidney samples from 7 birds (Naidoo, 2010[2]) were also used from the tissue bank of the Section of Pathology, Department of Paraclinical Sciences. The latter samples were collected during previous pathological evaluation by Prof N Duncan. The birds in question were euthanized through the administration of pentobarbitone (1ml/kg) into the *vena metatarsalis dorsalis*. Soon after euthanasia, a cross section sample was collected and placed into 10% buffered formalin. One sample was collected from each of the left and right kidney randomly.

3.3. Sample Evaluation

3.3.1. *Gross Morphology*

The vultures were opened by abdominal incision just cranial to the cloaca. The incision was extended laterally to the synsacrum and thereafter extended cranially to open the thoracic cavity. The covering abdominal organs were removed to expose the kidneys. Both kidneys were measured from the cranial to caudal poles to determine their length, and from the midline laterally to determine their width (Nabipour et al., 2009). Widths and lengths of the different lobes (cranial, middle and caudal) were also measured. All measurements were subjected to descriptive statistics in Excel (Microsoft Office 2010). Topographical positions of the lobes in relation to surrounding structures were described.

For the dissection of the *valva renalis portalis*, the kidneys were removed *in situ* following fixation, using the method described by Akester (1964) in the chicken. *V. renalis caudalis* was incised along its *facies ventralis* and the incision continued into the common trunk formed by the *v. iliaca externa* and *v. renalis portalis caudalis*, at the same location that *valva renalis portalis* was described in the chicken (Akester, 1964).

3.3.2. *Microscopic Evaluation*

Kidneys fixed in 10% buffered formalin were used. Sections from each lobe, ureter, *v. renalis portalis caudalis* and *v. iliaca externa* where they form the *v. iliaca communis*, and related structures were paraffin-fixed. For light microscopy, the protocols for the histopathology laboratory at the University of Pretoria were followed. All slides were first evaluated by a Specialist Pathologist (Prof N Duncan) to confirm the absence of overt pathology prior to histological descriptions.

30

3.4. Data Analyses

Arterial and venous supply to the kidney was digitally recorded and represented graphically by annotated sketches, macrographs, micrographs and diagrams. Macroscopic specimens were digitally photographed using a Canon 7D digital camera equipped with a Sigma 105mm Macro lens, described and annotated in Photoshop CS5. Smaller macro specimens were viewed with a Zeis surgical microscope, described and annotated in Photoshop CS5. Histological sections were viewed and digitally photographed using an Olympus BX63 light microscope equipped with a DP72 camera and Olympus CellSens imaging software, described and annotated in Photoshop CS5. When statistics were undertaken, all evaluation was undertaken using the analysis tool-pack addition on Microsoft Excel 2010.

3.5. Ethical Considerations

The collection of samples for this project was approved by the Animal Use and Care Committee (Animal Ethics Committee) of the University of Pretoria (SOP043-12). Research approval was also attained from South African Nature Conservation under the University's research permit (TOPS permit 07137)

4. Results and Discussion

4.1. Osteology of the Vulture

Four birds were boiled and defatted to obtain skeletal specimens. Of these, two were adults and two were sub adults. Of the two sub adults, one bird appeared to suffer from osteodystrophy, which resulted in the complete destruction of the bones during processing. On evaluation of the mid to caudal spinal column, the Cape griffon vulture had five free thoracic vertebrae, which was different to the chicken (Nickel et al, 1977) and turkey (*Meleagris gallapavo*) (Baumel et al, 1993) in which vertebrae T2 to T5 were fused. Caudally the fifth thoracic vertebra (T5) articulated with the synsacrum. While the presence of free thoracic vertebrae was also a feature of the Eurasian griffon vulture (Lamagère, 2011), the latter only had four free thoracic vertebrae (Figure 4-1). This also differed to the domestic goose (*Anser domesticus*), domestic fowl and domestic pigeon (*Columbar domestica*) where the synsacrum articulated with the sixth thoracic vertebrae (T6) (Nickel et al, 1977) (Figure 4-2). The synsacrum was fused to thoracic vertebrae six and seven, which were clearly identifiable as they articulated with the last two ribs (one full rib and one residual) (Figure 4-3). In two of the vulture specimens, the synsacrii at T6 had a ventral spinous process. The third bird differed slightly by having a residual ventral process on T7. This was in agreement with the Eurasian griffon vulture (Lamagère, 2011), where the last two thoracic vertebrae were fused to the synsacrum. However, unlike in the Cape giffon vulture, the Eurasian griffon vulture only had a ventral spinous process on T6 (Lamagère, 2011).
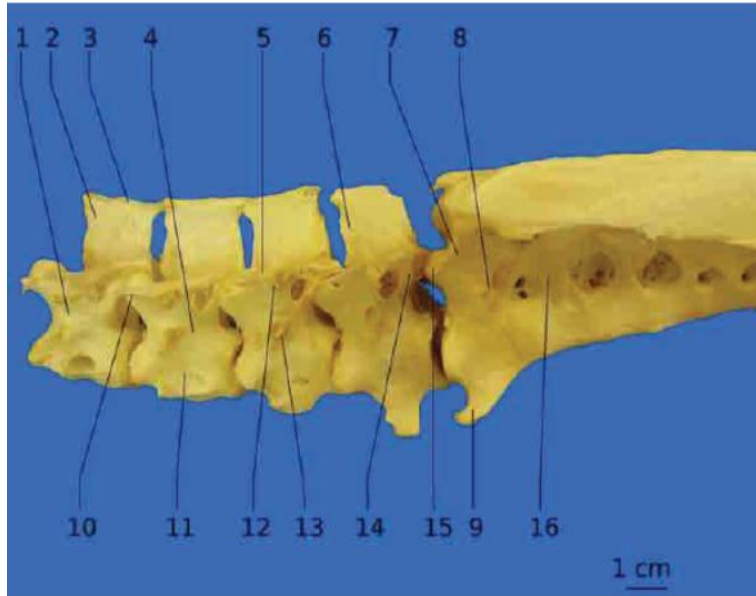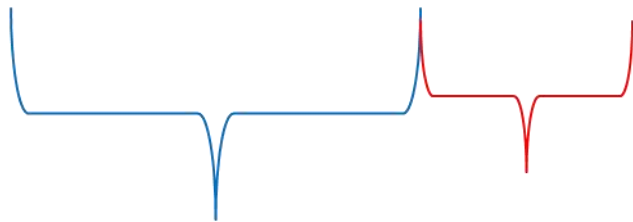
Figure 4-1: The synsacrum articulating with four thoracic vertebrae (labels 1 to 4) (blue bracket) in *G. fulvus* (adapted from Lamagère, 2011) with the latter two fused to the synsacrum (5&6) (red bracket) making six thoracic vertebra in this species (Left). In comparison *G. coprotheres* had five free thoracic vertebrae (blue bracket) and two fused (red bracket) making seven thoracic vertebrae (Right).

33
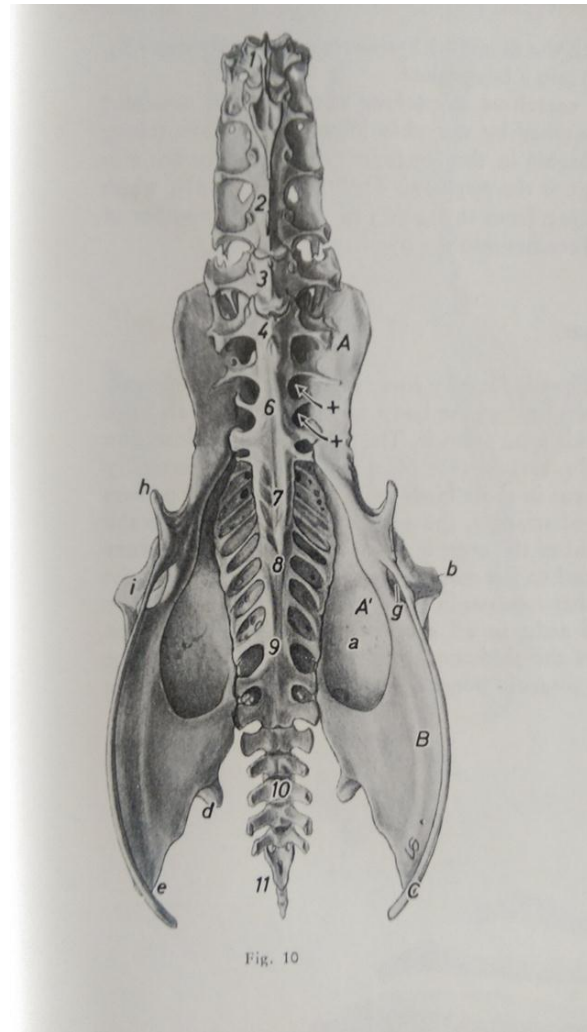
Figure 4-2: Comparison of the synsacrum and thoracic vertebrae of the Cape griffon vulture (left) next to an illustration from the domestic chicken (Right). The first five thoracic vertebrae are free while the last two are fused to the synsacrum in *G. corprotheres*. In the chicken, only thoracic vertebrae T1 and T6 (label 3) are free, while T2 to T5 are fused (Label 2). In addition only thoracic vertebra T7 (label 3) was attached to the synscarum in the *G. domesticus* (Nickel et al., 1977).

34
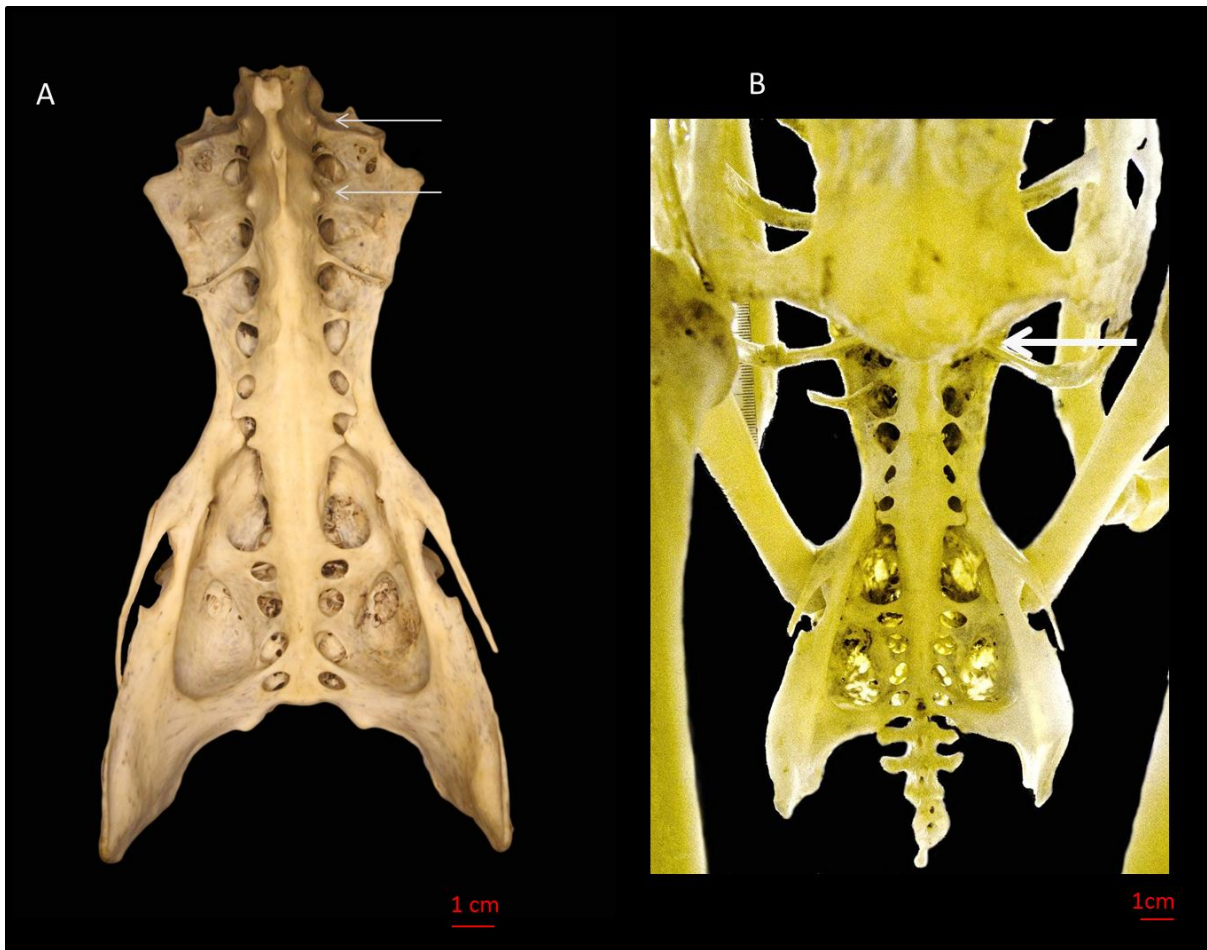
Figure 4-3: A- Cape griffon vulture synsacrum with the two articular surfaces for the last two ribs (Arrows). B- Assembled skeleton illustrating the articulation of the last two ribs with the synsacrum (Arrow). Of the two ribs, the last was a residual floating rib

The Sacrothoracic vertebrae were fused along their bodies (which, based on their transverse processes, appeared to be the fusion of five vertebral bodies) (Figure 4-5). The spinous processes of the synsacrothoracic vertebrae were fused dorsally to form a crest known as the *crista spinosa synsacri* (also called *crista dorsalis*) (Figure 4-4). The transverse processes of the synsacrothoracic vertebrae were also fused. Both the transverse process and dorsal processes were fused respectively with the medial and *margo lateralis*s of the preacetabular ileal wing. On the *facies ventralis*, the rib rudiments were present and attached to the vertebral bodies. Attached caudally to the sacrothoracic vertebrae by osseus fusion were the sacrolumbar vertebrae, which were also fused along their bodies. They were easily distinguished from the sacrothoracic vertebrae through the absence of rib rudiments and parapophyseal processes on their *facies ventralis* (Figure 4-5). The absence of the latter

35

structures gave formation to a dorsal space, in which part of the cranial lobe of the kidney lies (*fossae renalis*). The space was approximately 26.30 ± 1.20 mm.

Figure 4-4: Cranial view of the synsacrum. A - shows the fusion of the dorsal spinous process and transverse process of the synsacrothoracic vertebrae and the points of attachment with the pre-acetabular *ilium* (arrows) to form the *canalis iliosynsacrales* (c). The transverse (a) and dorsal spinous (b) process of the sixth thoracic vertebra (T6) can be clearly seen. B - shows the prominent crest formed by the fusion of the dorsal process of the synsacrothoracic vertebrae (Arrow)

36

The primary sacral vertebrae were caudal to the sacrolumbar vertebrae and also fused with the synsacrum (Figure 4-5). The primary sacral vertebrae were distinguished by the fusion of their parapophysis and diapophysis with the post-acetabular *ilium* (Figure 4-6). An interesting intra-species difference was present between the three birds in the number of the primary sacral vertebrae present, with one specimen having two and the others having three. This did not, however, result in a difference in the length of the pelvis, nor the angle of the pelvis. The sacrocaudal vertebra was followed by the primary sacral vertebrae which were distinguished by the fusion of their transverse process, and their articulation with the first coccygeal vertebrae (Figure 4-6). Six coccygeal vertebrae were present in the vulture, as described for other domestic bird species. The vertebrae articulated with one another through distinct transverse and spinous processes. The dorsal spines of the first coccygeal vertebrae were double while the remaining were just ridged, which is different to the fowl where all the dorsal processes were double. The articulating processes were prominent on the first four vertebrae and vestigial on the last two. The last two vertebral bodies had double ventral crests which was similar to the duck. The last coccygeal vertebra was the pygostyle, and was ploughshare in shape. While the pygostyle has been described as a fusion of a number of coccygeal vertebrae in the chicken, the points of fusion in the vulture specimens were not discernible. The spinal canal narrowed as it entered the pygostyle.

37
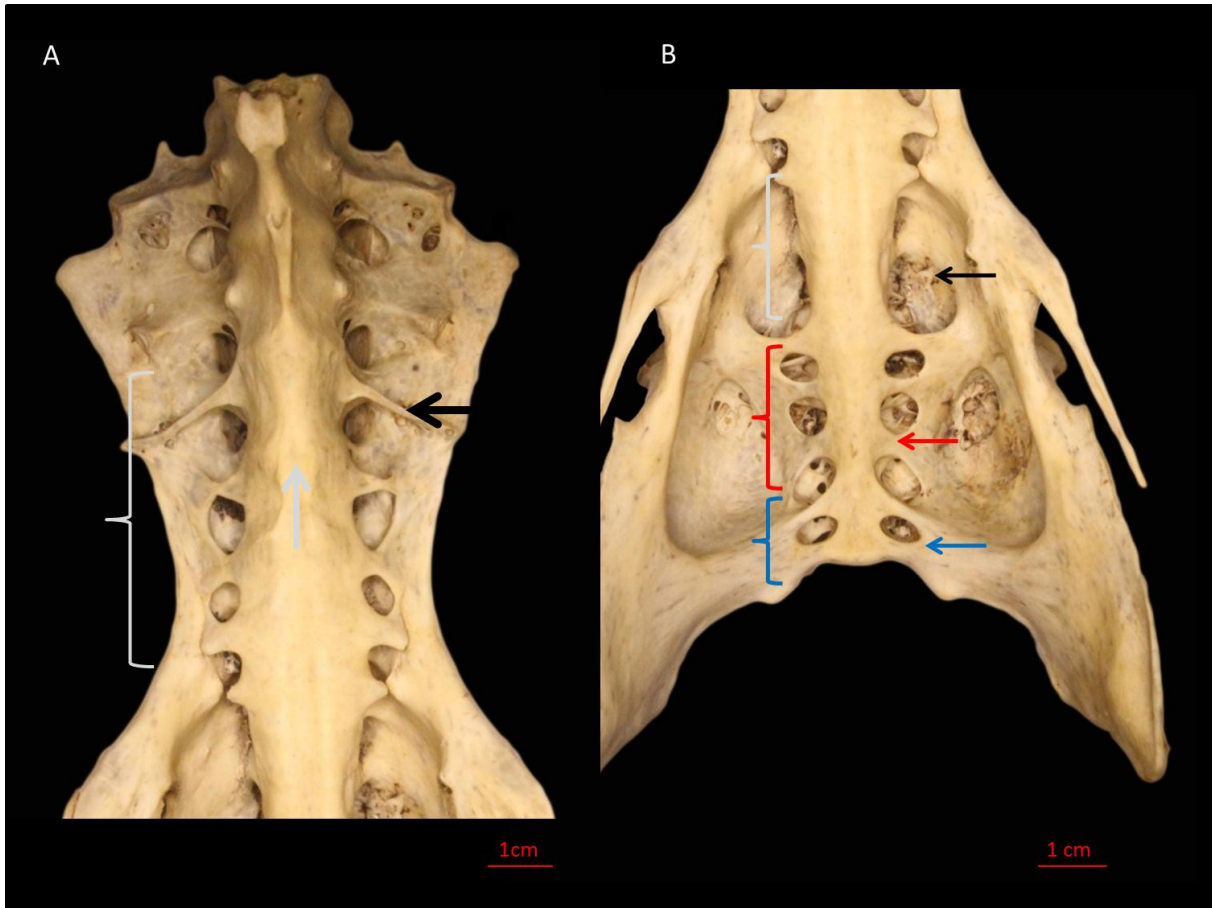
Figure 4-5: A- Ventral view of the sacrothoracic vertebrae (white bracket). Present are the residual rib remnants (dark arrow) and the fused ventral spinous processes (white arrow); B- Ventral view of the sacrolumbar vertebrae (white bracket), whose fused bodies don't have rib remnants and a hollow dorsal space (black arrow); ventral view of the primary sacral vertebrae (red bracket) and the fused parapophysis (red arrow) and the sacrocaudal vertebrae (blue bracket) with fused transverse processes (blue arrow)
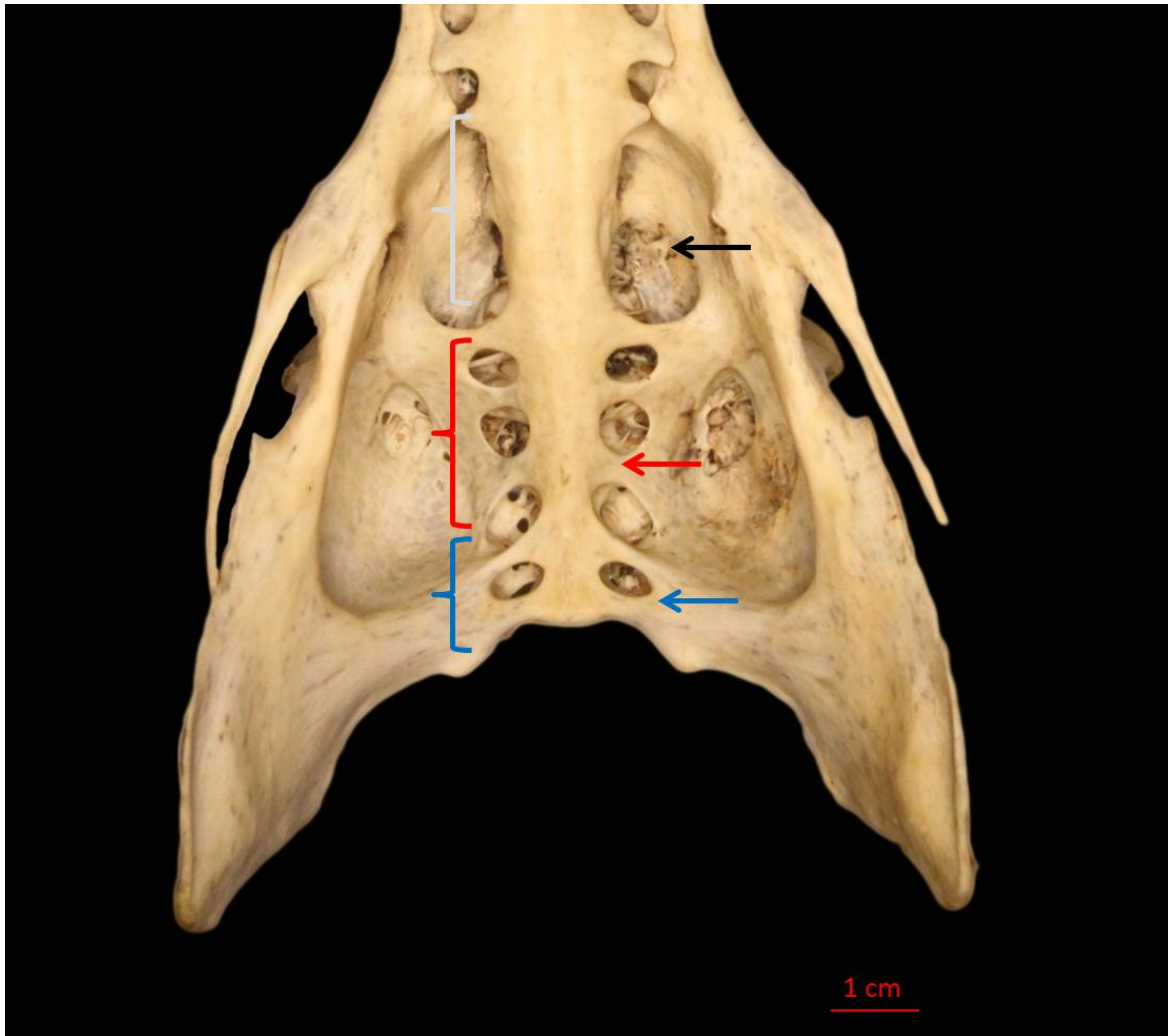
Figure 4-6: *Facies ventralis* **of the primary sacral vertebrae. The white arrow shows the diapophysis and the blue arrow the parapophysis. Both are fused with the post-acetabular** *ilium***.**

The pelvis was made up of two bones, the *os coxae*, each of which comprises an *ilium*, *ischium* and *pubis* (Figure 4-7 and Figure 4-8). In the examined specimens, the bones were fused. The os *ilium* appeared as an elongated bony plate and was differentiated into pre-acetabular and post-acetabular parts. The cranial portion of the pre-acetabular part was attached to the vertebrae of the synsacrum by osseous fusion, while caudally it is separated by small gaps, which in the complete specimen is characterised as a syndesmotic connection. The pre-acetabular portion is also fused medially with the sacrothoracic vertebrae to form the canales iliosynsacrales through which the epaxial muscles run. The part of the pre-acetabular *ilium* near the acetabulum was the ala preacetabularis. On the *facies ventralis* it formed the deep renal fossa. The pre-acetabular *ilium* was spoonbill-shaped, while the post-acetabular portion was dome-shaped. General measurements of the pelvis are presented in Table 4-1. The pelvis was defined by an angle of 140 degrees. The *ilium* was longer pre-acetabular

39

(78.30 ± 5.80 mm) than post-acetabular (54.70 ± 4.60 mm). The total length of the post-acetabular part of the *ilium* was shorter than the *ischium* (Ratio of 8.20 ± 0.5 mm). The *pubis* varied in length between the three birds at 35.70 ± 9.30 mm.

The *corpus ischium* was present caudo-vental to the *corpus ilium* and was shorter in length. The cranial portion of the *ischium*, which was much thicker, together with the *os ilium* formed the acetabulum. The *ischium* and *ilium* also formed the oval *foramen ischiadicum* (caudal to the acetabulum) and the obturator foramen (caudo-ventral to the acetabulum). Caudo-dorsal to the acetabulum was the antitrochanter to which the trochanter of the femur articulates. The *pubis* was a thin rib like bone that followed the ventral border of the *ischium*. The ventral part of the obturator foramen was formed in part by the *pubis*. The *pubis* did not appear to form part of the acetabulum in a similar manner to the fowl and duck. The *pubis* appeared to be residual and only extended half-way down to the *ischium*. It ended blindly and did not fuse caudally with the *ischium* as described in fowl, duck and Eurasian griffon vulture (Lamagère, 2011). While this was similar to that described in the hooded vulture, the bone in the latter was substantially longer. In the unboiled sample, the *os pubis* continued as a cartilaginous extension to reach the same length as the *os pubis* of the Eurasian griffon vulture (Figure 4-9). With the exception of the *pubis* the pelvis of the Cape griffon vulture appeared almost identical to that of the Eurasian griffon vulture (Figure 4-9) (Lamagère, 2011). In comparison to the New-World Black vulture (*Coragyps atratus*) and Hooded vulture (*Necrosyrtes monachus*) (Fisher, 1946), the pelvis of the Cape griffon vulture was more angled and more elongated (Figure 4-10) (Lamagère, 2011). This can most likely be explained by the more compact appearance of the new world vulture in comparison to the old world vulture, to which the Cape griffon vulture belongs.

40
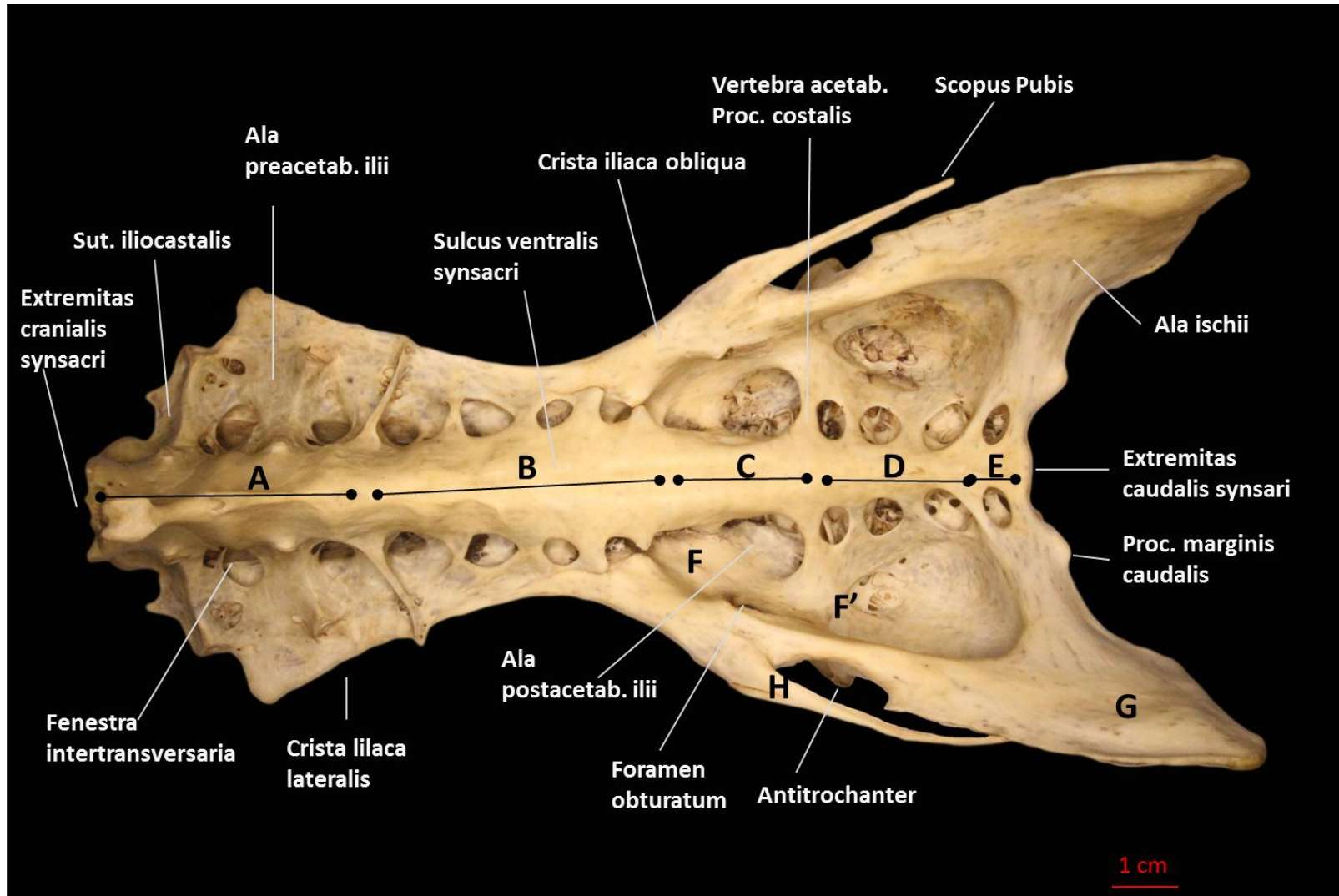
Figure 4-7: *Facies ventralis* of the synsacrum. A- last two thoracic vetebrae; B – sacrothoracic vertebrae; C- sacrolubar vertebrae; D- primary sacral vertebrae; E- sacrococcygeal vertebrae; F- preacetabular *ilium*; F'-postacetabular *ilium*; G – *ischium* and H-*pubis*.

Table 4-1: Measurements of the pelvis in three birds (mm).

Vulture	Interacetabular width	Preacetabular Length	Post-acetabular length	*Ischium* length	Ilium: Ischium Ratio	Pubis length	Renal fossa length	Inter-caudal process length	Angle of pelvis (°)
1	48	75	52	66	7.90	42	27	60	142
2	43	75	52	65	8.00	40	27	65	140
3	50	85	60	68	8.80	25.0	25	67	140
Mean	47	78.30	54.70	66.30	8.20	35.70	26.30	64.00	140.67
SD	3.60	5.80	46	1.50	0.50	9.30	1.20	3.60	1.15

Ilium: *Ischium* ratio: This is the ratio of the length of the post-acetabular to the ischial length. Angle of the pelvis was measure with zero being the *facies ventralis* of *ilium* wing and moving anti-clockwise.
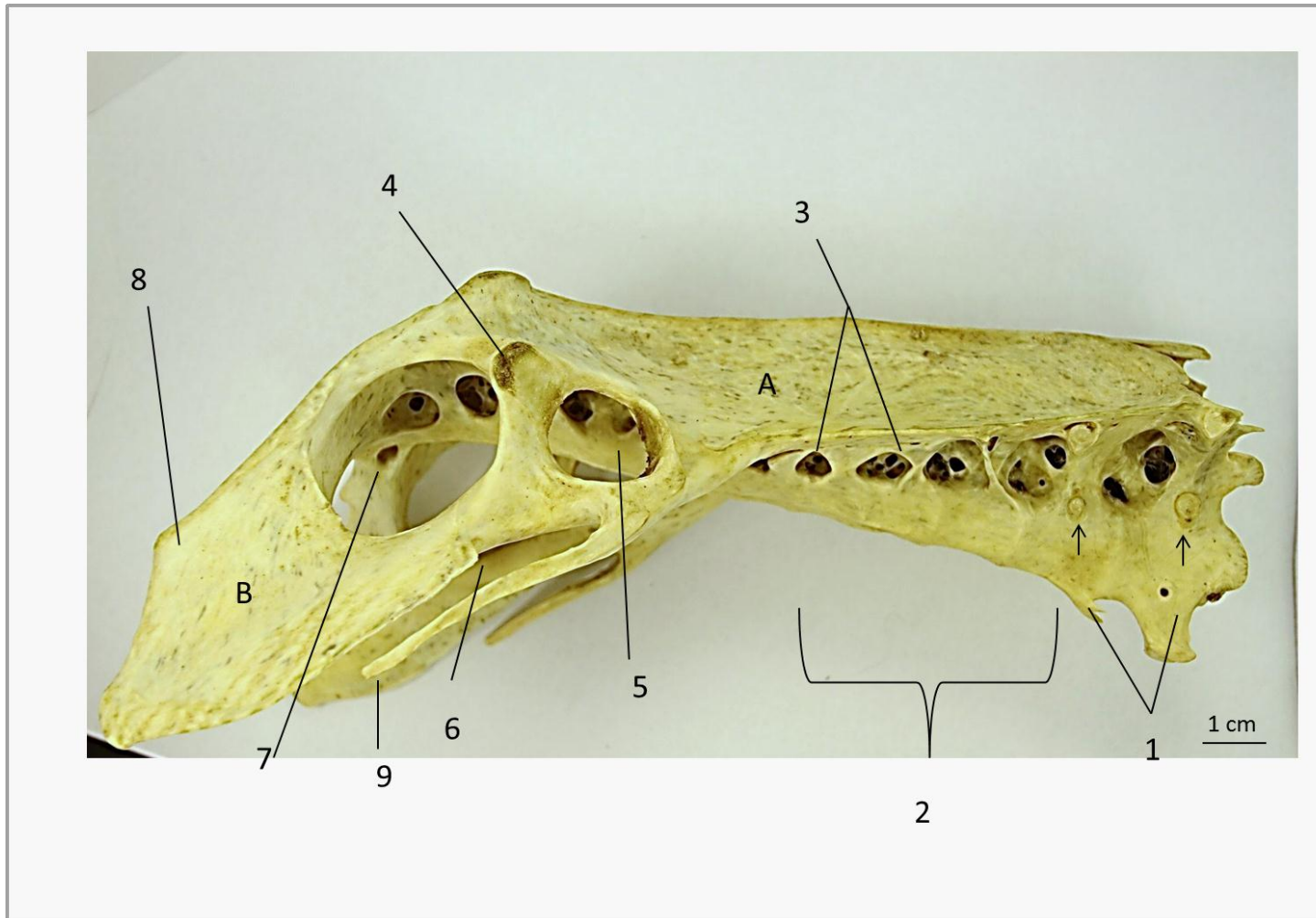
Figure 4-8: Lateral view of the pelvis of G. coprotheres. 1: Last two thoracic vertebrae (T6 and T7) with ventral spinous processes; *processus artularus capitulum costae* **(Black arrows); 2: synsacrothoracic vertebrae; 3:** *fenestrae intertransversariae***; 4: antitrochanter; 5: acetabulum: 6:** *Incisures puboischiatica***; 7:** *Foramina ischiadicum***; 8: caudal process of the** *ilium***; 9:** *pubis***; B-** *Ischium***; A –** *Ilium***.**

43

A

Vertebra acetab. Proc. costalis

Scopus Pubis

Ala preacetab. ilii

Crista iliaca obliqua

Sut. iliocastalis

Sulcus ventralis synsacri

Extremitas cranialis synsacri

Ala ischii

Extremitas caudalis synsari

A   B   C   D   E

Proc. marginis caudalis

F

F'

Ala postacetab. ilii

H

G

Fenestra intertransversaria

Crista lilaca lateralis

Foramen obturatum

Antitrochanter

1 cm

44
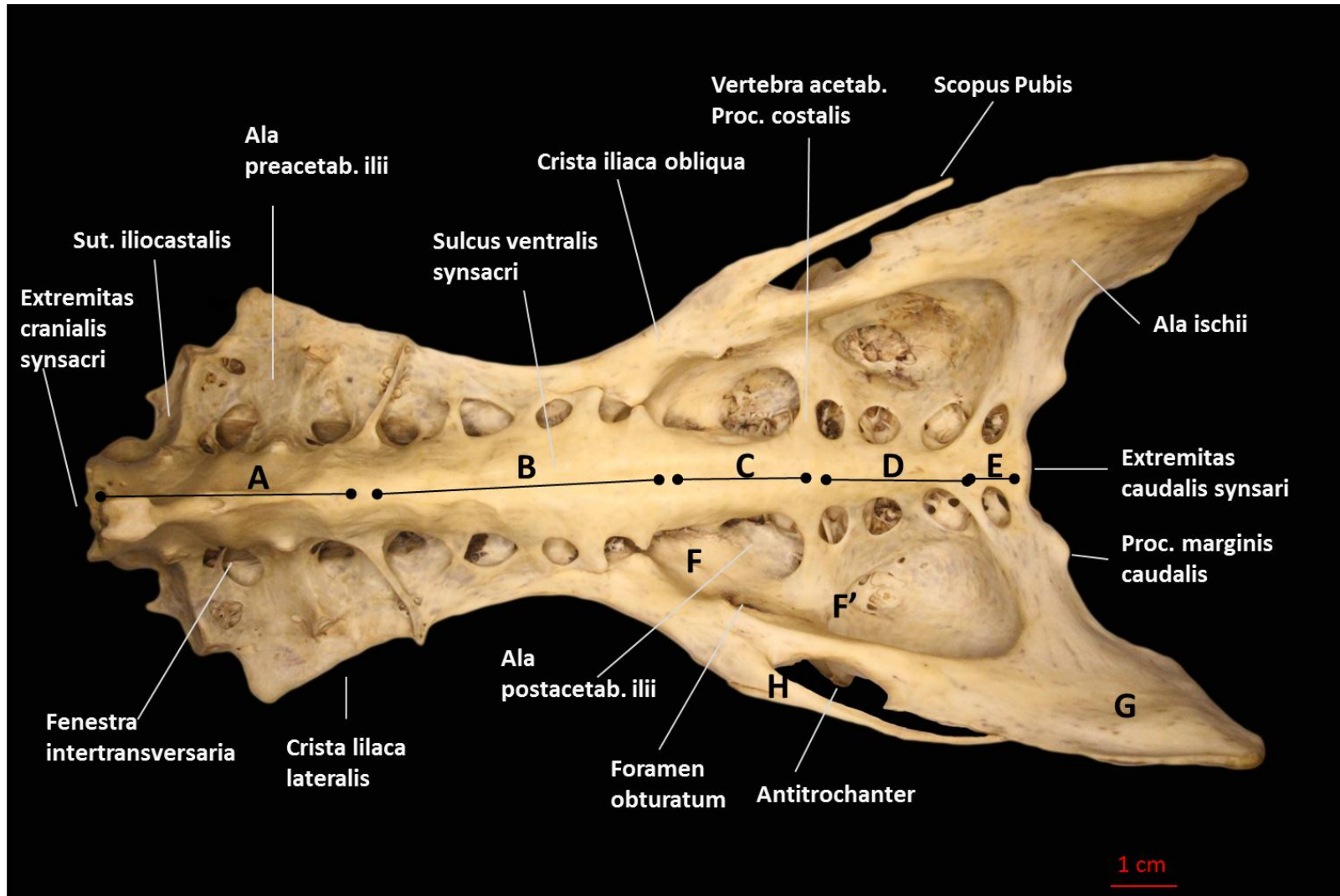
B
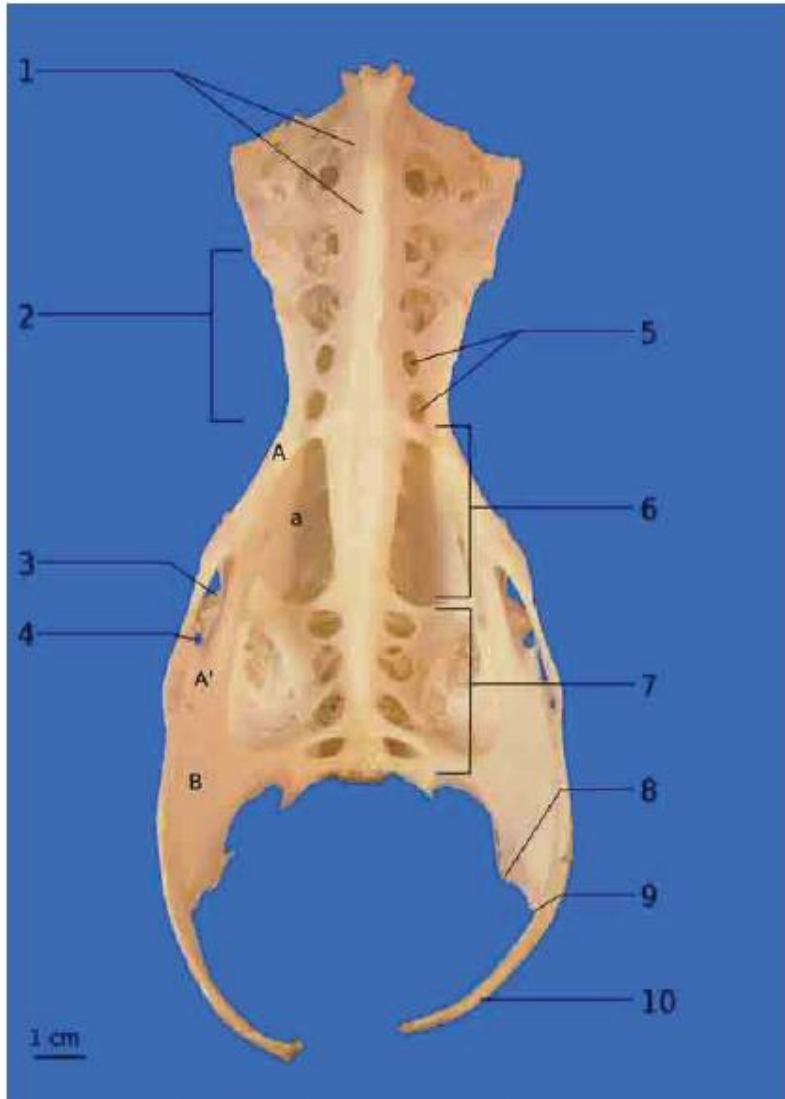
Figure 48 : Aspect ventral de la ceinture pelvienne

1 : Dernières vertèbres thoraciques
2 : Vertèbres synsacrothoraciques
3 : Antitrochanter
4 : Fenêtre ischiopubienne
5 : Fenêtres intertransversaires
A : Aile (partie) pré-acétabulaire de l'ilium
A' : Aile (partie) post-acétabulaire de l'ilium

6 : Vertèbres synsacrolombaires
7 : Vertèbres sacrées/synsacrocaudales
8 : Processus caudal de l'ilium
9 : Processus terminal de l'ischium
10 : Pubis
B : Ischium
a : Fosse rénale

45

C

Figure 4-9: Comparison of the *facies ventralis* of the pelvis of *G coprotheres* (A), and *G fulvus* (B) and overlay of an outline of the pelvis of *G. fulvus* (Lamagère, 2011) over the pelvis of *G. coprotheres* (C).

46
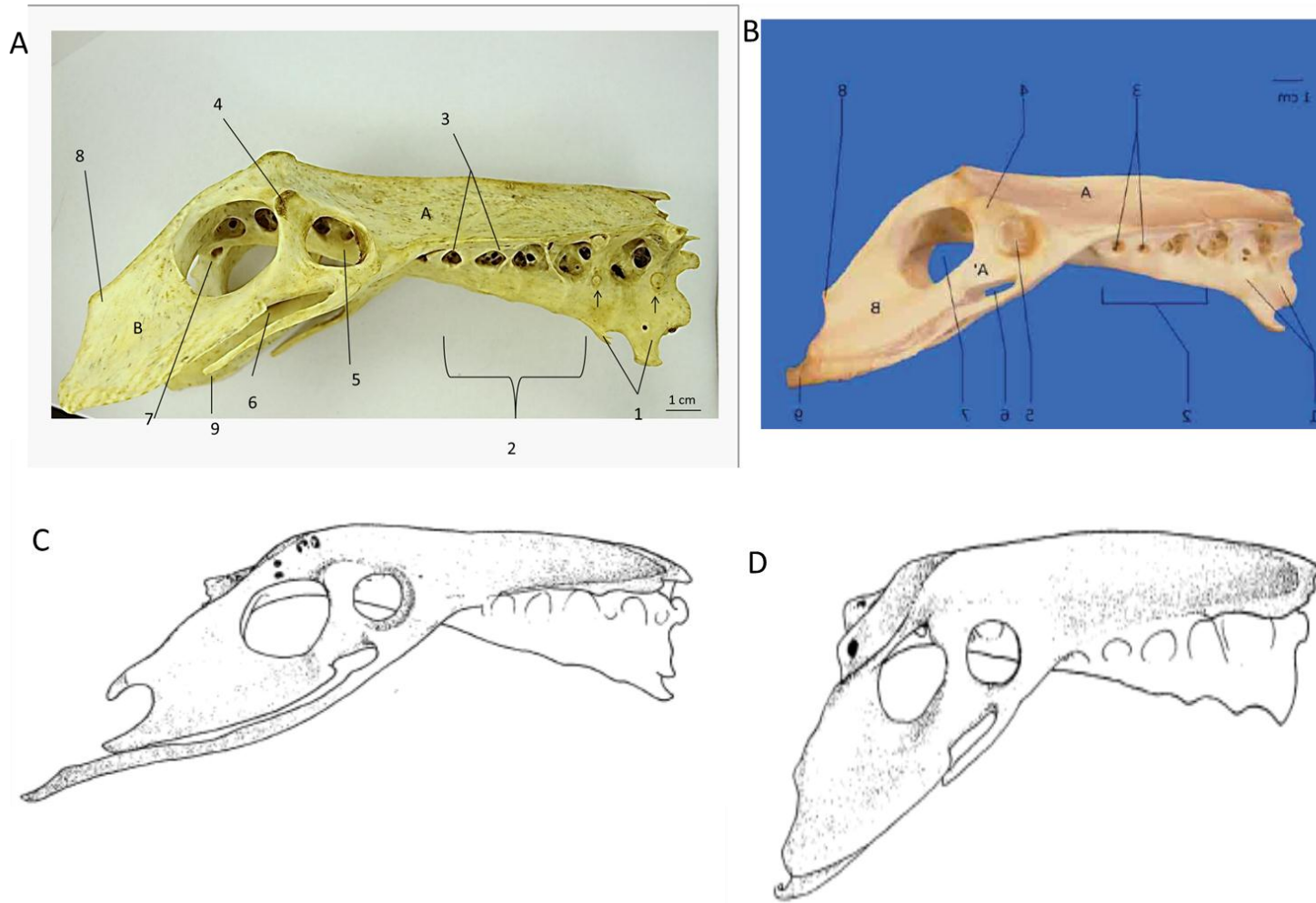
Figure 4-10: Ventral view of the pelvis of four different vulture species; Cape griffon vulture (A); Eurasian griffon vulture (B); Black vulture (C); Hooded vulture (D) 1: Last two thoracic vertebrae (T6 and T7) with ventral spinous process; *processus articularus capitulum costae* **(Black arrows); 2 synsacrothoracic vertebrae; 3:** *Fenestra intertransversaria***; 4: Antitrochanter; 5: acetabulum; 6: Incisures puboischiatic; 7:** *Foramina ischiatica***; 8: caudal process of the** *ilium***; 9:** *pubis***; B-** *Ischium***; A –** *Ilium***. Picture of** *G. fulvus* **from Lamagère, 2011, while the picture of the black vulture and hooded vulture were from Fisher, 1946.**

4.2. Topography

The paired kidneys were situated on either side of the dorsal midline (Figure 4-11). Each kidney, although one continuous structure, was comprised of three structurally distinct lobes namely the *lobalis renalis cranialis, media* and *caudalis* (Figure 4-12). Paired, deep fossae (*fossae renales*) on each side of the ventral synsacral sulcus (*Sulcus ventralis synsacri*) accommodated the kidneys and were formed partly by the *Os coxae* (mainly the *ilium*) and the synsacrum. However, the cranial lobes were not housed in the *fossae renales*. Each cranial lobe occupied a shallow depression on the *facies ventralis* of the corresponding pre-acetabular *ilium* and a soft tissue depression formed by the base of the lungs (cranially) and the abdominal wall (laterally). The extension of the kidneys from the caudal margin of the lungs to the caudal ends of the synsacral fossae was similar to findings of Nabipour, et al. (2009), who evaluated the Rock dove (*Columba livia*), the Collared dove, (*Streptopelia decaota*) and the owl (*Athene noctua*).

 Each kidney in its entirety (the three lobes in sequence) was an elongated, narrow bean-shaped structure and presented two margins, two extremities and two surfaces. The *margo lateralis* was concave due to the slender nature of the middle lobe in comparison to the cranial and caudal lobes, whereas the *margo medialis* was slightly convex and lay adjacent to the dorso-lateral surface of the synsacrum. Both the cranial and caudal poles or extremities (*Extremitas cranialis et caudalis*) were convex with the cranial pole corresponding to the *extremitas cranialis* of the cranial lobe and the caudal pole to the *extremitas caudalis* of the caudal lobe. The *facies ventralis* (*Facies ventralis*) faced the abdominal viscera (liver and small intestines predominantly) (Figure 4-12) and was the surface on which the major portions of the renal portal vasculature were visible. The *facies ventralis* of the cranial lobes was closely associated with the adrenal glands in all specimens and the testes in male birds. The *ductus deferens* ran along the ventromedial aspect of each kidney, and in the one mature female specimen dissected, the entire *facies ventralis* of the kidney was closely associated with the ovary craniomedially to the cranial lobe, the *infundibulum* ventromedially to the middle lobe and the *oviduct* running from ventromedial to the caudal lobe caudally to the cloaca.

48
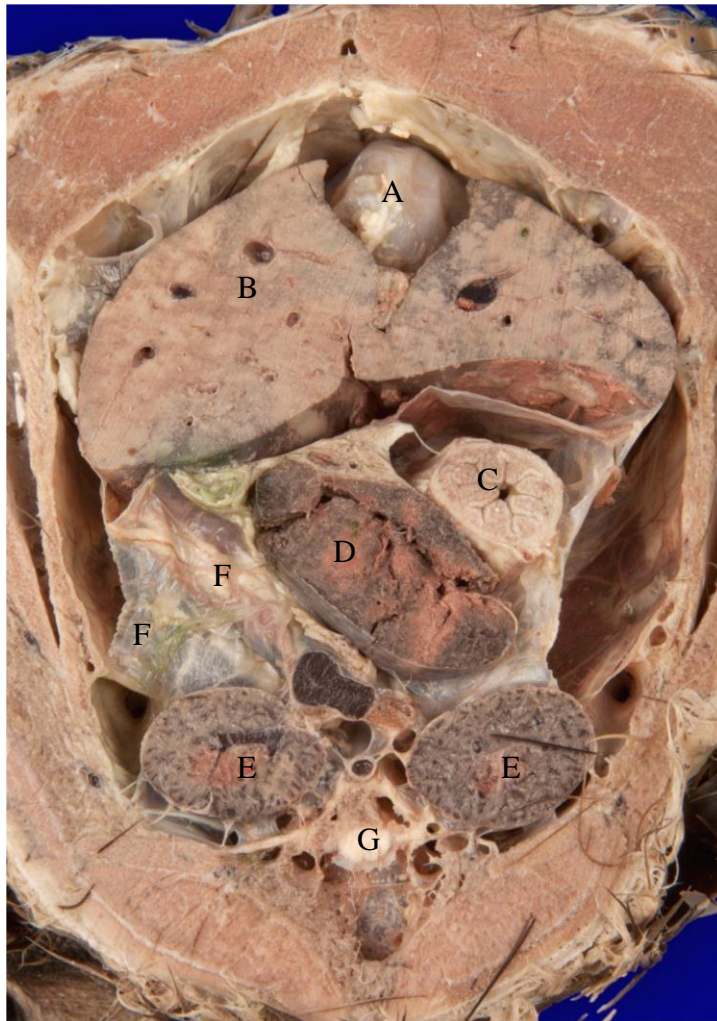
Figure 4-11: Cross section through the cranial lobes of the kidney. A- apex of the Heart, B- liver; C- gizzard (ventriculus), D- spleen; E- kidneys; F- loops of Small Intestine; G - spinal Column
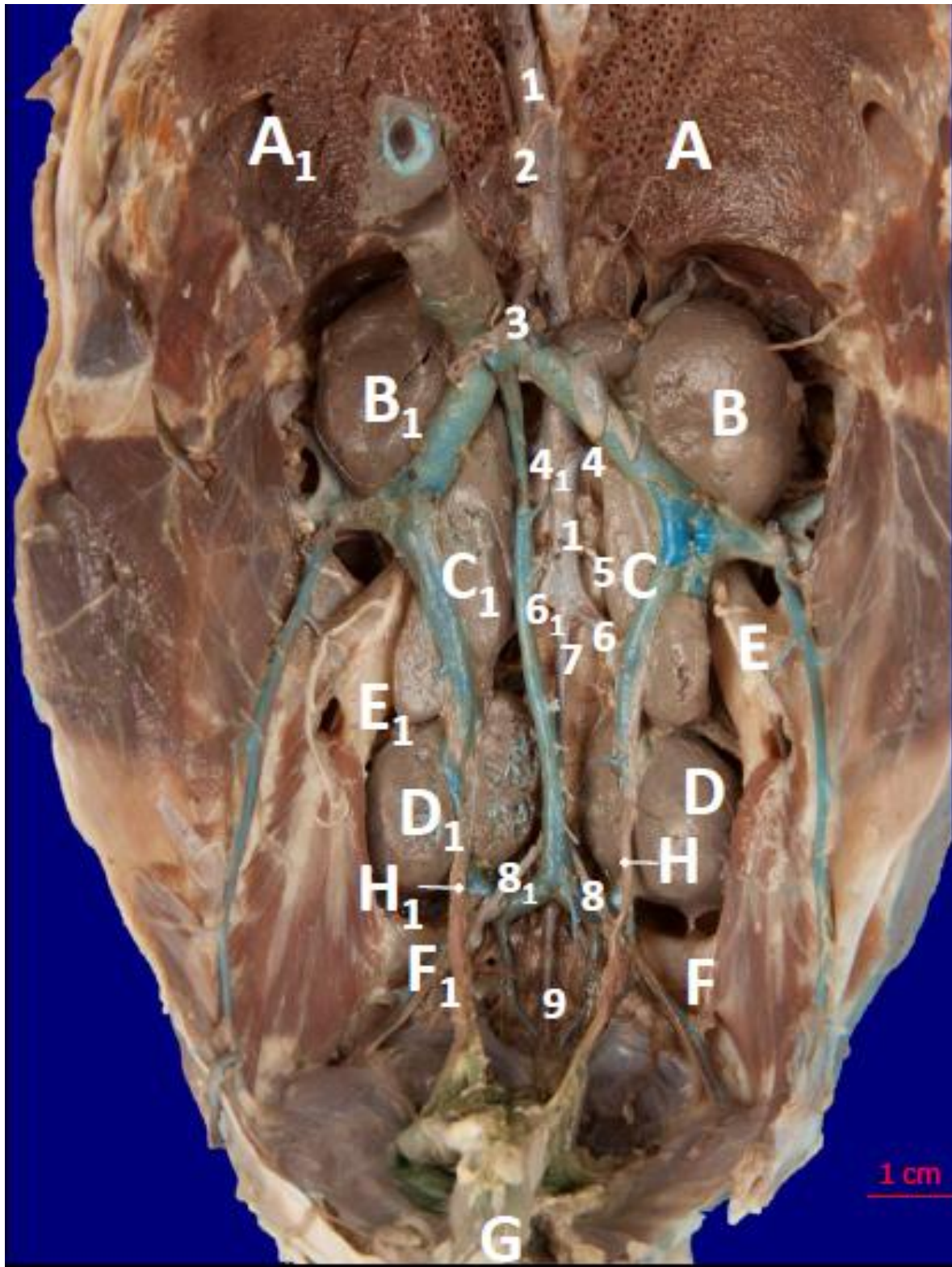
Figure 4-12: Photograph of arteries visible on the ventral aspect of the abdominal cavity of a one-year old Cape griffon vulture (of unknown sex) following removal of viscera to expose the retroperitoneal structures. A, A1 lungs, sin. and dext., B, B1 *divisio renalis cranialis*, *sin*. and *dext*., **C, C1** *lobalis renalis media*, *sin*. and *dext*., **D, D1** *divisio renalis caudalis sin*. and *dext*., **E, E1** *crista iliaca obliqua sin*. and *dext*., **F, F1** *pila postrenalis sin*. and *dext*., **G rectum, reflected. H, H1** *ureter sin*. and dext. **1** *aorta caudalis*, **2** *a. coeliaca*, **3** *a. mesenterica cranialis*, **4, 41** *a. iliac externa sin*. and *dext*., **5** *aa. sacrales*, **6, 61** *a. ischiadica externa sin*. and dext., **7** *a. sacralis*, **8, 81** *a. iliaca interna sin*. and <u>dext</u>., **9** *a. mediana caudae*.
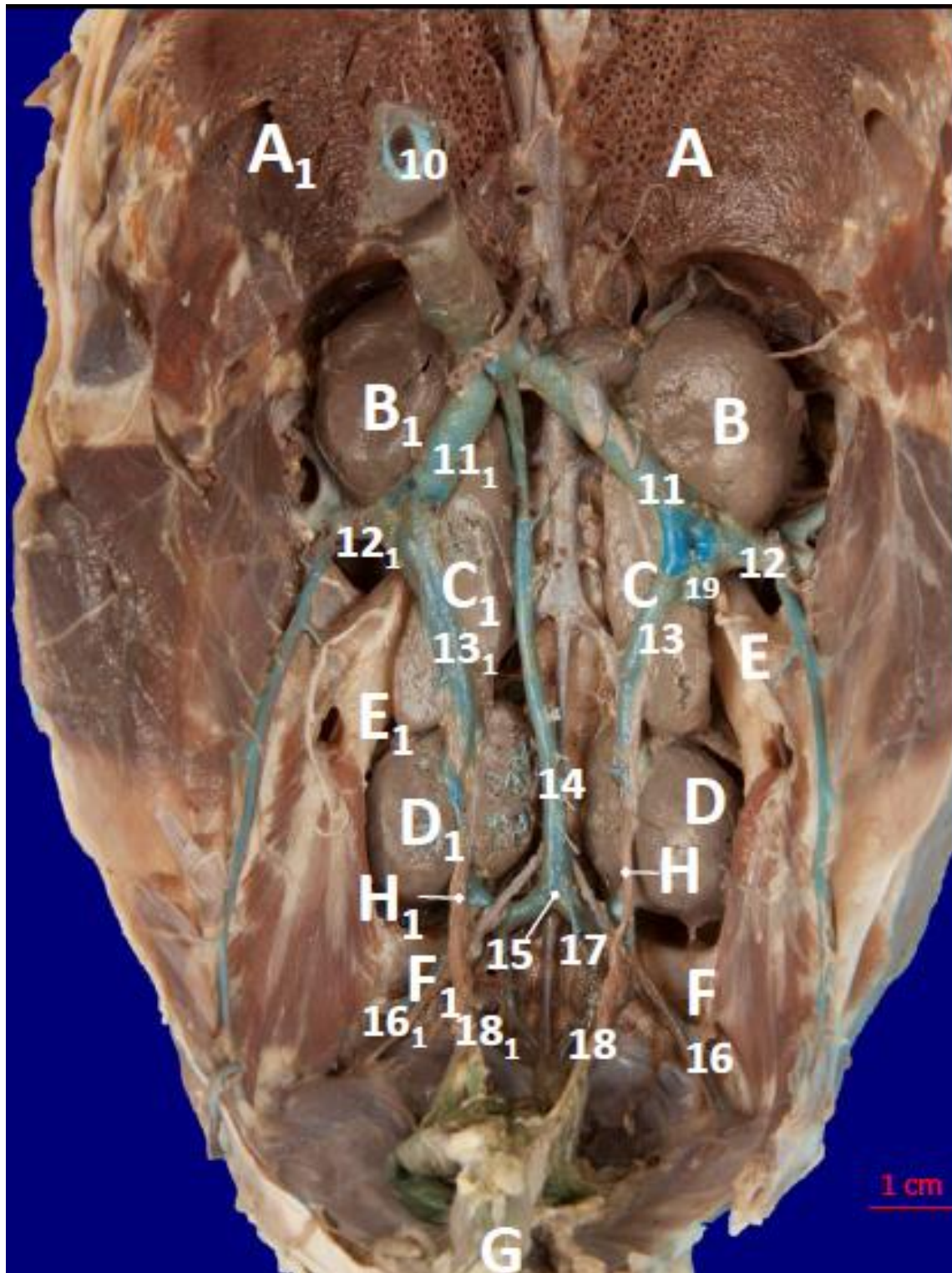
Figure 4-13: Photograph of veins on the ventral aspect of the abdominal cavity of a one-year old Cape griffon vulture (of unknown sex) following removal of viscera to expose the retroperitoneal structures. A, A₁ lungs, *sin*. and *dext*., B, B₁ *divisio renalis cranialis*, *sin*. and *dext*., C, C₁ *lobalis renalis media*, *sin*. and *dext*., D, D₁ *divisio renalis caudalis sin*. and *dext*., E, E₁ *Crista iliaca obliqua sin*. and *dext*., F, F₁ *pila postrenalis sin*. and *dext*., G rectum, reflected. H, H₁ *ureter sin*. and *dext*. 10 *vena cava*, 11, 11₁, *v. iliaca communis sin*. and *dext*., 12, 12₁ *v. iliaca externa sin*. and *dext*., 13, 13₁ *v. renalis caudalis sin*. and *dext*., 14 *v. mesenterica caudalis*, 15 *anastamosis interiliaca*, 16, 16₁ *v. iliaca interna sin*. and *dext*., 17 *v. efferentes sinus intervertebralis*, 18, 18₁ *v. hypogastrica sin*. and *dext*. 19, *v. renalis portalis caudalis sin*.

The dorsal surface (*facies dorsalis*) faced the recess in the synsacrum forming the *fossae renales* and the flat depression in the *facies ventralis* of the wing of the preacetabular *ilium*. Also found along the *facies dorsalis* were arteries originating off the *aorta descendens*, nerves forming *plexus lumbales, plesux sacralis* and plexus *pudendae*, as well as *sinous venosae* (Figure 4-14).
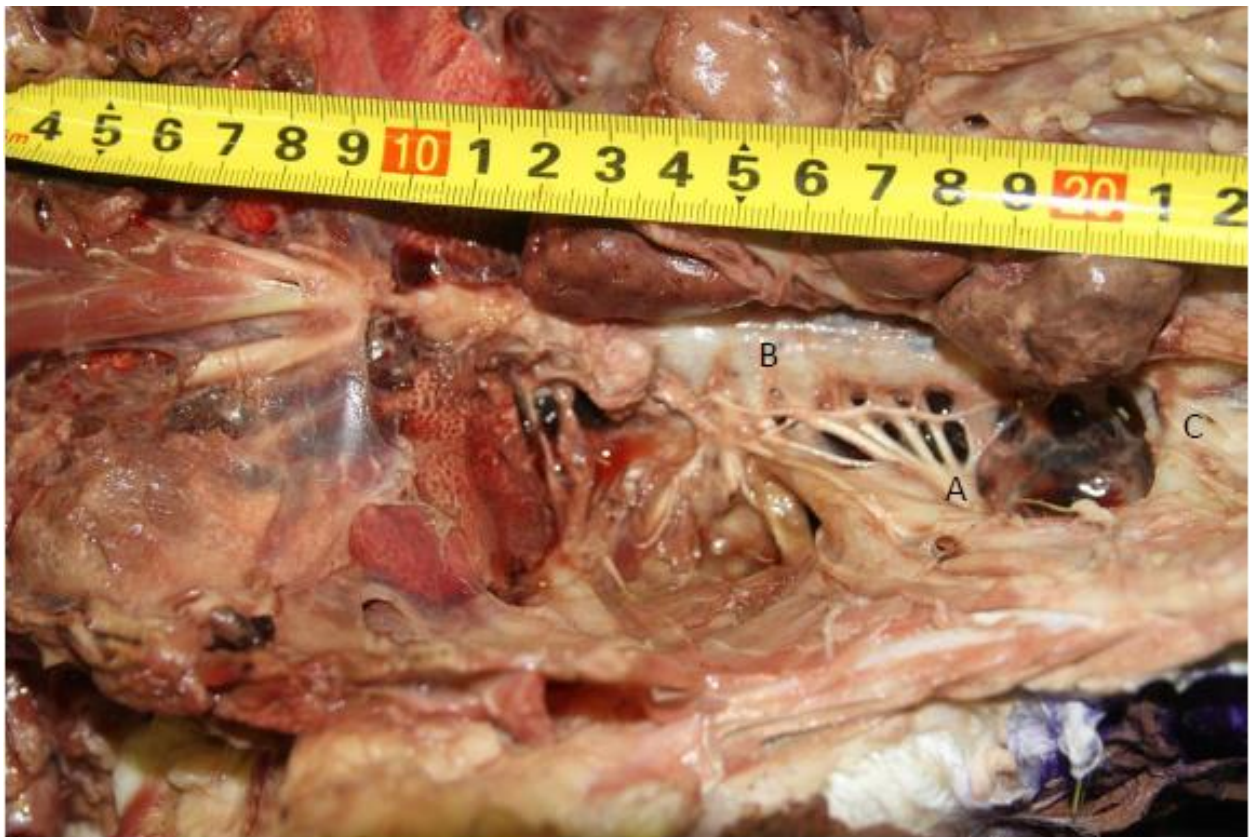
Figure 4-14: *Facies ventralis* **of the pelvis, after removal of the kidney. Visible are the nerve plexuses (A), the spinal column (B), and the wing of the** *ilium* **(C)**

Each lobe was surrounded by a thin fibrous capsule (*capsula fibrosa*). A fairly thick layer of adipose tissue formed a fat capsule (*capsula adiposa*) surrounding the *facies ventralis* of the middle and especially the *lobales caudales*. Ventral to the fat capsule was a notable fat deposit within the omentum which spanned the entire length of the kidneys. The structures bordering the *divisio renales craniales sin.* and *dext.* differed minimally. *Divisio renalis cranialis sin.*was bordered by the base of the left lung (cranially), the last rib (cranio-laterally), and abdominal

muscles (caudo-laterally), the *v. iliaca externa sin.* (caudally), the *v. iliaca communis sin.* (caudo-medially) and the *glandus adrenalis sin.* (cranio-medially).

Divisio renalis cranialis of each kidney was ovoid in shape and mirror-imaged one another across the midline, with the right cranial lobe (*divisio renalis cranialis dextra*) being marginally larger, more angular and located slightly cranial to the left cranial lobe (*divisio renalis cranialis sinistra*) (Figure 4-12). The long axis of each cranial lobe lay oblique to that of the midline and ran parallel to the *vv. iliacae communii*. The *extremitas cranialis* of the lobe was located immediately caudal to the last rib and corresponded with the cranial pole of each kidney. The *margo lateralis* was convex and formed the cranial part of the *margo lateralis* of the kidney. A shallow depression was present in the *facies ventralis* of the preacetabular *ilium* and the dorsal margin of the *divisio cranialis* followed the shape of the depression. The caudo- lateral margin of the cranial lobe was continuous with the cranio-*lateral* of the *divisio media* dorsal to the *v. iliaca communus* (Figure 4-13 and Figure 4-15). This vein was the major external feature demarcating the *divisio renales craniales* and *mediales*. The *v. iliaca externa* partially obscured the most caudal part of *divisio cranialis* and was therefore the external feature which marked the caudal extent of *divisio cranialis.*

The *divisio renalis media sinistra* was comma-shaped, with the long axis parallel to the *sulcus ventralis synsacri,* which demarcated the midline, and was within *the pars ischiadica* of the renal fossa (Figure 4-12). The *margo medialis* ran along the midline of the synsacrum. While the middle lobe was fused with the cranial lobe along its oblique cranio*margo lateralis*, it was clearly demarcated by the common iliac trunk. The *v. renalis caudalis sin.* separated the head of the comma from the tail of the comma on the *facies ventralis* of the lobe. The *v. caudalis renalis portalis sin.* entered the middle lobe at the cranio-*margo lateralis* of the head of the comma. The *margo lateralis* was formed by *crista iliaca obliqua sin.* The *ureter sin.* exited the lobe under the head of the comma medial to the *v. renalis portalis caudalis* and ran along the *margo medialis* of the vein until crossing it at the caudal pole of the caudal lobe. Unlike the *extremitas caudalis* of the *divisio renalis cranialis*, the *extremitas caudalis* of the *divisio renalis media* was more distinct and only appeared to be attached to the caudal lobe by vessels, the ureter and a very small bridge of kidney parenchyma.

The *divisio renalis media detra* was roughly triangular in shape, with the long axis parallel to the *sulcus ventralis synsacri* (midline) and lay in the *pars ischiadica* of the *renal fossa* (Figure 4-12).

53

The *divisio media* appeared to be subdivided into a *pars cranialis* and a *pars caudalis* by the *v. renalis caudalis dextra*, with the *extremitas cranialis* of the *pars caudalis* being slightly raised above the *extremitas caudalis* of the *pars cranialis*, to which it was tightly fused. The *margo medialis* of the cranial portion ran along the midline of the synsacrum. While the middle lobe was fused with the cranial lobe along its oblique craniolateral border, it was clearly demarcated by the *v. iliaca communis*. The *v. caudalis renalis portalis dext.* was not visible on the *facies ventralis*. The *margo lateralis* of the *division media* was against the *crista iliaca obliqua dextra*. The *ureter dext.* exited the lobe lateral to the *v. renalis caudalis* at the *extremitas caudalis* of the caudal portion of the lobe. Unlike the *extremitas caudalis* of the *divisio cranialis*, the *extremitas caudalis* of the *divisio media* was more distinct and only appeared to be attached to the *divisio caudalis* by vessels, the *ureter* and a small bridge of kidney parenchyma.

The *divisio caudales* were well developed and separated by an obvious connective-filled septum and distinct indentation, as described by Johnson 1968, in his classification of the avian kidney based on morphology (Figure 4-16). The *divisio caudalis sin.* was rhomboid in shape, and was deeply embedded in the *pars pudenda* of the *fossa renalis*, with its *margo medialis* also running parallel to the midline (Figure 4-12). The *extremitas cranialis* ran oblique to the midline at an angle of 115 degrees. The *margo lateralis* was roughly convex, and ran parallel to the *margo medialis*. In this area the *ureter* and *v. renalis caudalis sin.* ran parallel to the midline approximately one quarter width of the lobe from its medial border. The *division renalis caudalis dext.* was also rhomboid in shape, and was deeply embedded in the *pars pudenda* of the *fossa renalis*, with its *margo medialis* also running parallel to the midline (Figure 4-12). It was larger and extended more cranially than the corresponding *divisio caudalis sin.* The *extremitas cranialis* ran oblique to the midline at an angle of 260 degrees. The *margo lateralis* was also roughly convex, and ran in the parallel plane to the *margo medialis*. The *ureter dext.* and *v. renalis portalis caudalis dext.* ran in a cranial to caudal direction to divided the lobe into roughly equal halves. The *extremitas caudalis* was parallel to the *extremitas cranialis*, and moulded to fit the *fossa renalis*.

54
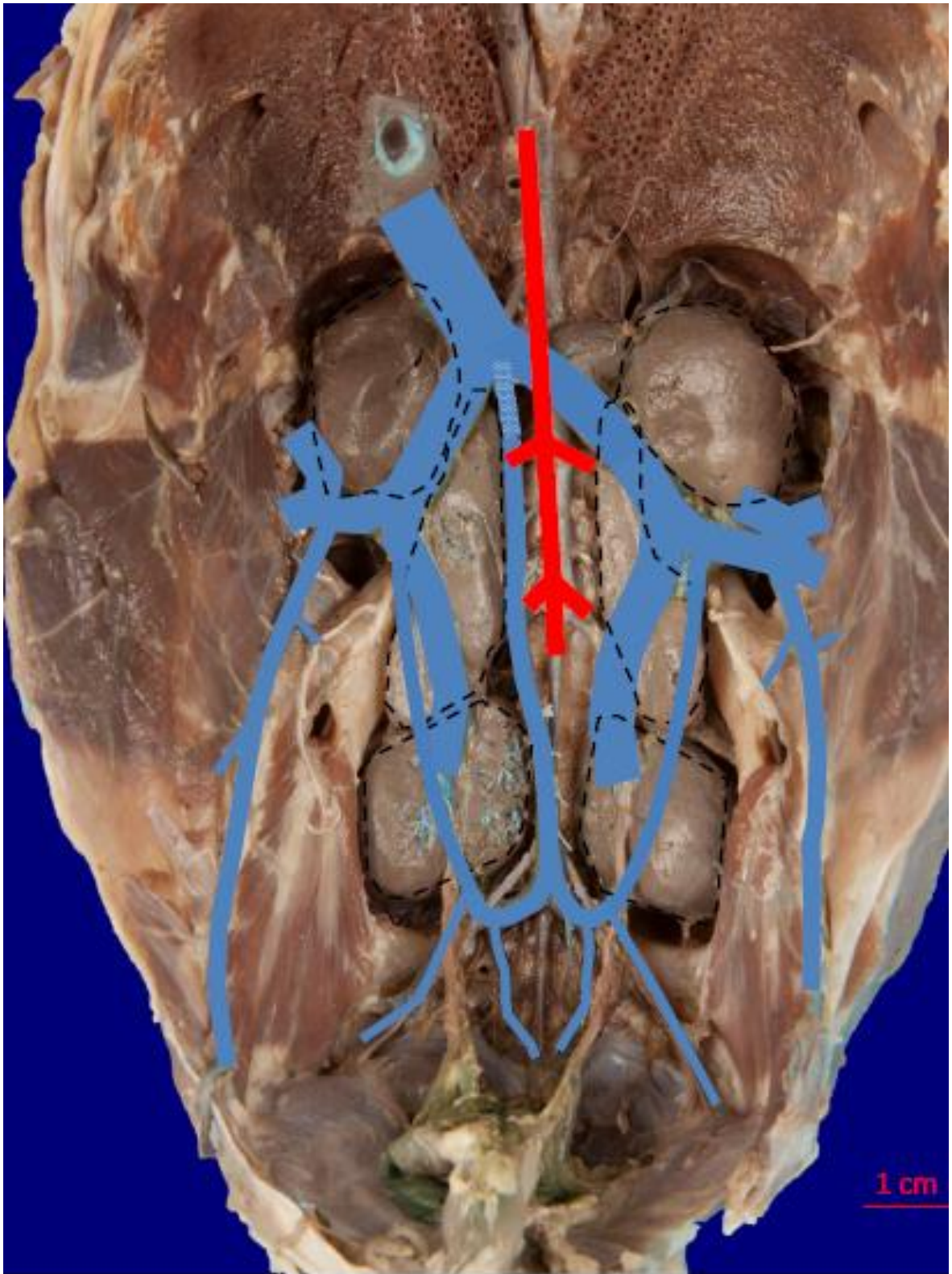
B
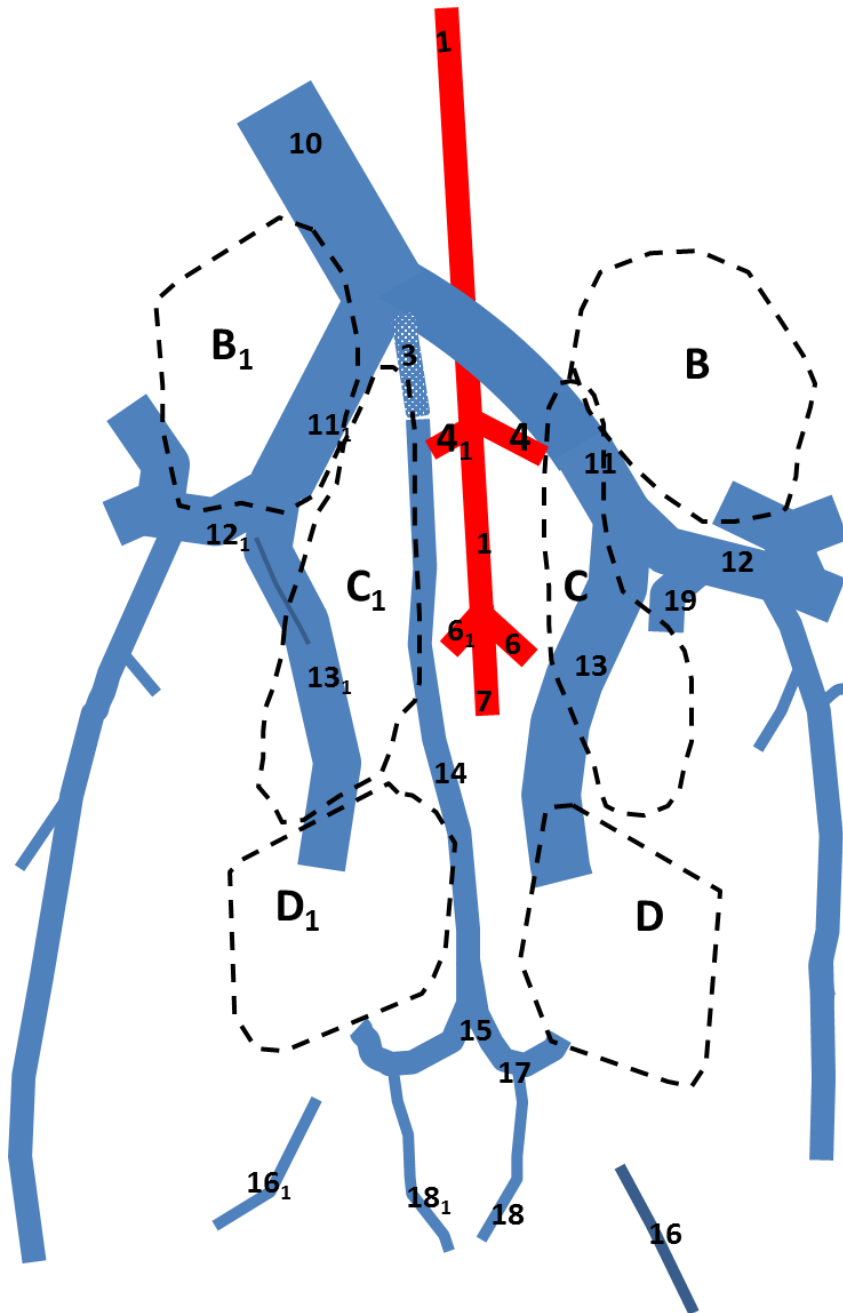
Figure 4-15: A and B: Simple line diagram superimposed on the blood vessels (A) and line diagram independent of underlying architecture (B) illustrating the shape of the various lobes of the kidney (Ventral view). B, B$_1$ *Divisio* renalis cranialis, *sin*. and *dext*., C, C$_1$ *Lobalis renalis media*, *sin*. and *dext*., D, D$_1$ *Divisio renalis caudalis sin*. and *dext*., 1 aorta caudalis, 4, 4$_1$ *a*. iliac externa sin. and *dext*., 6, 6$_1$ *a*. ischiadica externa sin. and dext., 7 a. sacralis, 10 v*ena cava*, 11, 11$_1$, *v. iliaca communis sin*. and *dext*., 12, 12$_1$ *v. iliaca externa sin*. and *dext*., 13, 13$_1$ *v. renalis caudalis sin*. and *dext*., 14 *v. mesenterica caudalis*, reflected cranially, 15 *anastamosis interiliaca*, 16, 16$_1$ *v. iliaca interna sin*. and *dext*., 17 *v. efferentes sinus intervertebralis*, 18, 18$_1$, *v. hypogastrica sin*. and *dext*., 19, *v. renalis portalis caudalis sin*. (*v. renalis portalis caudalis dext*. not visible as it was dorsal to the *v. renalis caudalis sin*. and *dext*., and shown here as a black line)

The ventral topography of the Cape griffon vulture was compared to an extensive review by Johnson (1968), in which the topography of 180 birds from 20 orders were compared. Johnson divided the kidneys based on the size and degree of separation of the lobes. With the vulture kidney showing three distinct lobes and with the *divisio renalis cranialis* being approximately the same length as the *divisio renalis caudalis* (32.32 ± 3.96 mm versus 28.95 ± 4.80 mm for the left; and 34.81 ± 3.74 mm versus 30.28 ± 9.97 mm for the right) (Tables 4-2 and 4-3), this bird's kidneys will fall in category III of Johnson's classification. This was similar to *Perdix perdix* (Gray partridge), *Charadrius vociferous* (Killdeer), and *Pitangus sulphuratus* (Great Kiskadee). The presence of the trilobular kidney differentiates this vulture species from other Passeriformes, for which the division between the *diviso renalis media* and *divisio renalis caudalis* is not distinct. The trilobular structure of the vulture was similar to that for the red-tailed hawk, although the latter appears to be more of a type-I appearance. Batah (2012) measured the length and width of the kidney lobes of Coot birds (*Fulica atra*). It was found that each kidney consisted of three parts, namely a large cranial lobe (*divisio renalis cranialis)* with a mean length of 28 ± 0.15 mm and a width of 13 ± 0.08 mm, a middle lobe (*divisio renalis media)* with a length of 30+- 0.08mm and width of 7.5 ± 0.10 mm, and a small caudal lobe (*divisio renalis caudalis)* with a length of 13 ± 0.07 mm and a width of 4 ± 0.08 mm. This would put the coot bird in Type I of Johnson's Classification, characterised by a well-developed middle lobe and small caudal lobe.

57
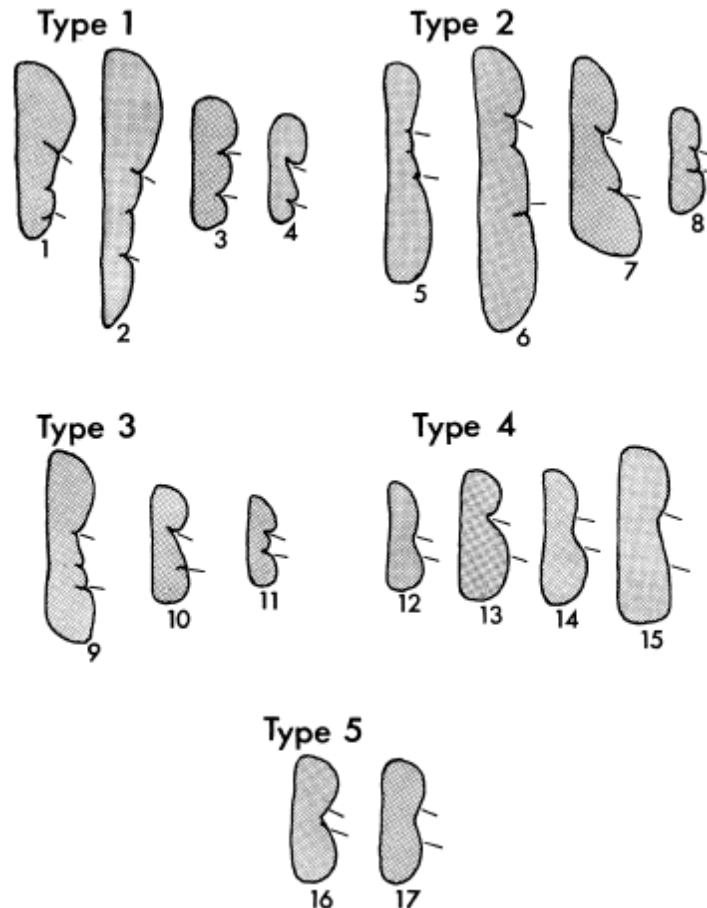
Figure 4-16: Classification of avian kidneys based on the morphology (Johnson, 1968). Type 1-Three lobes present, middle lobe well developed and separated from the caudal lobe by a distinct indentation or obvious connective tissue-filled septum, cranial lobe largest. Type 2-As for I, except caudal lobe largest. Type 3-As for I, except caudal and cranial lobes approximately equal in size. Type 4-Middle lobe not well defined as it is apparently fused closely to the other lobes (especially to the caudal), the latter combination exceeding the size of the cranial portion. Type 5-As per IV, except cranial portion larger than or approximately equal to the caudal portion.

Not all avian species have three well demarcated lobes as described in the domestic hen and seen in the Cape griffon vulture. Two lobes have been described for the hornbill (Feinstein, 1962), four lobes in long billed species such as storks, herons, egrets and ibis (Johnson, 1979; King, 1993) and five lobes in the kiwi species (Kurod, 1963). Structures crossing the kidney are often responsible for lobular division, for example blood vessels or a ureter crossing the kidney may give the impression of external divisions without internal divisions being evident on further examination (Johnson, 1979; King, 1993). This can be misleading and give the impression of supernumerary lobation.

When the kidneys were measured, the left kidney and the right kidney were 85.14 ± 9.02 and 86.29 ± 9.97 mm at their longest respectively. At their widest part, they measured 25.34 ± 5.21 and 24.33 ± 2.93 mm respectively (Tables 4-2 and 4-3). The widest part of the kidney was

58

accounted for by the caudal lobe for both kidneys. In terms of length the middle lobe accounted for the greatest length. When the lobes were compared by a student t-test, no significant differences were present between the kidneys or between their respective lobes. This compared well to measurements taken during dissection by Nabipour, et al. (2009). In this study the Rock dove (*Columba livia*), Collared Dove, (*Streptopelia decaota*) and owl (*Athene Noctua*) had kidneys that measured 27 x 10, 21 x 7 and 25 x 7 mm respectively. While these birds had smaller kidneys, the ratio of the length to width was similar to that of the vulture at ± 3.

Table 4-2: Measurements of the Left Kidney and Lobes (mm)

Sample	Cranial Lobe		Middle Lobe		Caudal Lobe		Total Length	Renal Fossa Length
	Width	Length	Width	Length	Width	Length		
1	26.46	33.62	23.78	33.98	20.96	32.29	82.15	84.73
2	29.36	37.23	25.29	46.38	32.61	26.77	96.57	98.15
3	21.42	28.19	15.14	35.31	22.3	23.23	75.04	81.09
4	23.86	30.25	25.53	45.64	25.48	33.49	86.78	97.03
Mean	25.28	32.32	22.44	40.33	25.34	28.95	85.14	90.25
Max	29.36	37.23	25.53	46.38	32.61	33.49	96.57	98.15
Min	21.42	28.19	15.14	33.98	20.96	23.23	75.04	81.09
SD	3.41	3.96	4.93	6.59	5.21	4.80	9.02	8.62
%CV	13.51	12.26	21.95	16.34	20.55	16.60	10.60	9.55

Table 4-3: Measurements of the Right Kidney and Lobes (mm)

| Sample | Cranial | | Middle | | Caudal | | Total | Renal Fossa |
	Width	Length	Width	Length	Width	Length	Length	Length
1	22.49	31.84	24.77	40.23	26.18	29.67	81.61	84.72
2	27.62	37.88	28.87	46.83	26.9	35.99	97.72	98.13
3	17.65	38.2	18.78	75.14	20.4	26.17	75.08	81.04
4	26.1	31.32	20.43	49.11	23.84	29.28	90.73	97.06
Mean	23.47	34.81	23.21	52.83	24.33	30.28	86.29	90.24
Max	27.62	38.2	28.87	75.14	26.9	35.99	97.72	98.13
Min	17.65	31.32	18.78	40.23	20.4	26.17	75.08	81.04
SD	4.43	3.74	4.54	15.34	2.93	4.12	9.97	8.64
%CV	18.89	10.74	19.56	29.04	12.04	13.61	11.55	9.57

60

4.3. Vasculature of the Vulture Kidney

The major blood vessels are presented in Figure 4-17 and Figure 4-20; and as a line diagram in Figure 4-18 and Figure 4-21. At the level of the last thoracic to first lumbar vertebra (At the point that the *vv. iliacae communii* the *vena cava caudalis*) the abdominal *aorta descendens* gives off *a. renalis cranialis* which supplies the *division renalis cranialis*. The hind limb of the bird is supplied with blood by the *a. iliaca externa* and by the *a. ischiadica externa* The *a. iliaca externa* arises from the *aorta descendens* on the *facies ventralis* of the synsacrum between the *divisio renales mediales* (at the junction of *divisio renales mediales* and *caudales*) and leaves the pelvic cavity above the hip joint and branches into the *a. circumflexa femoris, a. glutea* and the *a. pelvina.* The *aa. ischiadicae ext*ernae take their origin from the *aorta descendens* at the middle axis of the *division renalis media*. They traverse the *renalis sin.* and *dext.* respectively in the groove between the *divisio renales mediales* and *caudales* and leave the pelvic cavity through the *foramen ischiadicum.* While still within the kidney, the *a. ischiadica* gives rise to the *aa. renales mediales* and *caudales* on each side. The *aorta descendens* terminates in the *a. sacralis*. The arterial blood supply of the vulture kidney followed closely the path described for the chicken (Figure 4-19), with the exception that the *a. spermatica int.* and *a. testicularis* were not visible, most likely as result of the birds being immature or the birds being in the quiescent phase of their reproductive cycle being seasonal breeders. A major difference was evident for the *a. renalis caudalis,* which in the chicken arises from the common trunk.

61
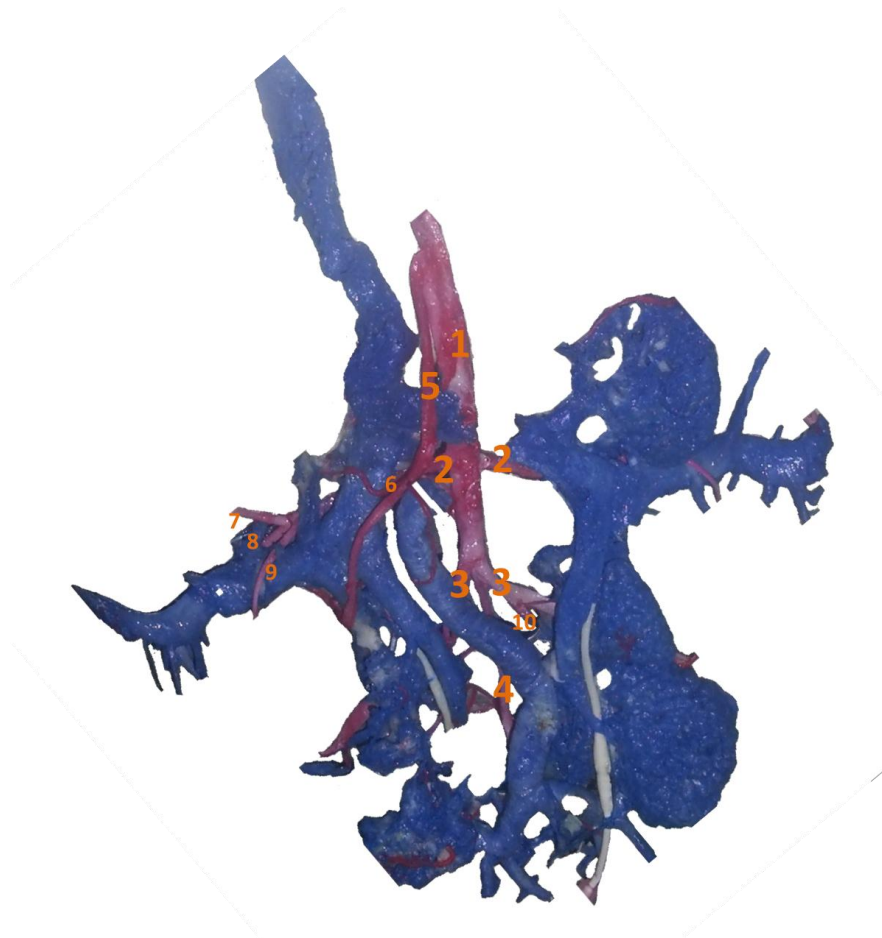
Figure 4-17: Vascular cast of the arteries of the vulture kidney (ventral view). 1 *aorta*; **2** *a. iliaca externa dext.* **and** *sin.*; **3** *a. ischiadica externa dext.* **and** *sin.*; **4** *a. sacralis*; **5 a. common stem of the** *a. renalis cranialis dextra* **and** *sin.*;**6 branch of the** *a. renailis cranialis dext.* **and** *sin.*; **7** *a. circumflexa femoris*; **8** *a. glutaea*; **9** *a. pelvina*; **10** *a. renalis caudalis.*
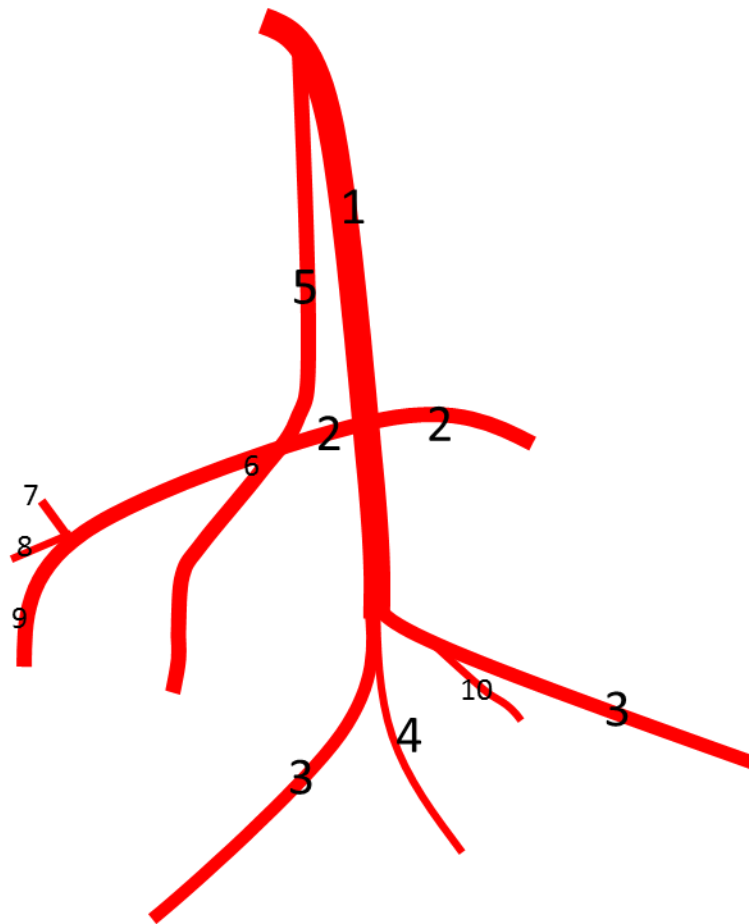
Figure 4-18: Line diagram of the arteries visible. 1 *aorta***; 2** *a. iliaca externa dext.* **and** *sin.***; 3** *a. ischiadica externa dext.* **and** *sin.***; 4** *a. sacralis***; 5 a. common stem of the** *a. renalis cranialis sin.***; 6 branch of the** *a. renalis cranialis dext.* **and** *sin.* **7** *a. circumflexa femoris***; 8** *a. glutaea***; 9** *a. pelvina***; 10** *a. renalis caudalis.*
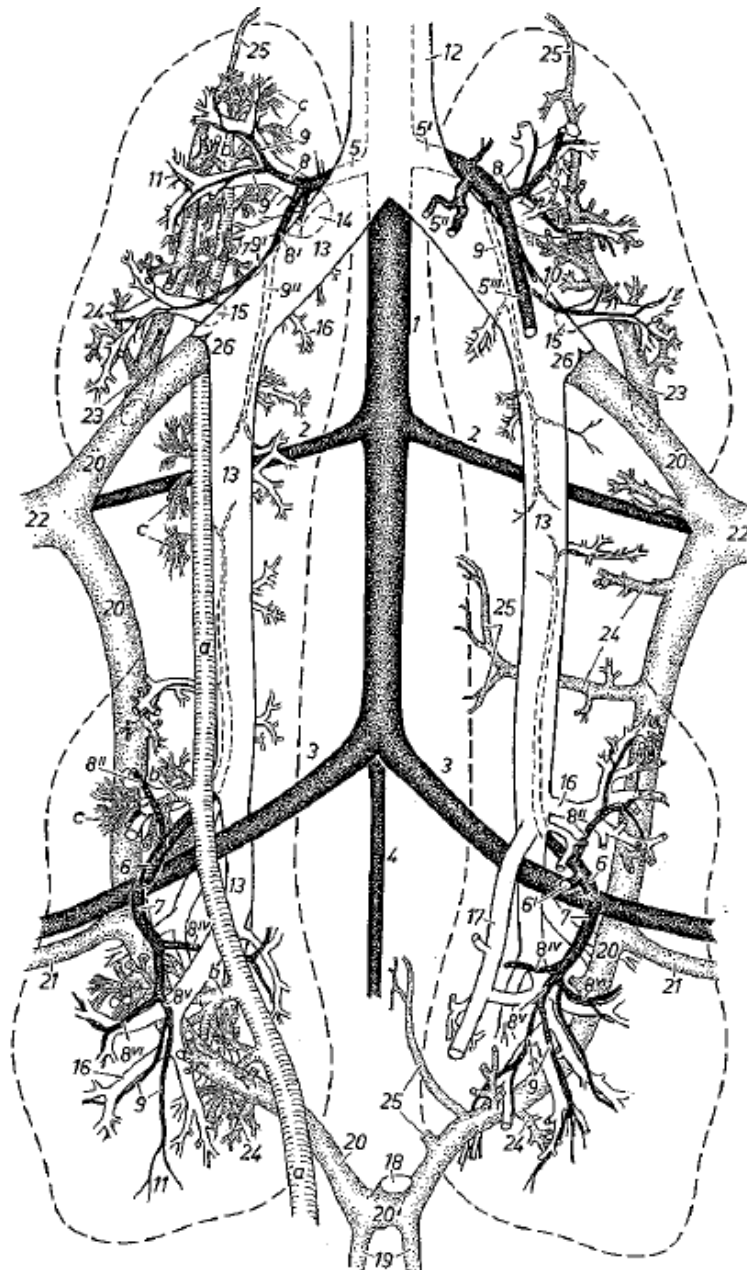
Figure 4-19: *Aorta descendens* and branches in the chicken. *a* ureter; *b* branch of the *ureter*; *c* collecting duct *1 Aorta descendens*; *2, 2 a. iliaca externa dext.* and *sin.*; *3, 3 a. ischiadica externa dext.* and *sin.*; *4 a. sacralis*; *5 a. renalis ·cranialis dext.*; *5′* common stem of the *a. renalis cranialis sin.*; *5″ a. ovarica* and *5‴ a. oviduct cran*ialis; *6, 6 a. renalis media dext.* and *sin.*, *6′* a. oviducta media; *7, 7 a. renalis caudalis dext.* and *sin.*; *8, 8′, 9, 9′, 9″, 10, 11* branches of the *a. renalis cranialis dext.* and *sin.* (5, 5′); *8″* branch of the *a. renalis media* (**6**); *8[iv-vi], 9, 11* branches of the *a. renalis caudalis* (**7**); *12 v. cava caudalis*; *13, 13 v. renalis efferens dext.* and *sin.*; *14,15, 16* branches of the *v. renalis efferens dext.* and *sin.*; *17 v. oviducta caud*alis; *18* stump of the *vv coccygomcsenterica* (Caudal mesenteric vein); *19 v. hypogastrica*; *20,20 v. renalis afferens dext.* and *sin.*; *20′* anastomosis between the *v. renalis afferens dext.* and *sin.*; *21 V. ischiadica*; *22 v. iliaca ex*terna; *23, 24* branches of the *vv. renalis afferentes*; *25* branches from the intervertebral veins; *26* valve (**Nickel et al, 1977.**)

64

The major veins of the vulture kidney are annotated in Figure 4-20 and as a line diagram in Figure 4-21. On the right the *v. iliaca externa* from the hind leg enters the abdominal cavity cranial to the *os pelvis* and divides on entering the kidney to form the *v. iliaca communis* and the *v. renalis portalis caudalis* which enters in the parenchyma of the middle and caudal lobes. The *v. renalis portalis caudalis* varied in its exit from the *V. iliaca communis*, exiting slightly caudo-dorsal (under) to the *v. renalis caudalis* or slightly cranio-medial (adjacent) to it (Figure 4-20). The latter was a major difference on the left side, where the *v. renalis portalis caudalis* always exited from the *v. iliaca communis* caudo-laterally to the *v. renalis caudalis*. Cranially the *vv. Iliacae communii sin.* and *dext.* unite to form the *vena cava caudalis.* Immediately prior to the junction of the common iliac veins the *v. renalis cranialis* arose and entered the craniomedial aspects of the *divisio renalis cranialis dext.*

The *v. renalis portalis cranialis* arose from the *v. iliaca communis* lateral to the entry of the *v. portalis caudalis renalis.* The *v. portalis caudalis renalis* is not evident from the *facies ventralis* and transverses within the parenchyma of the kidney. At their caudal ends, the two *vv. renales portales caudales* form a circumflex bilaterally before merging on the midline to form an *anastomosis interiliaca* to which the *v. mesenterica caudalis* (also referred to as the *v. coccygeomesenterica*) joins at their junction. Also joining the *anastomosis interiliaca* are the *v. iliaca interna* and *v. hypogastrica.* These portal vessels form the renal portal venous ring spanning the *facies ventralis*s of both kidneys, which is well described in other avians. In comparison to the chicken, the ventral topography of the vulture appeared to be almost identical with the only difference being the entrance of the *v. portalis renalis caudalis* and *v. renalis caudalis* into the *v. iliaca communis* which in the chicken were described as being the same on both the right and left sides (Figure 4-22).

65
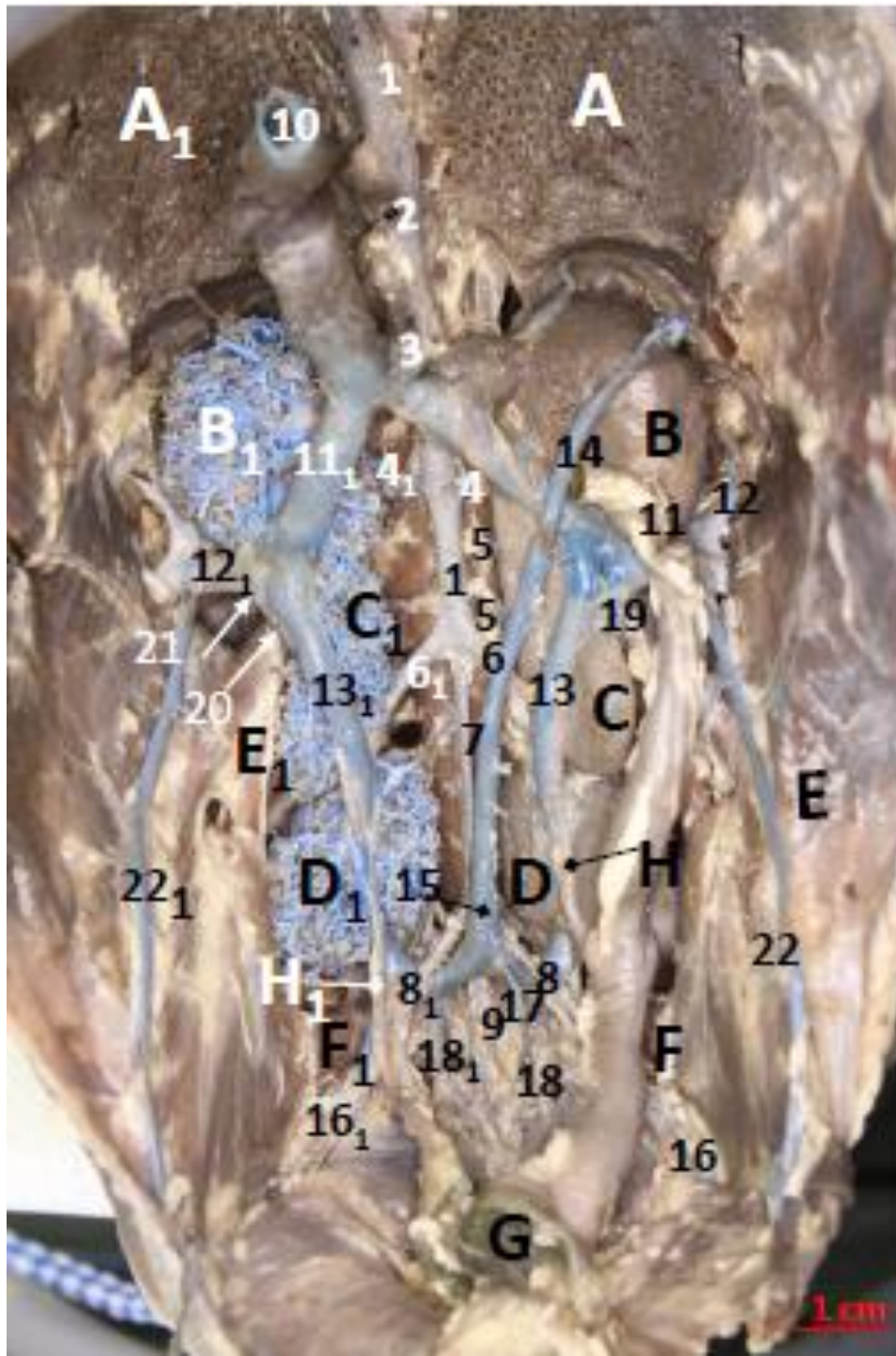
Figure 4-20: Veins of the vulture kidney following vascular casting. A, A₁ lungs, *sin*. and *dext*., B, B₁
divisio renalis cranialis, sin. and *dext*., C, C₁ divisio renalis media, *sin*. and *dext*., D, D₁ *divisio renalis*
caudalis sin. and *dext*., E, E₁ *crista iliaca obliqua sin*. and *dext*., F, F₁ *pila postrenalis sin*. and *dext*., G
rectum, reflected. H, H₁ *ureter sin*. and *dext*. 1 *Aorta descendens*, 2 *a. coeliaca*, 3 *a. mesenterica cranialis*, 4,
4₁ *a. iliac externa sin*. and *dext*., 5 *aa. sacrales*, 6, 6₁ *a. ischiadica externa sin*. and *dext*., 7 *a. sacralis*, 8, 8₁ *a.
iliaca interna sin*. and *dext*., 9 *a. mediana caudae*,10 *vena cava*, 11, 11₁, *v. iliaca communis sin*. and *dext*., 12,
12₁ *v. iliaca externa sin*. and *dext*., 13, 13₁ *v. renalis caudalis sin*. and *dext*., 14 *v. mesenterica caudalis*, 15
anastamosis interiliaca, 16, 16₁ v. *iliaca interna sin*. and *dext*., 17 *v. efferentes sinus intervertebralis*, 18, 18₁
v. hypogastrica sin. and *dext*.. 19, *v. renalis portalis caudalis sinistra*, 20, point at which the *v. renalis
portalis caudalis dextra*. exits the *v. iliaca communis* OR 21, point at which the *v renalis accessorius dextra*.
could exit the *v. iliaca communis*, 22, 22₁ *v. pelvina sin*. and *detr*.

66
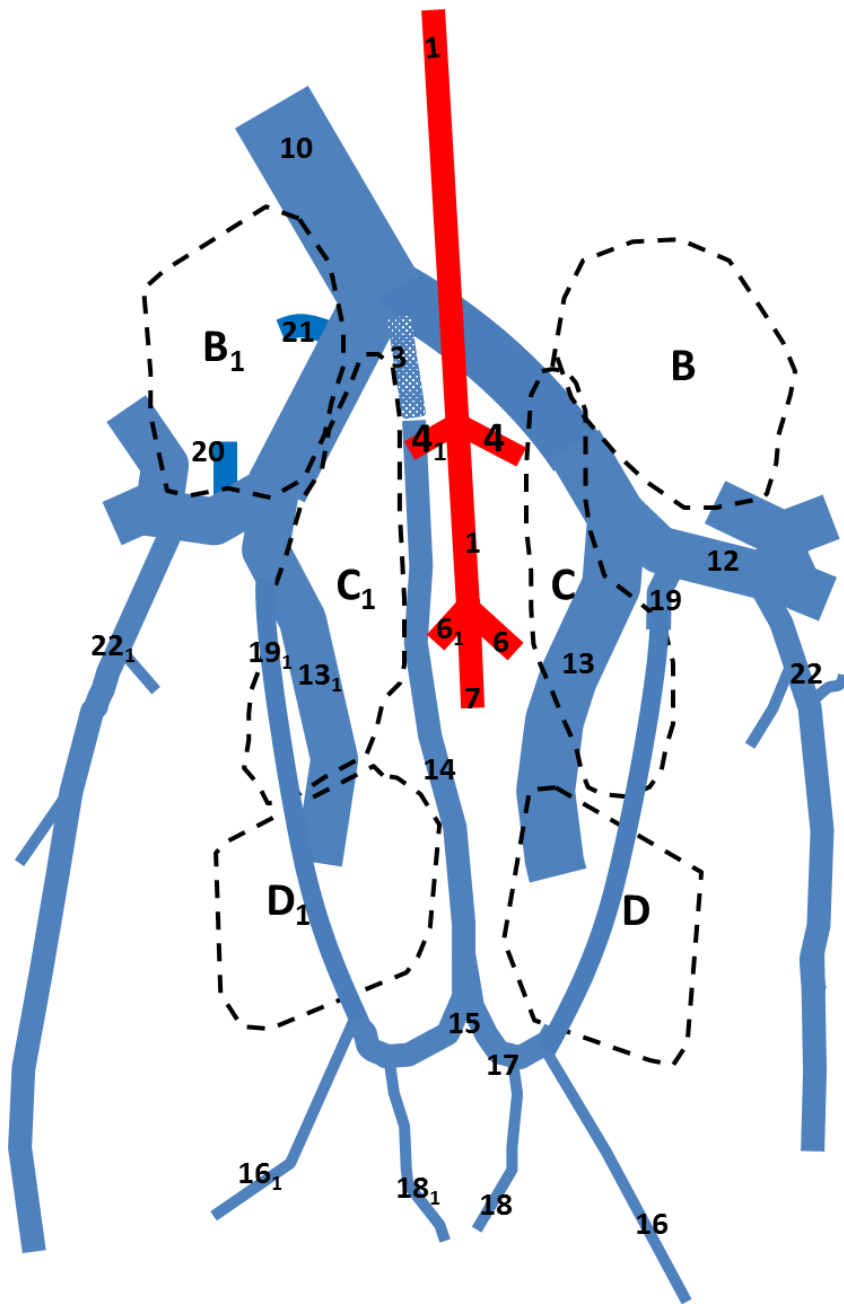
Figure 4-21: Line diagram of the venous vasculature of the vulture from the *facies ventralis* visible after removal of the tissue around the vasculature cast. B, B$_1$ *divisio renalis cranialis, sin.* and *dext.*, C, C$_1$ *lobalis renalis media, sin.* and *dext.*, D, D$_1$ *divisio renalis caudalis sin.* and *dext.*, 1 *aorta caudalis*, 4, 4$_1$ *a. iliac externa sin.* and *dext.*, 6, 6$_1$ *a. ischiadica externa sin.* and *dext.*, 7 *a. sacralis*, 10 *vena cava*, 11, 11$_1$, *v. iliaca communis sin.* and *dext.*, 12, 12$_1$ *v. iliaca externa sin.* and *dext.*, 13, 13$_1$ *v. renalis caudalis sin.* and *dext.*, 14 *v. mesenterica caudalis*, reflected cranially, 15 *anastamosis interiliaca*, 16, 16$_1$ *v. iliaca interna sin.* and *dext.*, 17 *v. efferentes sinus intervertebralis*, 18, 18$_1$, *v. hypogastrica sin.* and *dext.*, 19, 19$_1$ *v renalis portalis caudalis sin.* and *dext.* 20, *v. renalis portalis cranialis dext.* 21, *v. renalis cranialis dext.* 22, 22$_1$, *v. pelvina sin.* and *detr.*

67
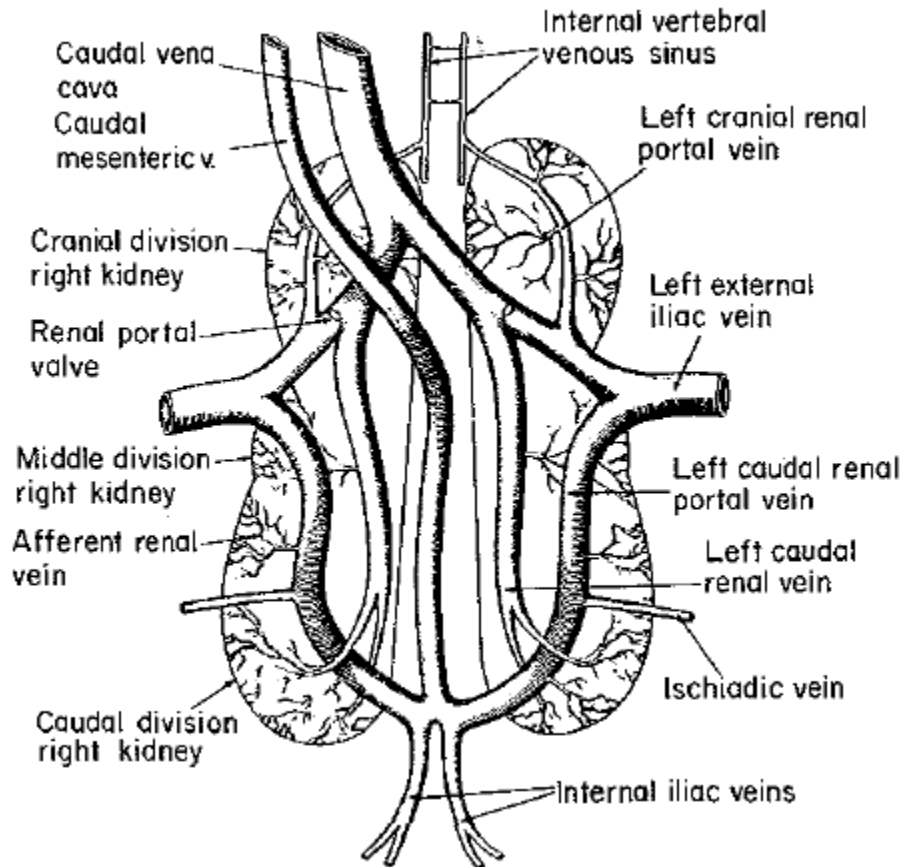
Figure 4-22 Illustration of the veins of the kidney of the chicken (Akester, 1967)

4.4. Renal Portal Valve

The *valva renalis portalis* was opens into the lumen of the *v. iliaca communis* between the *v. renalis caudalis* and the *v. renalis caudalis*. The valve was conical in shape with the apex appearing wider than its base (Figure 4-23). The apex of the valve was characterised by finger-like processes. The valve itself was also hollow. The valve was identical to the description of those present in the chicken as described by Akester (1964).

68
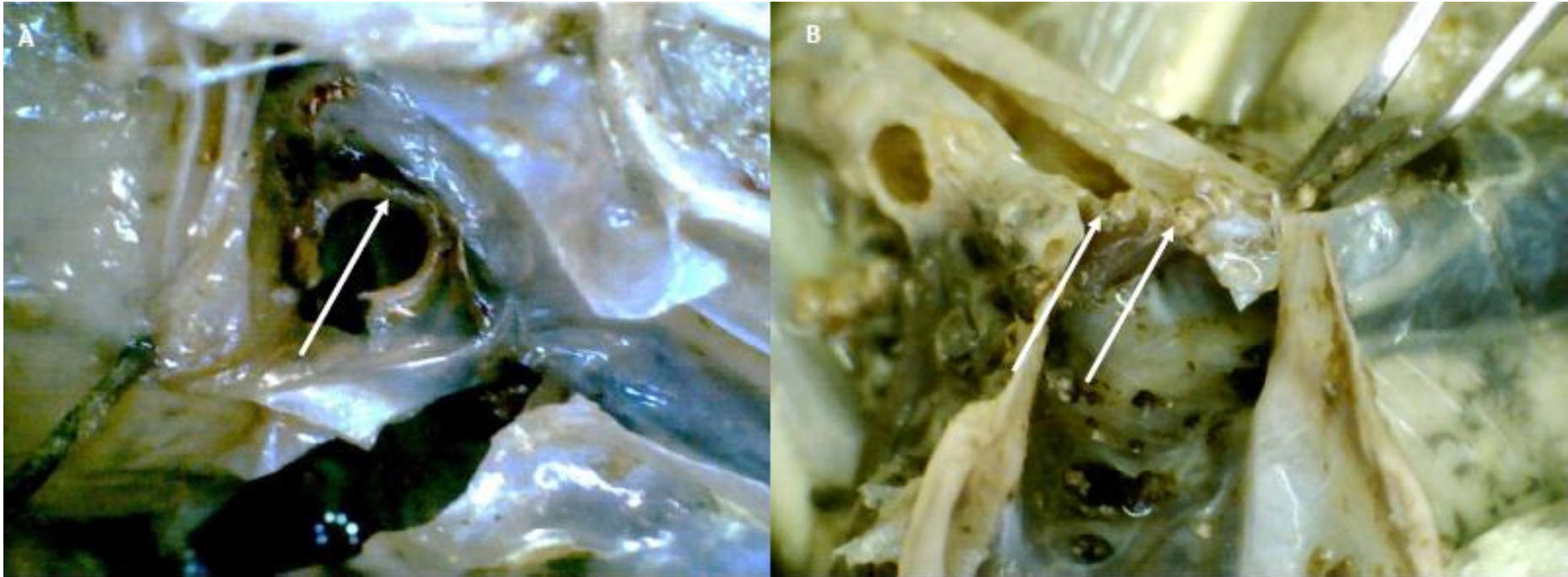
Figure 4-23: Picture of the *valva renalis portalis* in the *v. iliaca communis*. A – shows the ring- like appearance of the valve; B – shows the finger-like projections (Arrows) at the apical surface into the lumen of the *v. iliaca communis*

69

4.5. Histology

The kidney was made up of *cortex renalis* and *medulla renalis*. Unlike in mammals, the *cortex renalis* was larger and far more extensive than the *medulla renalis* (Figure 4-24), with no contiguous distinct cortico-medullary junction, but rather was composed of cloud-shaped cortex surrounding a medullary cone (Figure 4-25). This was similar to the findings of Warui (1989) who evaluated the kidneys of fourteen avian species from six orders. In this study the *medulla renalis* formed only 5-15% of the total kidney volume, 10-13% was blood vessels larger than capillaries, 0.3-5% was formed by the ureter and ureteral ducts, and the *cortex renalis* the remaining 70-80% (Warui, 1989). The cortex and medulla were arranged in cones that are analogous to the outer medulla of the mammalian kidney (Nabipour, et al, 2009)(Figure 4-28).
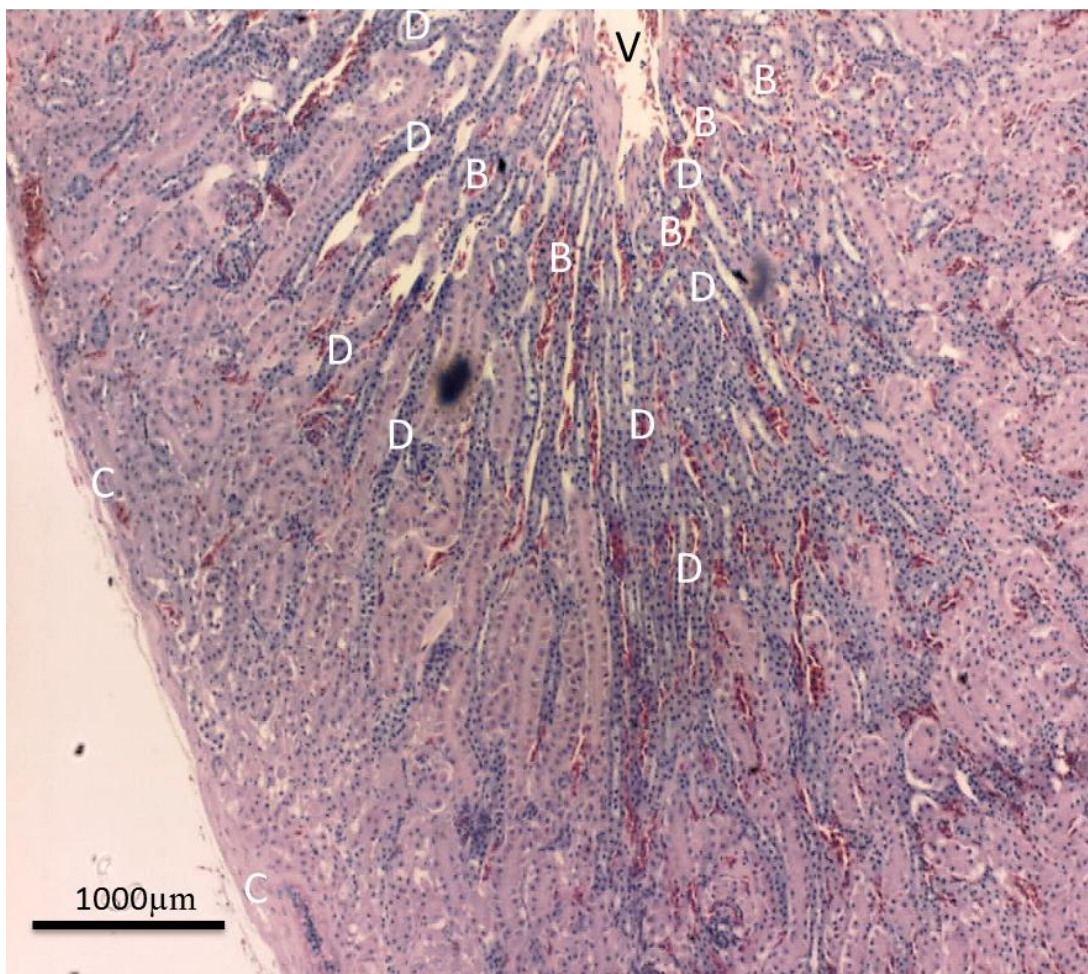
Figure 4-24: Cortex of the kidney of *G. coprotheres*. Visible around the *vena intralobularis* (V) are cortical collecting ducts (D) and blood in the peritulular plexus (B). The connective tissue capsule (C) is visible surrounding the kidney lobe. 40x magnification.

70

4.5.1. *Capsule*

The kidney was covered by a thin capsule of connective tissue comprised of collagen fibres. Subcapsular venous sinuses were present and contained red blood cells (Figure 4-25).
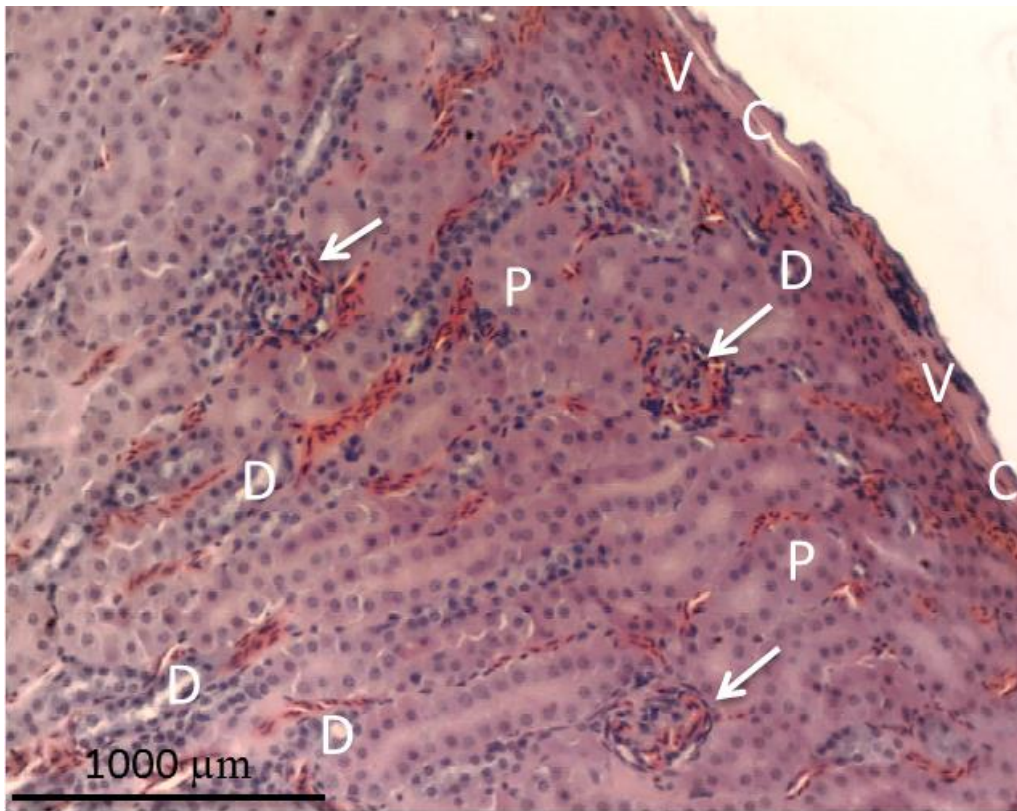
Figure 4-25: Capsular surface of the kidney. Subcapsular venous sinuses (V) are visible below the collagen fibres of the connective tissue capsule (C). Reptilian nephrons are visible (white arrows). The proximal convoluted tubule (P) lacks a distinct lumen as it is filled with eosinophilic microvili. The distal convoluted tubules (D) stain more basophilic than the proimal convoluted tubules, lack brush border microvili and have a clear lumen. 100x magnification.

4.5.2. *The Cortex renalis*

The *cortex renalis* was made up of nephrons of three different sizes. The majority of the *cortex renalis* was made up of convoluted tubules, both distal and proximal; and the cortical collecting ducts:

- Nephrons: Three nephrons were identified by the size of their *glomerulus*. While all three structures appeared to be similar, they differed in size and number of cells. Based on description of Batah, (2012) the smallest corpuscles, nearest the cortical surface, were identified as reptilian nephrons. The reptilian nephrons are devoid of a loop of Henlé and the entire structure lies in the *cortex renalis*. While the tubules are distributed randomly, Nabipour and associates found that most of the reptilian

71

glomeruli were located peripherally and the distal tubules around the *vena intralobularis* (Nabipour, et al, 2009). Closer to the *medulla renalis* were the two other types of glomeruli of intermediate and larger size (Figure 4-26). Based on their size difference relative to the reptilian *glomerulus*, they were identified as the intermediate and mammalian nephrons respectively. Unlike the reptilian nephron, the mammalian nephron has a loop of Henlé, which extends into the *medulla renalis* the large renal corpuscles of medullary nephrons lie close to the *medulla renalis*.
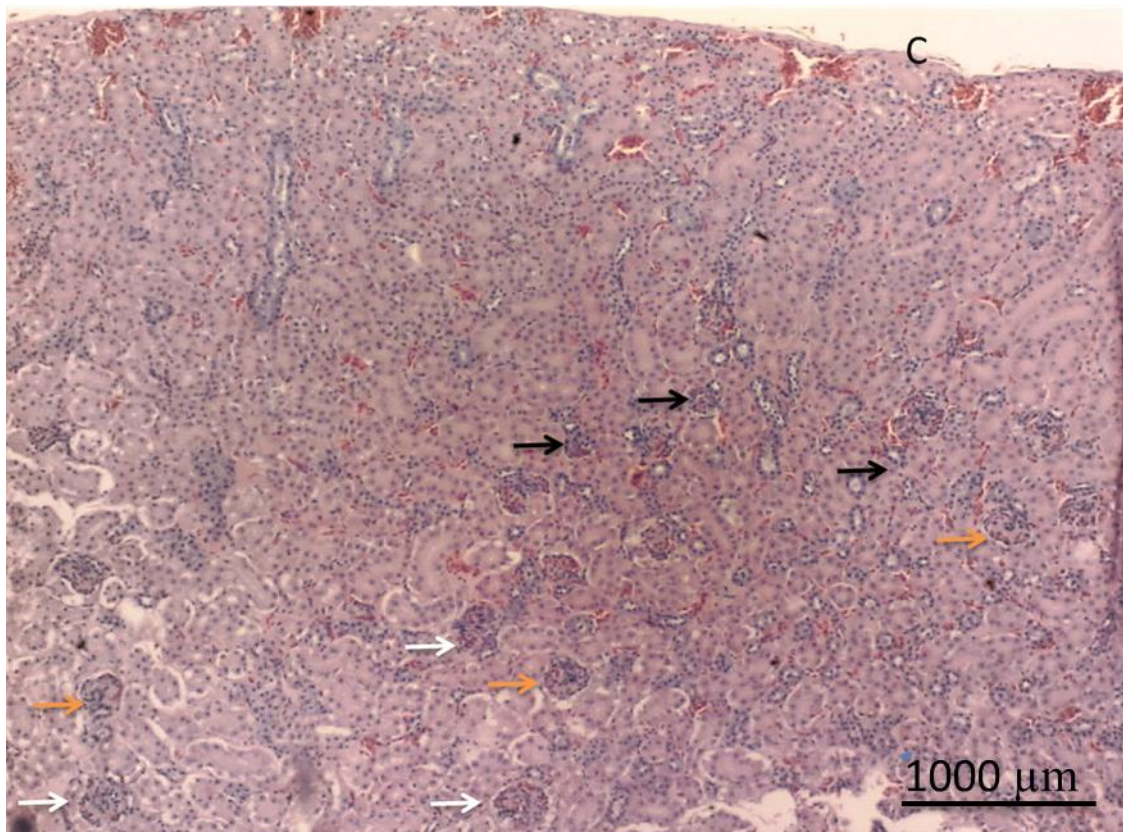
Figure 4-26: Cortex of the kidney of *G. coprotheres*. Three sizes of glomerulus are present, namely reptilian (black arrows), intermediate (orange arrows) and mammalian (white arrows). C- capsular surface of the renal lobe. 40x magnification.

- <u>Renal Corpuscle:</u> The renal corpuscle was fairly round, and comprised of a central *glomerulus* made up of tightly grouped central mesangial cells with their smaller basophilic nuclei, while at their periphery were podocytes with larger basophilic nuclei and eosinophilic cytoplasm that surrounded the mesangial cells and their protruding finger-like processes associated with the capillary loop (Figure 4-27). The *glomerulus* was surrounded by the urinary space (Bowman's space) and the Bowman's capsule comprised of deeply basophilic squamous epithelial cells. This is

consistent with Naipour et al (2009). The *glomerulus* was connected to two blood vessels, separated by a tubule with an open lumen. The tubule in question was flattened at the point it attached to the capsule. Based on studies in other avian species, the first arteriole was identified as the afferent arteriole by the presence of different nuclei identified as macula densa cells at the point of attachment to the capsule.
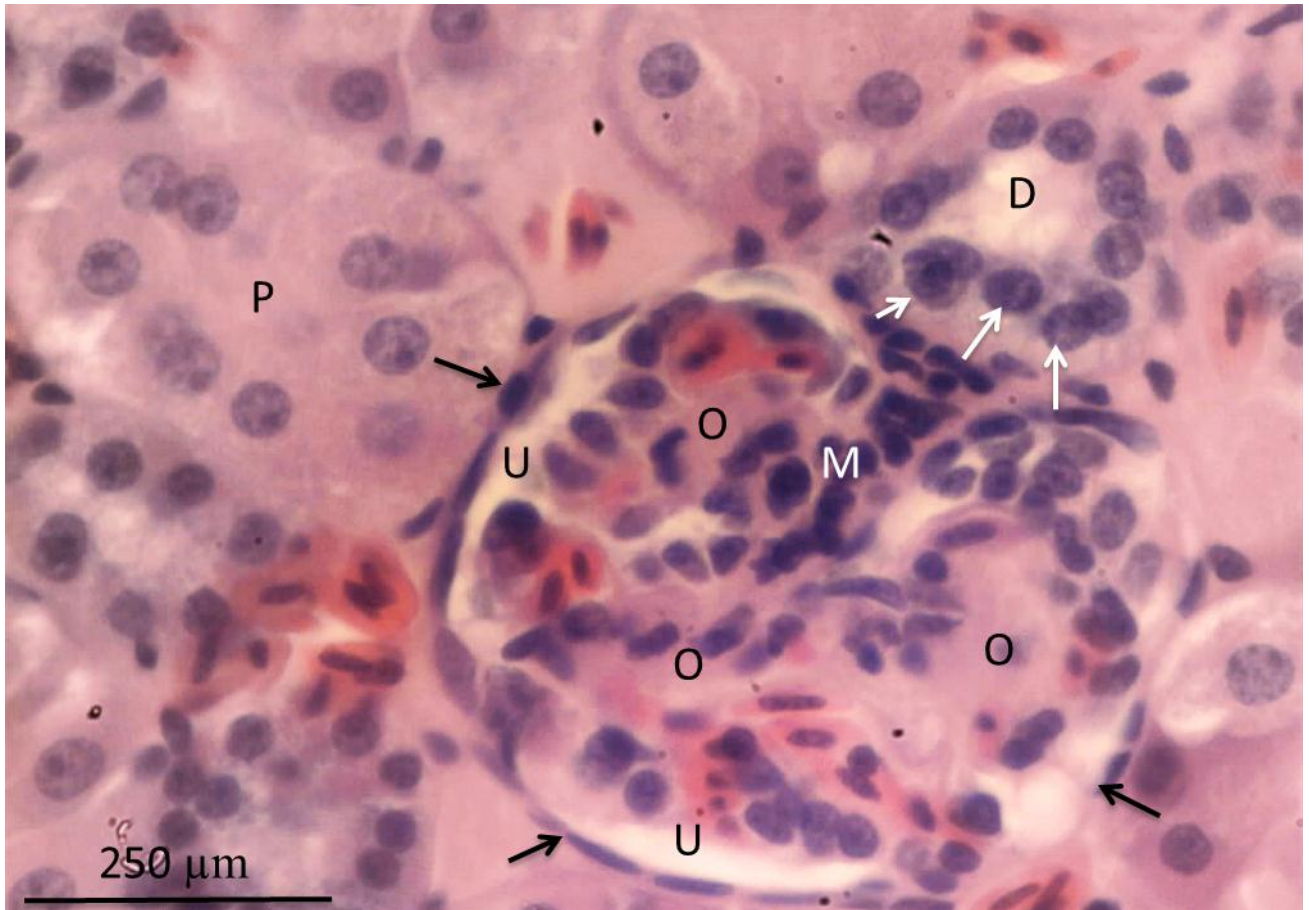
Figure 4-27: Mammalian glomerulus of *G. coprotheres*. O- Podocytes. U- urinary space. D- distal convoluted tubule. P- proximal convoluted tubule. White arrows indicating macula densa cells in the distal convoluted tubule. Black arrows indicating the glomerular capsule. Ms- mesangeal cells. A- afferent arteriole associated with the proximal convoluted tubule. 400x magnification.

- **Proximal Convoluted tubules:** The proximal convoluted tubule (PCT) was made of eosinophilic columnar epithelial cells (Figure 4-27). The proximal tubule was identified as such by the absence of a clearly evident lumen, which is mostly due to the presence of a large number of apical microvilli forming a brush border (Batah, 2012). The cells were separated by clearly visible cell junctions. This was similar to

73

chicken (Casotti et al., 2000; Cazmir et al., 2008) but different to the findings of Nabipour who described the PCT cells as cuboidal in the rock dove, collared dove and owl and that of Batah who described the cells as simple low cuboidal in the coot bird.

- **<u>Distal convoluted Tubules:</u>** The tubule attached to the glomerular capsule was identified as the distal convoluted tubule (DCT) based on descriptions from other avian species viz. the more basophilic columnar epithelial cells (Nabipour, 2009), presence of an empty lumen, lack of microvilli at the apical pole and attachment to the capsule (Figure 4-27). The macula densa cells, evident by their basal nucleus and darker staining, in comparison to the rest of the tubule (Figure 4-27), were attached to the vascular pole of the *glomerulus* at the DCT. The macula densa therefore marks the origin of the DCT (Cazmir, et al, 2008).

- **<u>Cortical Collecting Ducts:</u>** Numerous tubules with clear lumens and simple to low cuboidal cells that were darker staining were present around a large *v. interlobularis* that was surrounded by concentric glomeruli (Figure 4-24). Based on their pattern, they were identified as the cortical collecting ducts of the reptilian nephrons. These were different to that of the chicken, for which the cells were described as cuboidal to low columnar and different staining to the PCT and DCT (Nabipour, 2009)

- **<u>V. interlobularis:</u>** Identified as the large vein (Figure 4-24) present in the center of the *cortex renalis* and surrounded by the collecting tubules.

4.5.3. *The Medulla renalis*

The *medulla renalis* was composed of groups of tubules, properly delineated from each other by a fibrous tissue sheath (Figure 4-28). These corresponded to the description of the medullary cones of other avian kidneys (Bacha & Bacha, 2012). Within each cones, three tubules of different sizes were present (Figure 4-29 and Figure 4-30). Although all three tubules were lined by cuboidal epithelial cells, lumen size varied. The largest were suspected to be collecting ducts, while the two smaller were believed to be the ascending and descending loops of Henle. For the loop of Henlé cells, the larger was twice the diameter of

74

the smaller. In addition the smaller tubules' cells were darker staining. Due to the size difference, the larger were identified as the thick loop of Henlé and the smaller as the thin loop of Henlé (Casotti, 2000)
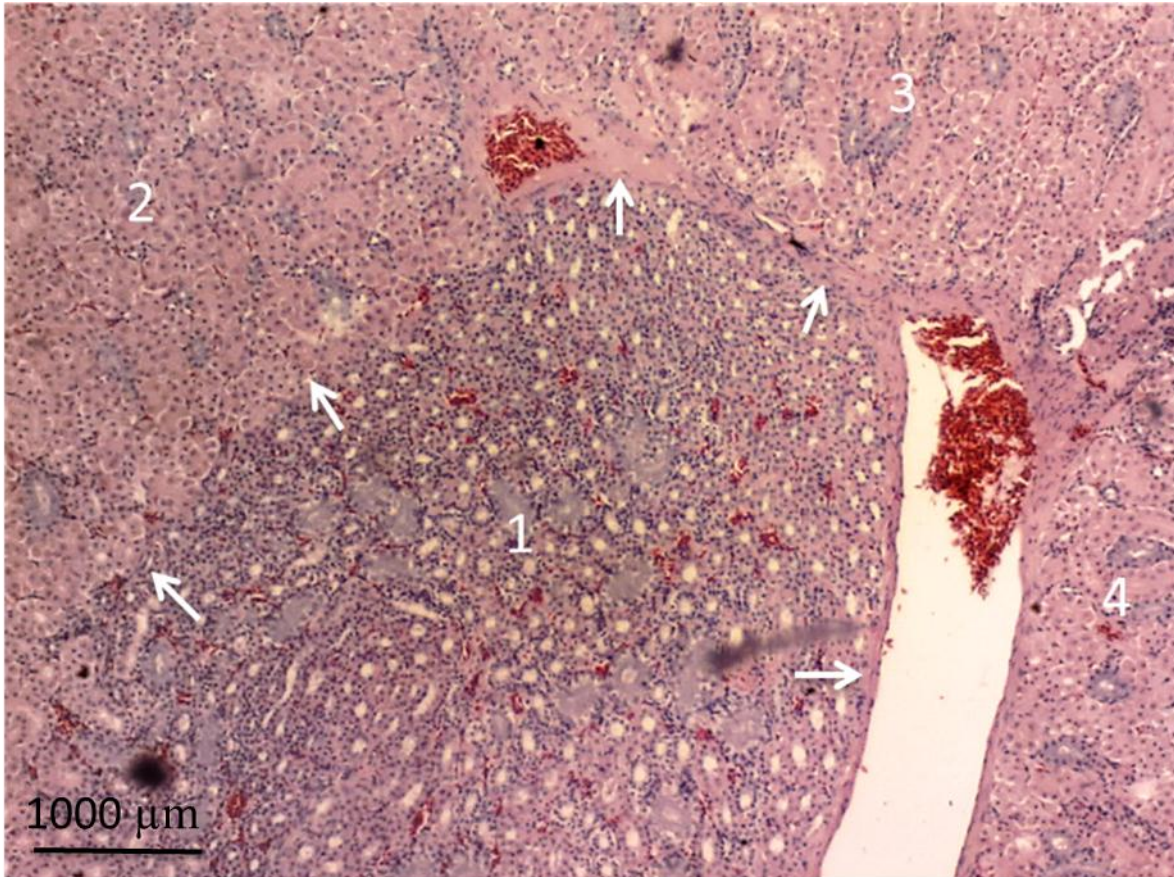
Figure 4-28: Four (1-4) *lobuli renales* from the kidney of *G. coprotheres*. The connective tissue sheath surrounding each *lobulus renalis* (white arrows) indicates that this is a medullary cone. 40x magnification.

75
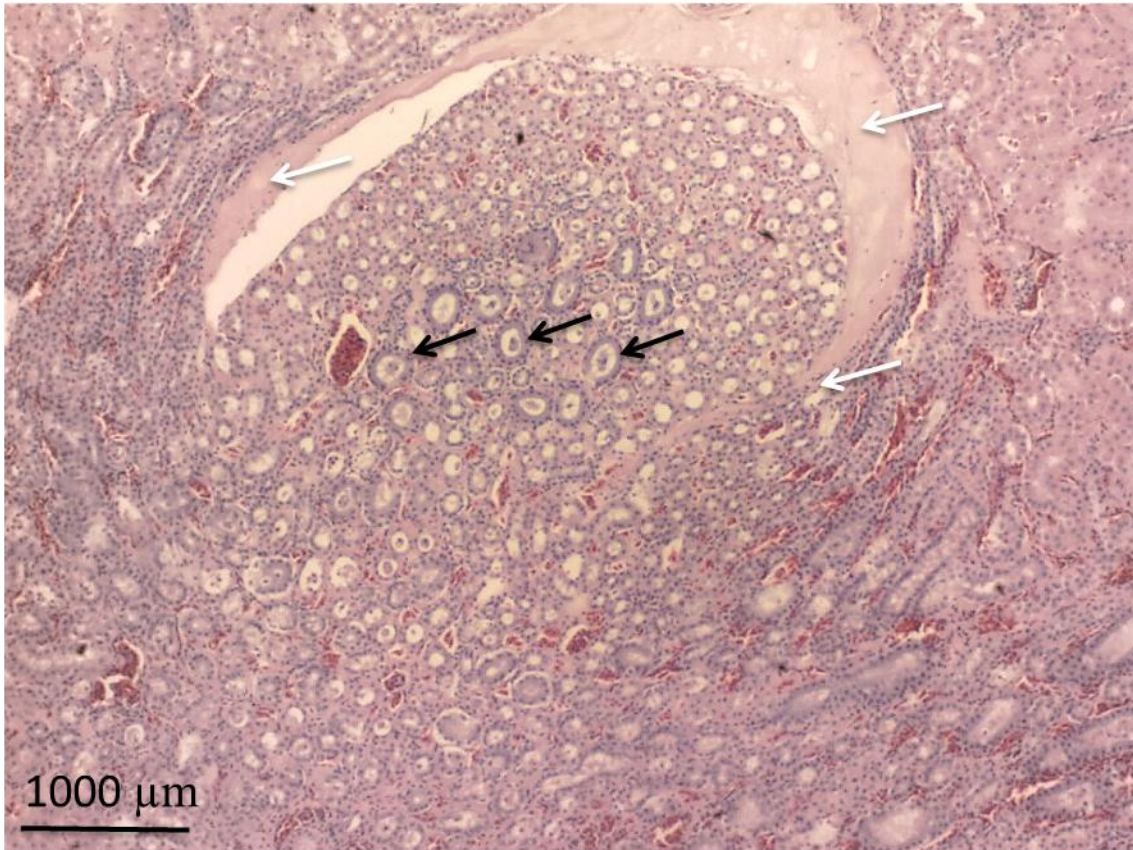
Figure 4-29: Cross-section of a medullary cone of the kidney of *G. coprotheres*. Black arrows indicate collecting ducts which stain more basophilic than the ascending and descending loops of Henlé, which cannot be differentiated at this magnification. White arrows indicate the connective tissue sheath surrounding cone. 40x magnification.

76
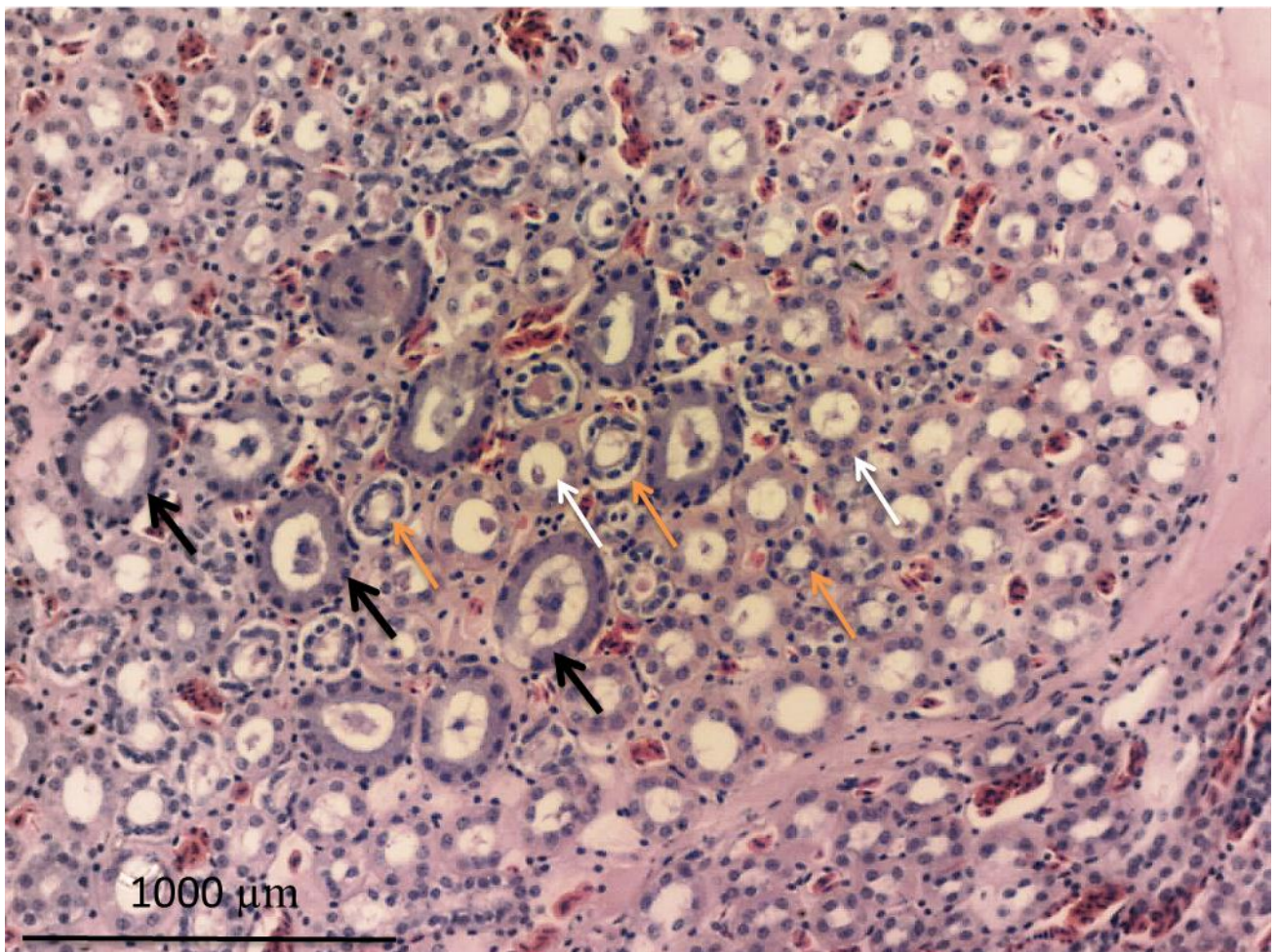
Figure 4-30: Medullary cone (100x magnification). Collecting ducts (Black arrows) and thick ascending loops (White arrows) of Henlé have clear cytoplasmic blebs, whereas thin descending loops of Henlé have a clear lumen (Orange arrows).

4.5.4. *Histology of the Valve*

The valve was easily found in the lumen of the *v. iliaca communis*. On cross section, the valve was made up predominantly of smooth muscle and was lined by a layer of endothelial cells (Figure 4-31 and Figure 4-32). The valve was both vascularised and well innervated. The valve looked identical to the valve described in the chicken. Two prominent nerve plexus was present next to the valve (Figure 4-33). The latter agreed with the description of Akster & Mann (1969), who described the renal portal valve as being the only intravascular structure in any invertebrate species to be comprised mainly of smooth muscle and to have a rich nerve

77

supply comprising of a double innervation viz. adrenergic and cholinergic. Gilbert (1961) described considerable innervation to the basal two-thirds of the valve with large trunks in the basal third giving off fine bundles to the middle third (Figure 2-5). He also described the apical third of being comprised of epitheloid cells and collagen fibres. Akster and Mann (1969), however, described a more uniform distribution of smooth muscle throughout the valve without large nerve trunks within the basal third of the valve, which is more consistent with the findings of this study.
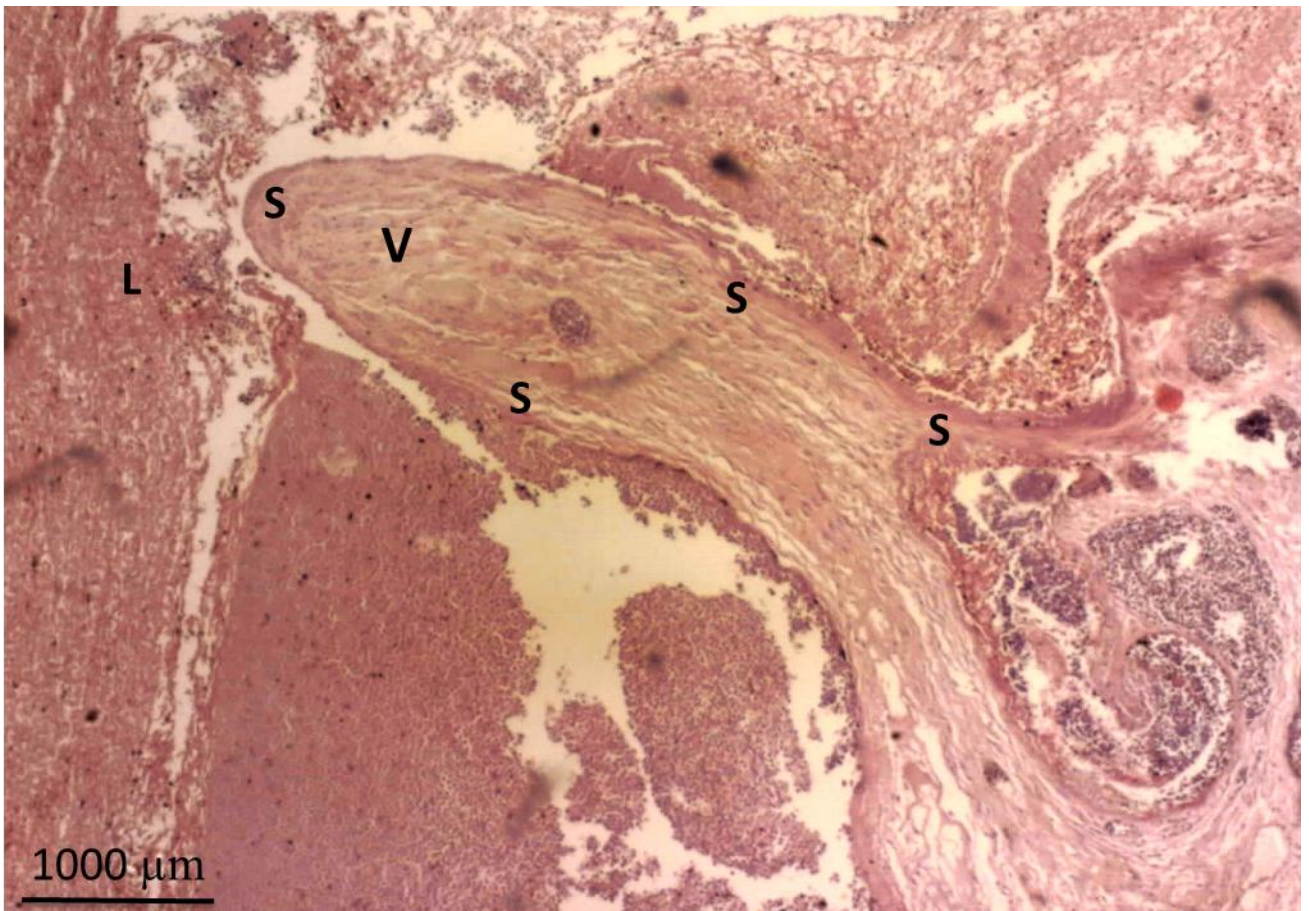
Figure 4-31: Cross-section of the well-vascularised *valva renalis portalis (V)* in *G. coprotheres*. L- lumen of *v. iliaca communis*. The smooth muscle fibres that comprise the majority of the valve are clearly evident (S). Magnification 40x.
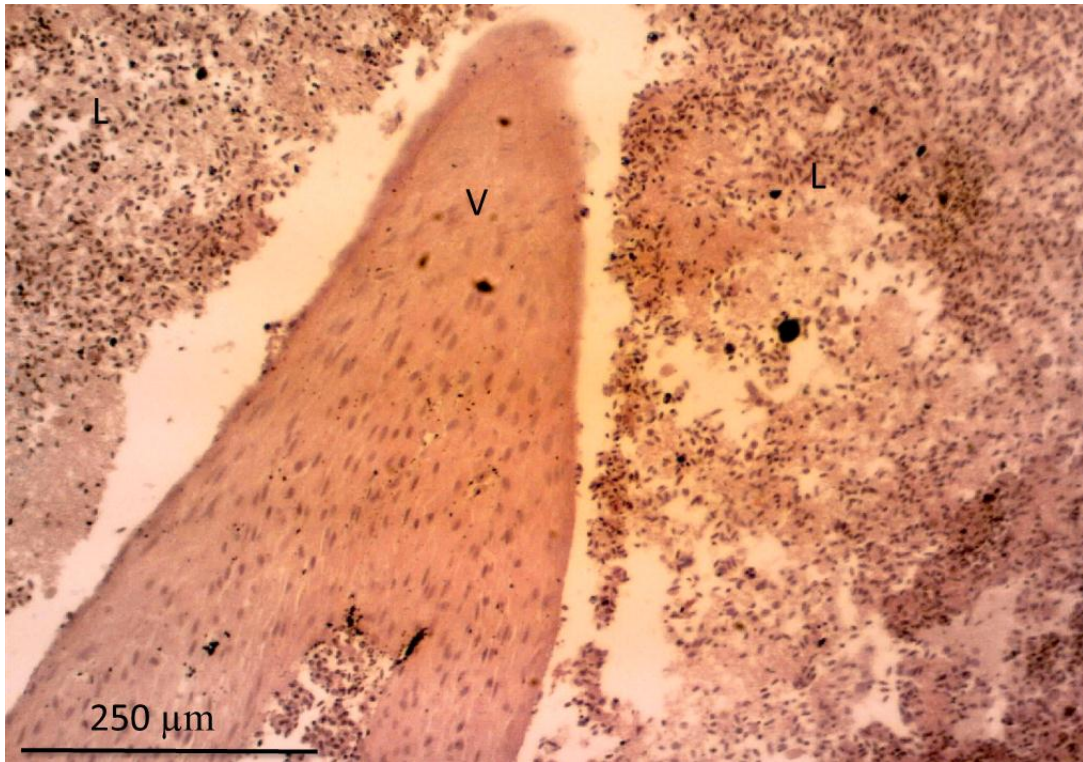
Figure 4-32: Magnification of a valve leaflet (400x) illustrating the smooth muscle (S0 composition of the *valva renalis portalis* **(V) in the lumen of** *v. iliaca communis* **(L).**
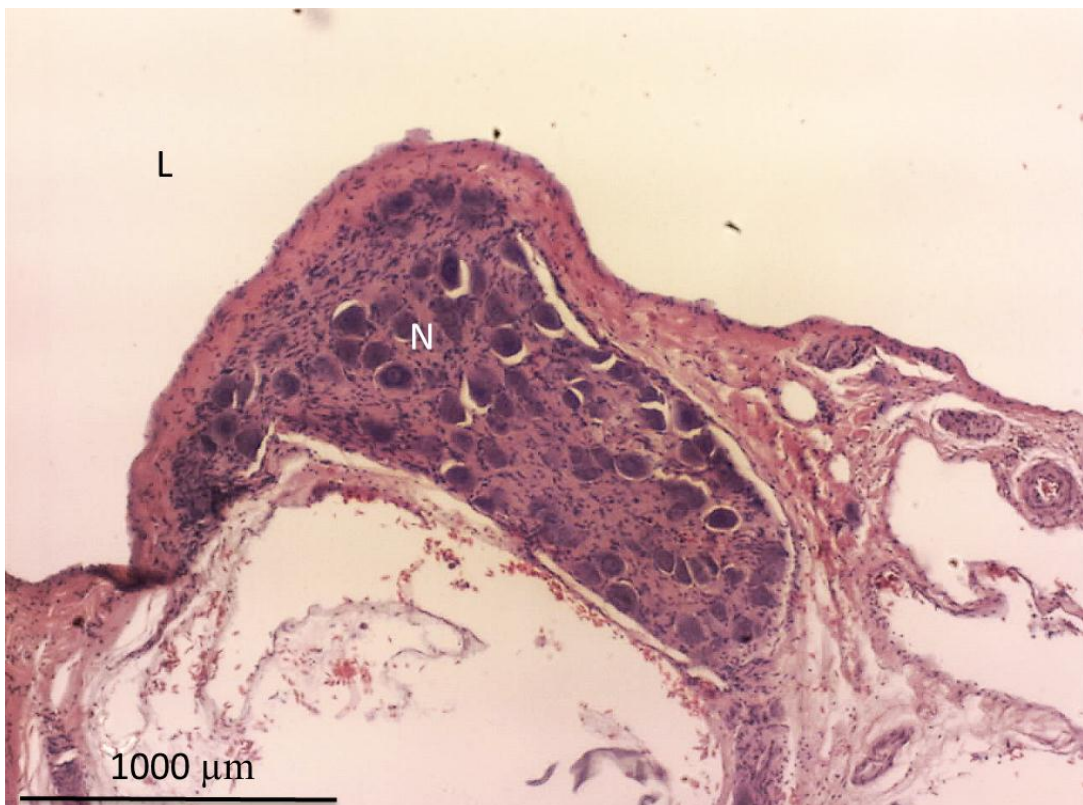
Figure 4-33: Smooth muscle and endothelium overlying a large nerve plexus (N) found in cross-section near the *valva renalis portalis* **of** *G.coprotheres***. L- lumen of** *v. iliaca communis* **(100x magnification).**

79

5. General Discussion

In the 1990's, a major catastrophe hit the vulture populations on the Asian subcontinent, with millions of birds dying through their inadvertent exposure to diclofenac in the food chain, making diclofenac one of the most toxic substances identified in a bird species. While the deaths of vultures were clearly evident, the mechanism behind their death remained unknown. All that was evident on necropsy was severe visceral and articular gout and associated urate tophi causing renal and hepatic necrosis. With the mechanism being unknown, a few suppositions were put forward to explain the toxicity. In one of the theories, Meteyer et al (2005), postulated that the acute necrosis of the proximal convoluted tubules in the cranial lobes, seen on histopathology, was likely caused by ischaemia. She also speculates that the effect could be due to the abnormal functioning of the *valva renalis portalis*. The valve has been a bit of an enigma, with current literature suggesting that the valve allows for shunting of venous blood from the hind limb to the vena cava instead of the cranial renal lobe to increase cardiac output in times of stress, or alternatively to protect the cranial lobe from hyperperfusion when the muscular pump of the hind limbs are active during exercise (Gilbert, 1961). Meteyer speculated that if the former mechanism was in place, diclofenac could potential induce shunting away from the renal lobe, resulting in hypoperfusion, ischaemia and necrosis of the cranial lobe. While Meteyer's theory appears plausible, the *valva renalis portalis* has only been described in a small number of other bird species such as the chicken and ostrich (*Struthio camelus*), which actually has 6 *valvae renales portales* (de Carvalho, et al. 2007). The aim of this study was to therefore evaluate the renal anatomy and related vasculature, in order to establish the merit of Meteyer's theory, with special attention being given to comparison to the domestic chicken.

As expected the kidneys of the vulture were present within the *fossae renales*, and were well attached to the *synsacrum* and the wings of the *ilium*. The kidneys were also of the expected size with most of the kidneys fitting within the entire space of the *fossae renales*, with just the cranial portion of the *division cranialis* lying in the space cranial to the *fossa renalis*. The kidney was trilobular with the *divisio cranialis*, *media* and *caudalis* being readily identifiable on each side of the midline. The three lobes were formed by the pathway of the *v. iliaca communis* between the *divisio media* and *cranialis*, while the *divisio media* and *caudalis* were physically separated by a connective tissue sheath. While this demarcation was much more prominent than in the chicken, the physiological significance of this separation is unknown at

80

this stage. Nonetheless, with the divisions being similar to the red tailed hawk and the lobe not being a functional unit of the kidney (viz. the *lobulus renalis* is the functional unit), it is probably not of physiologically significance.

The vasculature of the vulture appeared to be almost identical to that described in the domestic chicken, with the only differences being the entrance of the *v. portalis renalis caudalis* into the *v. iiaca communis* and the exit of the *v. renalis caudalis* from the *v. iliaca communis*. In the chicken, these vessels were described as being the same on both sides. In the Cape griffon vulture, the *v. renalis portalis caudalis* varied in its exit from the *v. iliaca communis* on the right, exiting slightly caudo-dorsal to (under) the *v. renalis caudalis* or slightly cranio-medial (adjacent) to it, while on the left where the *v. renalis portalis caudalis* always exited the *v. iliaca communis* caudo-laterally to the *v. renalis caudalis*. While this anatomical difference was rather prominent, this difference is probably of no physiological significance, as the blood vessels of the vulture still appeared to supply blood to the same areas as described in the chicken i.e. no difference in supply characteristics were evident. The *valva renalis portalis* was also present in same location and had a similar appearance as described in the chicken. The valve was present in the *v. iliaca communis* between the *v. renalis caudalis portalis* and the *v. renalis caudalis* and appeared as conical shaped, with finger-like processes.

Histologically, the Cape griffon vulture kidney was similar to that to other avian spp, with reptilian, mammalian and intermediate nephrons being evident. The latter was evident by glomeruli being present of roughly three size classes. The kidney also had the expected appearance with the cortex consisting of the glomeruli and the medulla being made up of medullary cones. On cross section the renal portal valve was composed of smooth muscle finger-like projections that protruded into the lumen of the lumen of the *v. iliaca communis*. The valve was well vascularised and was innervated by its own nerve plexus.

6. Conclusion

Based on the findings of this study, the proposed mechanism of toxicity of Meteyer et al. (2005) is anatomically possible. The similarity of the chicken and vulture in their anatomical structure may also explain previous finding that the chicken could serve as a physiological model of the study of the pathophysiology of diclofenac's toxicity.

6. Future Studies

With the *valva renalis portalis* being identified in the Cape griffon vulture, further studies should focus on the importance of the valve in toxicity. One manner in which this can be facilitated would be real time radiographic studies looking at changes in perfusion to the cranial lobe in the presence and absence diclofenac.

82

7. References

1. Abdalla, M. A. & Abdalla, O. (1979). Morphometric observations on the kidney of the camel, *Camelus dromedarius*. *Journal of Anatomy, 129*, 45-50.

2. Akester, A. R. (1964). Radiographic studies of the renal portal system in the domestic fowl (*Gallus domesticus*). *Journal of Anatomy, 98*, 365-376.

3. Akester, A. R. (1967). Renal portal shunts in the domestic fowl. *Journal of Anatomy, 202*, 569-594.

4. Akester, A. R. & Mann, S. P. (1969). Adrenergic and cholinergic innervation of the renal portal valve in the domestic fowl. *Journal of Anatomy*, *104*, 241-252.

5. Almansour, M. I. (2007). Anatomy, histology and histochemistry of the salt lands of the greater flamingo *Phoenicopterus ruber roseus* (Aves, Phoenicopteridae). Saudi Journal of Biological Sciences, 14, 145-152.

6. Anderson, M. D., Mundy, P. J. & Virani, M. Z. (2002). The demise of vultures in southern Asia: research and conservation recommendations for Africa. In Katzner, T. & Parry-Jones, J. (Eds.), *Proceedings of Conservation of* Gyps *vultures in Asia. 3rd North American Ornithological Conference.* New Orleans: United States of America.

7. Anon. (2002). *World agriculture: towards 2015/2030. Summary report.* Rome: Food and Agriculture Organization of the United Nations. Website: ftp://ftp.fao.org/docrep/fao/004/y3557e/y3557e.pdf. 29th May 2011.

8. Anon. (2011). The International Union for Conservation of Nature (IUCN). Website: http://www.iucnredlist.org/. 14th November 2011.

9. Bacha, W. J., & Bacha, L. M. (2012). *Color Atlas of Veterinary Histology*. Chichester. John Wiley & Sons.

10. Batah, A.L. (2012). Morphological and histological study for the kidneys of the coot bird (*Fulica atra*), Basrah Journal of Veterinary Research, 11, 128-136.

11. Baumel, J.J. and Witmer, L.M. (1993). Osteologica. In J. J. Baumel (Ed.), Handbook of Avian Anatomy: Nomina Anatomica Avium (pp. 329-347). Cambridge, Massachusetts: The Nuttall Ornithological Club

12. Burke, A., Smyth, E. M. & FitzGerald, G. A. (2005). Analgesic-Antipyretic-Agents; Pharmacotherapy of Gout. In, Brunton, L., Lazo, J., Parker. K., Buxton. I & Blumenthal, D. (Eds.), *Goodman & Gilman's The Pharmaceutical Basis of Therapeutics* (pp. 671-716). United States of America: McGraw Hill.

13. Burrows, M. E., Braun, E. J. & Duckles, S. P. (1983). Avian renal portal valve: A re-examination of its innervation. *American Journal of Physiology, 245*, 628-634.

83

14. Casotti, G., Beuchat, C. A. & Braun, E. J. (1998). Morphology of the kidney in a nectivrous bird, the Anna's hummingbird *Caypte anna. London Journal of Zoology*, 244, 175-184.

15. Casotti, G. & Braun, E. J. (1995). Structure of the glomerular capillaries of the domestic chicken and desert quail. *Journal of Morphology, 224*, 57-63.

16. Casotti, G. & Richardson, K. C. (1993). A qualitative analysis of the kidney structure of Meliphagid honeyeaters from wet and arid environments. *Journal of Anatomy, 182*, 239-247.

17. Casotti, G., Braun, E. J. & Lindberg, K. K. (2000). Functional morphology of the avian *medulla renalis*ry cone. *American Journal of Physiology: Regulatory Integrative Comparative Physiology, 279*, 1722-2730.

18. Cazmir, I., Cornila, M., Predoi, S., Marta, D. & Constantinescu, C. (2008). Histo- and ultrastructural aspects concerning renal corpuscle in *Coturnix Coturnix Japonica. Lucrari Stiintifice Medicina Veterinara, 41*, 64-72.

19. Cuthbert, R., Parry-Jones, J., Green, R. E. & Pain, D. J. (2007). NSAIDs and scavenging birds: potential impacts beyond Asia's critically endangered vultures. *Biology Letters, 3*, 91-94.

20. Cuthbert, R., Taggart, M. A., Prakash, V., Saini, M., Deverndra, S., Upreti, S., Mateo, R., Chakraborty, S. S., Deory, P. & Green, R. E. (2011). Effectiveness of action in India to reduce exposure of Gyps vultures to the toxic veterinary drug diclofenac. *PLoS ONE 6*, e19069.

21. de Carvalho, H. S., Ciboto, R., Baitelo, C. G., Dias, A. R., & Cortopassi, S. R. (2007). Anatomy of the renal portal system and its implications for the use of anesthetic agents in the restraint of ostriches (*Struthio camelus*). *Coemcoa Rural, Santa Maria, 37*, 1688-1694.

22. Deygout, C., Gault, A., Sarrazin, F. & Bessa-Gomes, C. (2009). Modelling the impact of feeding stations on vulture scavenging service efficiency. *Ecological Modelling, 220,* 1826-1935.

23. El-Gohary, Z. M., Khalifa, S. A., El-Said Fahmy, A. M., & Tag, Y. M. (2011). Comparative studies on the renal structural aspects of the mammalian species inhabiting different habitats. *Journal of American Science,* 7, 556-565.

24. Feinstein, B. (1962). Additional cases of bilobated kidneys in hornbills. *The Auk, 79*, 709-711.

25. Fisher, H. I. (1946). Adaptations and comparative anatomy of the locomotor apparatus of New World vultures. *American Midland Naturalist*, 545-727.

26. Gilbert, A. B. (1961). The innervation of the renal portal valve of the domestic fowl. *Journal of Anatomy*, *95*, 594-598.

84

27. Gilbert, M., Watson, R. T., Ahmed, S., Asim, M. & Johnson, J. A. (2007). Vulture restaurants and their role in reducing diclofenac exposure in Asian vultures. *Bird Conservation International*, 17, 63-77.

28. Goodchild, W. M. (1969). Biological aspects of the urinary system of Gallus domesticus with particular reference to the anatomy of the ureter. MSc Thesis, University of Bristol.

29. Green, R. E., Taggart, M. A., Senacha, K. R., Raghavan, B., Pain, D. J. & Jhala, Y. (2007). Rate of decline of the Oriental white-backed vulture population in India estimated from a survey of diclofenac residues in carcasses of ungulates. *PLoS ONE: e686*.

30. Guo, X., Huang, K. & Tang, J. (2005). Clinicopathology of gout in growing layers induced by high calcium and high protein diets. *British Poultry Science, 46*, 641-646.

31. Harris, M., Bose, N. K., Klass, M., Mencher, J. P., Oberg, M. K & Vayda, M. P. (1966). The cultural ecology of India's Sacred cattle. *Current Anthropology, 7,* 51-66.

32. Hodges, R. D. (1974). *The Histology of the Fowl.* London: Academic Press.

33. Inoue, H. (1953). An experimental study of the upper urinary tract and in the fowl. *Acta Medica et Biologica (Niigata), 1*, 127-136.

34. Islam, K. N., Khan, M. Z., Siddiqui, M. S., Islam, M. R., Lucky, N. S., Hossain, M. K. & Adhikary, G. N. (2004). The anatomical studies of the kidneys of Rhode Island Red (RIR) and White Leghorn (WLH) chicken during their postnatal stages of growth and development. *International Journal of Poultry Science*, *3*, 369-372.

35. Johnson, O. W. (1968). Some morphological features of avian kidneys. *The Auk, 85*, 216-228.

36. Johnson, O. W. (1974). Relative thickness of the renal *medulla renalis* in birds. *Journal of Morphology, 142*, 277-284.

37. Johnson, O. W. (1979). Urinary Organs. In A. S. King & J. McLelland (Eds.), *Form and Function in Birds* (Vol. 1, pp. 184-235). London: Academic Press.

38. King, A. S. (1993). Apparatus Urogenitalis. In J. J. Baumel (Ed.), *Handbook of Avian Anatomy: Nomina Anatomica Avium* (pp. 329-347). Cambridge, Massachusetts: The Nuttall Ornithological Club.

39. King, A. S. & McLelland, J. (1984). *Birds: Their Structure and Function.* Bath, Great Britain: The Pitman Press.

40. Kumar, A. (2006). Diclofenac for veterinary use. No. 18-03/2006/DC, Letter to all State Drug Controllers. Drug Controller General (India).

41. Kurod, N. (1963). *A fragmental observation on avian kidney.* misc., Yamashina Institution of Ornithology.

85

42. Lamagère, M. (2011). *Atlas radiographique du vautour fauve (Gyps fulvus)*(Doctoral dissertation), Université Paul-Sabatier de Toulose, Available online at http://oatao.univ-toulouse.fr/4870/.

43. Layton, H. E., Davies, J. M., Casotti, G. & Braun, E. J. (2000). Mathematical model of an avian urine concentrating mechanism. *American Journal of Physiology- Renal Physiology, 279*, 1139-1160.

44. Meteyer, C. U., Rideout, B. A., Gilbert, M., Shivaprasad, H. L. & Oaks, J. L. (2005). Pathology and proposed pathophysiology of diclofenac poisoning in free-living and experimentally exposed Oriental white-backed vultures (Gyps bengalensis). *Journal of Wildlife Diseases,* 41 707-716..

45. Mundy, P. J., Benson, P. C. & Allan, D. G. (1997). Cape Vulture. In Harrison, D. G., Underhill, L. G., Herremans, A. J., Parker, V. & Brown, C. J. (Eds). *The Atlas of Southern African Birds* Volume 1. Birdlife, Johannesberg, South Africa.

46. Mundy, P., Butchart, D., Ledger, J. & Piper, S. (1992). *Vultures of Africa.* Randburg, South Africa: Acorn Books.

47. Nabipour, A., Alishahi, M. & Asadian, M. (2009). Some histological and morphological features of the avian kidney. *Journal of Applied Animal Research, 36*, 195-198.

48. Naidoo, V. & Swan, G. E. (2008). Diclofenac toxicity in Gyps vulture is associated with decreased uric acid excretion and not renal portal vasoconstriction. *Biochemistry and Biophysics Part C: Pharmacology and Toxicology*, 149, 269-274.

49. Naidoo, V., Duncan, N., Bekker, L. & Swan, G. E. (2007). Validating the domestic fowl as a model to investigate the pathophysiology of diclofenac in Gyps vultures. *Environmental Toxicology and Pharmacology, 24*, 260-266.

50. Naidoo, V., Venter, L., Wolter, K., Taggart, M. & Cuthbert, R. (2010)[1]. The toxicokinetics of ketoprofen in *Gyps coprotheres*: toxicity due to zero-order metabolism. *Archives of Toxicology, 84*, 761-766.

51. Naidoo, V., Wolter, K., Cuthbert, R. & Duncan, N. (2009). Veterinary diclofenac threatens Africa's endangered vulture species. *Regulatory Toxicology and Pharmacology, 53*, 205-208.

52. Naidoo, V., Wolter, K., Diekman, M., Duncan, N., Meharg, A. A., Taggart, M. A., Venter, L. & Cuthbert, R. (2010)[2]. Toxicity of non-steroidal anti-inflammatory drugs to *Gyps* vultures: a new threat from ketoprofen. *Biology Letters, 6*, 339-341.

53. Nicholson, J. K. (1982). The microanatomy of the distal tubules, collecting tubules and collecting ducts of the starling kidney. *Journal of Anatomy*, *134,* 11-23.

54. Nicholson, J. K. & Kendall, M. D. (1983). The fine structure of dark or intercalated cells from the distal and collecting tubules of avian kidneys. *Journal of Anatomy, 136*, 145-156.

86

55. Nickel, R., Schummer, A. & Seiferle, E. (1977). *Anatomy of the Domestic Birds.* (W. G. Siller & P. L. Wight, Trans.) Berlin: Parey.

56. Oakes, J. L., Gilbert, M., Virani, M. Z., Watson, R. T., Meteyer, C. U., Rideout, B. A., Shivaprasad, H. L., Ahmed, S., Chaudhry, M. J. I., Arshad, M., Mahmood, S., Ali, A. & Kham, A. A. (2004). Diclofenac residues as the cause of vulture population decline in Pakistan. *Nature, 427*, 630-633.

57. Pain, D. J., Cunningham, A. A., Donald, P. F., Duckworth, J. W., Houston, D. C., Katzner, J. T., Parry-Jones, J., Poole, C., Prakash, V., Round, P. & Timmins, R. (2003). Causes and effects of temporospatial declines of *Gyps* vultures in Asia. *Conservation Biology, 17*, 661-671.

58. Peterson, D. W., Hamilton, W. H. & Lilyblade, A. L. (1971). Hereditary susceptibility to dietary induction in selected lines of chickens. *The Journal of Nutrition, 101*, 347-354.

59. Pountos, I., Georgouli, T., Bird, H. & Giannoudis, P. V. (2011). Non-steroidal anti-inflammatory drugs: prostaglandins, indications and side effects. *Journal of Interferon, Cytokine and Mediator Research, 3*, 19-27.

60. Robertson, A. S. (1986). Notes on the breeding cycle of cape vultures (*Gyps coprotheres*). *Raptor Research, 20,* 51-60.

61. Satheesan, S. M. (2000). The role of poisons in the Indian vulture crash. *Vulture News, 42*, 4.

62. Scott, J. T. (1978). New knowledge of the pathogenesis of gout. *Journal of Clinical Pathology, 3*, 205-213.

63. Sherrill, J., Ware, L. H., Lynch, W. E., Montali, R. J. & Bush, M. (2001). Contrast radiography with positive-pressure insufflation in Northern Pintails. *Journal of Avian Medicine and Surgery, 15*, 178-186.

64. Shimada, K. & Sturkie, P. D. (1973). Renal portal circulation in chickens. *Japanese Journal of Veterinary Science, 35*, 57-63.

65. Siller, W. G. & Hindle, R. M. (1969). The arterial blood supply to the kidney of the fowl. *Journal of Anatomy, 104*, 117-135.

66. Sperber, I. (1949). Investigations on the circulatory system of the avian kidney. *Zoologiska Bodrag Fran Uppsala, 27*, 429-448.

67. Sturkie, P. D. (1986). Kidneys, Extrarenal Salt Excretion and Urine. In P. D. Sturkie, *Avian Physiology* (pp. 359-382). New York: Springer.

68. Swan, G. E., Cuthbert, R., Quevedo, M., Green, R. E., Pain, D. J., Bartels, P., Cunningham, A. A., Duncan, N., Meharg, A. A., Oaks, J. L., Parry-Jones, J., Shultz, S., Taggart, M. A., Verdoorn, G. & Wolter, K. (2006). Toxicity of diclofenac to *Gyps* vultures. *Biology Letters, 2*, 279-282.

87

69. Tisher, C. C. (1971). Relationship between renal structure and concentrating ability in the Rhesus monkey. *American Journal of Physiology, 220*, 1100-1106.

70. Warui, C. N. (1989). Light microscopic morphometry of the kidneys of fourteen avian species. *Journal of Anatomy, 162*, 19-31.

71. Warui, C. N. & King, A. S. (1985). Stereological observations on the kidney of the domestic fowl. *Journal of Anatomy, 142*, 129-139.

72. Witter, F. J. (1976). The history of avian medicine in the United States. *Avian Diseases, 20*, 621-630.

73. Zorrilla, I., martinez, R., taggart, M. A., & Richards, N. (2014). Suspected Flunixin Poisoning of a Wild Eurasian griffon Vulture from Spain.*Conservation Biology*.

88

Appendix 1

UNIVERSITEIT VAN PRETORIA
UNIVERSITY OF PRETORIA
YUNIBESITHI YA PRETORIA

ANIMAL USE AND CARE COMMITTEE (AUCC)

Standard Operating Procedure (2012)

Submission Date	14-5-2012	For Administrative Purposes	SOP No.	043-12.
Effective Start Date	June 2012		Review Date	June 2013
AUCC approval Date	2012-06-29		Signature (only on approval)	

SOP TITLE

Use of Vulture Carcasses for research

1. APPLICANT / RESPONSIBLE SUPERVISOR

Name	Prof V Naidoo
Contact Number	X6212
e-mail address	Vinny.naidoo@up.ac.za
Contact Address	UPBRC
Qualifications	BVMCh, MSc(Vet), PhD
Appropriate experience in animal handling	Director of UPBRC, Specialist Vet Pharmacologist and Authorised Expert in Laboratory Animals.

2. PURPOSE / AIM / JUSTIFICATION
(Describe the purpose of the process NOT MORE than 500 words)

Vultures are a ubiquitous part of the African landscape. Unfortunately all the vultures species across Africa, including the White-backed vultures (*Gyps africanus*), are endangered. In southern Africa, our most endangered species is the Cape Griffon vulture (*Gyps coprotheres*)(CGV), with an estimated 2400 breeding pairs in the wild. The Magaliesberg cliffs just outside Hartbeestpoort are home to the second largest breeding colony of CGVs in the Country. On average the colony can product 180 chicks annually. While the majority of these chicks fledge, a small portion of these birds are "non-viable" in that they're weak, undernourished, have metabolic bone disease, or are injured from their first attempts at flight. Some of these "non-viable" chicks are often presented at the Onderstepoort Veterinary Academic Hospital for veterinary treatment. In most cases treatment is not possible (e.g. metabolic diseases or non-aligned fractures) with the result that the birds are euthanased.

At present these carcasses are usually incinerated and present a major loss to science. We intend on preserving some if not all of these carcasses for potential future studies. Ethics approval is required as the birds will be treated with heparin 5 to 15 minutes prior to euthanasia. In addition the CGV is a TOPS appendix I listed species, which necessitates ethics approval. VulPro already has the necessary permits to treat rehabilitate birds, while the faculty of Veterinary Science has permission to treat birds on site. Permits are in process for the storage of these specimens, which are a restricted item to have in one's possession.

3. SPECIES & NUMBER OF ANIMALS INVOLVED

The intention of the study is to preserve as many fresh carcasses in formalin as possible. For this the animals will be initially given a dose of heparin 5 to 15 minutes prior to the pentobarbitone overdose. This will allow for the adequate exsanguination post-mortem for tissue fixation.

1

S4528/12
(Replace S4525/12)

89

Training Phase: While it is hoped that only one person will be involved in the process, this is not feasible. We would therefore like to also be able to teach students/technicians and other vets the proper manner to preserve "non-valuable" species. At this stage I request for the use of up to ten chickens per year. The chickens will all be at slaughter weight and destined for human consumption.

Preservation: *Gyps coprotheres* mainly. However we will attempt to preserve any vulture species that is euthanased.

The potential studies:
- Study of the vasculature to the kidneys
- Study of the vomeronasal organs of the head
- Endoscopic study of internal vasculature structure
- Morphological anatomy of the vulture
- Description of the skeleton and associated flight muscles.
- Studies in the aerodynamics of vulture flight: Size versus structural adaptations

4. REDUCTION / REFINEMENT / REPLACEMENT

Not applicable for the vulture phase. To prevent any question on the need for euthanasia, an independent vet from the Exotics Animal Clinic of the OVAH will always make the decision to euthanase without prior consultation with the study director. The latter is an important component of the TOPS regulation i.e. this prevents unethical euthanasia where animals are killed for sample harvest for muti, which in the case of the vulture are the feet and head.

For the training phase: The number of birds will be kept to a minimum by ensuring that no person will ever use more than 3 carcasses in their training. If more are required, the study director will need to use their discretion e.g. multiple techniques attempted, which require multiple carcasses.

5. HOUSING / SOURCE OF ANIMALS *(where will the work be done)*

The chickens will be sourced from a commercial broiler rearing farm (e.g. Kroon's Gourmet chickens). The animals will not be housed for the study. Birds will undergo euthanasia on arrival at the faculty.

6. PROCEDURE
(Give a clear step-by-step description of all procedures to be carried out on the animals. Include full details where relevant of handling and restraint, manipulations (e.g. rectal palpations), age/gender of animal, number and volume of blood samples taken.)

The following procedure will apply to all birds:
1) The birds will be given a 1ml/5kg heparin bolus, 5 to 15 minutes prior to euthanasia via a Jelco placed in the tarsal, wing or jugular vein. During this period animals will be monitored for potential complications. If any complications arise the animals will be immediately euthanized. This step is unfortunately necessary to allow for flushing of the blood vessels post-mortem. Without the heparin clotting will result, which will interfere with the perfusion in step 2 and fixation in step 3.
2) Following euthanasia with pentobarbitone, blood will be flushed out of the jugular with heparinised saline.
3) This will be followed by perfusion with embalming fluid
4) The carcasses will be placed in a formalin tank for hardening and anatomical studies
5) After a period, one of the following may be applied for vascular studies
   a. The veins will be injected with coloured latex; OR
   b. The arteries will be injected with coloured latex; OR
   c. The vessels will be cast in resin

7. TREATMENT / SUBSTANCES ADMINISTERED
(Give full details of any treatment/substances administered as described in procedure)

Heparin
Pentobarbitone

8. ANIMAL WELFARE
(Identify all known/anticipated welfare issues and specify how each issue will be monitored and dealt with)

2

S4528/12
(Replace S4525/12)

90

(a) Pain, discomfort, stress classification *(Please indicate)*

A1	Experiments on embryonated eggs or cephalopods and decapods	☐
A2	Studies on vertebrate animals during the course of routine examination, teaching procedures and treatment. **Examples:** *Animals held under proper conditions for later use or for teaching non-invasive procedures.* *Observational studies e.g. on wild animals in the field*	☐
B	Procedures on vertebrate species that are expected to produce stress but no pain requiring anaesthesia. **Examples:** *Wild animals caught in the field, caged & transported for observation.* *Administration of medication.* *Collection of blood samples.* *Rectal examination*	☐
C	Experiments that produce minor or short-duration pain requiring the use of pain relieving drugs. **Examples:** *Subcutaneous implants.* *Docking in sheep.* *Collection of tissues from animals after euthanasia.*	☐
D	Experiments that involve significant but unavoidable stress or pain requiring anaesthesia or a humane endpoint. **Examples:** *Non-survival surgery in teaching.* *Survival surgical procedures.* *Infectivity or toxicity studies with a high probability of producing disease.* *Large animals kept in boma.*	☐
E	Procedures that involve inflicting severe pain at or above the pain tolerance threshold and the use of pain relievers are contra-indicated. **Examples:** *Toxicity/virulence testing where death is the endpoint.* *Disease/cancer models involving chronic clinical signs.*	☐

Definitions from Special Issue, Laboratory Animal Science, January 1987, p 12

(b) Monitoring and method

Animals will at all times be under veterinary observation following the administration of the heparin.

(c) Analgesia / Anaesthesia
(It is expected that analgesia will be used routinely after every painful procedure)

Not applicable

(d) Endpoints / Euthanasia criteria if applicable

If any animal shows suffering after the administration of the heparin, the animal will be immediately terminated.

9. SAFETY HAZARDS / BIOSAFETY

Staff will wear appropriate protective equipment when working with formalin

10. EQUIPMENT / CONSUMABLES USED

Formalin

11. WASTE MANAGEMENT / DISPOSAL OF CARCASES
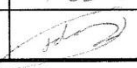
Carcasses will be incinerated once utilised in a study

12. ADDITIONAL

13. RECORDS
(Annual reporting of animals used is required)

3

S4528/12
(Replace S4525/12)

91

A list of animals will be kept for TOPS purposes

14. GENERAL VETERINARY CARE *(When welfare procedures are involved requiring veterinary supervision by law)*
(Provide details, including emergency contact details, of the veterinarian who will be responsible to provide the general veterinary care and who will have the authority to enforce the endpoints stipulated under Point 8(d). The veterinarian must be registered or authorised with the SAVC and is preferably independent of the research group.) *(Please type)* It is the responsibility of the veterinarian to arrange for a locum if he/she is not available

PERSON RESPONSIBLE FOR VETERINARY CARE OF ANIMALS	Prof V Naidoo
EMERGENCY Contact details	X 6212
Signature & Date	12/06/12

15. DECLARATION

I, (full name) ....V.....Naidoo...............declare that the use of animals in the proposed course or diagnostic procedure is justified. I have actively pursued and investigated the use of alternatives and declare that there are no acceptable non-animal alternatives. The course participants or personnel will be suitably prepared to perform the procedures required. I undertake to ensure that high ethical standards, as prescribed in the South African National Standards (SAN 10386-2008), are maintained throughout the course. I understand that the Animal Use and Care Committee may appoint a supervisor to attend the course and that this person, in consultation with the Committee, will have the authority to terminate the course if the animals are treated unethically.

_____
SIGNATURE

_____12/06/12_____
DATE